

THE ROLE OF YAP SIGNALLING IN STRESSORS ASSOCIATED WITH MYOCARDIAL  
INFARCTION

by

Victoria Lynn Nelson

Submitted in partial fulfilment of the requirements.  
for the degree of Master of Science

at

Dalhousie University  
Halifax, Nova Scotia  
July 2023

## TABLE OF CONTENTS

LIST OF TABLES .....	iv
LIST OF FIGURES .....	v
ABSTRACT .....	vii
LIST OF ABBREVIATIONS AND SYMBOLS USED .....	viii
ACKNOWLEDGEMENTS .....	x
<b>Chapter 1: Introduction .....</b>	<b>1</b>
1.1 Clinical Characteristics and Management of Myocardial infarction (MI) .....	1
1.1.1 Clinical treatment of ST-elevation MI and non-ST-elevation MI .....	2
1.2 Preclinical Models of Myocardial Infarction .....	4
1.2.1 Myocardial Infarction by Surgical Ligation .....	4
1.3 Molecular Mechanisms of Myocardial Infarction .....	5
1.3.1 Necrosis and apoptosis after Myocardial Infarction .....	5
1.3.2 Cardiac Hypertrophy After Myocardial Infarction .....	6
1.3.3. Fibrotic Response After Myocardial Infarction .....	8
1.3.4 Vascular Remodelling After Myocardial Infarction .....	9
1.3.5 Inflammatory Response After Myocardial Infarction .....	10
1.4 Yap Signalling Pathway .....	11
1.4.1 Regulation of the Yap Signalling .....	12
1.4.2 Yap Signalling in Cardiac Development .....	15
1.4.3 Yap Signalling in Cardiac Regeneration .....	16
1.5 Summary and Rationale .....	17
<b>Chapter 2: Materials and Methods .....</b>	<b>18</b>
2.1 <i>In Silico</i> Microarray Analyses of Myocardial Infarction in Rats .....	18
2.2.1 Volume Overload Heart Failure (AMI) .....	18
2.3 Tissue Collection and Preparation .....	19
2.3.1 Fixing Tissue and Sectioning .....	19
2.4 Immunohistochemistry Chromogen Staining .....	19
2.5 Cell Culture .....	20
2.5.1 Cell Treatments .....	20
2.6 Resazurin Metabolic Assay .....	22
2.7.1 Cell Collection and Whole Cell Lysate Preparation .....	22
2.7.2 Nuclear and Cytoplasmic Protein Extraction .....	23
2.7.3 Bicinchoninic Acid (BCA) Assay .....	23

2.7.4 Bradford Assay .....	24
2.7.5 Western Blotting.....	24
2.7.6 Densitometry.....	25
2.8 Isolation and Measurement of Free Amino Acids .....	25
2.9 Quantitative Polymerase Chain Reaction (qPCR) .....	26
2.9.1 Extraction of RNA from Tissue.....	26
2.9.2 RNA Isolation from H9c2 Cells .....	26
2.9.3 Complementary DNA (cDNA) Synthesis.....	27
2.9.4 SYBRGreen Quantitative Polymerase Chain Reaction (qPCR).....	27
2.9.5 qPCR Gradient.....	29
2.9.6 Primer Validation - Agarose DNA Electrophoresis.....	30
2.10 Immunocytochemistry .....	30
2.11 Statistical Analysis.....	31
<b>Chapter 3: Results.....</b>	<b>32</b>
3.1 Yap Signalling in Mice After Myocardial Infarction .....	32
3.2 Effects of Ischemic Stressors on Yap Signalling in H9c2 Rat Cardiomyotubes .....	32
3.3 Yap Signalling Related Protein Levels Changes in Sub-Cellular Fractionation .....	39
3.4 The Effect of Fatty acids and Glucose on Yap Signalling Protein Levels.....	39
3.5 Changes in Amino Acids Impact Yap Signalling in H9c2 Rat Cardiomyotubes .....	43
3.6 Hepes Supplementation Does Not Impact the Response to Nutrient Deprivation in Rat Cardiomyocytes .....	51
3.7 Nutrient Deprivation Conditions Alters Gene Expression.....	55
3.8 Nutrient Deprivation Conditions Alters Metabolic Activity .....	59
<b>Chapter 4: Discussion .....</b>	<b>64</b>
4.1 Summary of findings.....	64
4.2 Yap Expression in Response to Acute Nutrient Deprivation.....	65
4.3 Compartmentalization of Yap After Nutrient Deprivation in Rat Cardiomyotubes .....	66
4.4 Connective Tissue Growth Factor in Yap Signalling and the Heart.....	68
4.5 Clinical Relevance of Yap, Isoleucine, and Ctgf.....	69
4.6 Limitations and Future Directions .....	70
4.7 Conclusions.....	71
<b>References.....</b>	<b>73</b>

## LIST OF TABLES

Table 1. Primer Sequences and Annealing Temperatures of Oligonucleotides used in qPCR...	27
Table 2. Summary of Compartmentalization Patterns Results in Nutrient Deprivation and Nutrient Deprivation with Isoleucine Compared to DMEM Controls.....	67

## LIST OF FIGURES

Figure 1.1: Cell Progression After MI .....	7
Figure 1.2 Simplified Yap Signalling Pathway .....	13
Figure 1.3 Regulation of Yap Signalling .....	14
Figure 3.1: Positive Yap Signalling 28-day Post MI in Mice.....	33
Figure 3.2: Increase in peri-infarct Yap Levels after MI.....	34
Figure 3.3: Screen of ischemic stressors experienced during an MI effect on Yap signalling...	35
Figure 3.4: Increased Phosphorylation at Two Key Sites in Nutrient Deprivation Conditions..	37
Figure 3.5: No Changes in Apoptosis or Cell Stress Markers in Nutrient Deprivation Conditions at 1hr. ....	38
Figure 3.6: Evidence of Nuclear Compartmentalization in Nutrient Deprivation Conditions. ..	40
Figure 3.7: Increased Nuclear and Cytoplasmic Yap Phosphorylation in Nutrient Deprivation Conditions.....	41
Figure 3.8: Schematic of ischemic components. ....	42
Figure 3.9: Unsuccessful Fatty Acid Supplementation in Nutrient Deprivation Conditions. ....	44
Figure 3.10: Effects of D-glucose Supplementation on Yap Signalling.....	45
Figure 3.11 Deduction and Reduction Approach to Focus on Amino Acids. ....	46
Figure 3.12: Effects on Free Amino Acids in Nutrient Deprivation Conditions.....	48
Figure 3.13: Effects of Amino Acid Supplementation in Nutrient Deprivation Conditions. ....	49
Figure 3.14: Threonine and Isoleucine Feedback Inhibition. ....	50
Figure 3.15: L-Isoleucine Decreased Cytoplasmic Yap (p-S397) Back to Control Levels.....	52
Figure 3.16: Validation That Hepes Supplementation at Utilized Concentration Does Not Affect Yap Levels.....	53
Figure 3.17: The Effects of Re-addition of DMEM After One Hour of Nutrient Deprivation. ..	54
Figure 3.18: Determination of Reference Genes for qPCR Analysis. ....	56
Figure 3.19: Five Themes Associated with Myocardial Infarction Recovery.....	57

Figure 3.20: Supplementation of Isoleucine Results in an increase of mRNA Expression of a Matrix Related Gene ..... 58

Figure 3.21: Expression of Known Yap Regulated Genes from a Gene Expression Omnibus (GEO) Data Set. .... 60

Figure 3.22: L-isoleucine Supplementation Suggest More Cell Survival/Adhesion Compared to Nutrient Deprivation Alone. .... 61

Figure 3.23: The effects of Nutrient Deprivation and Nutrient Deprivation supplemented with L-isoleucine..... 62

## ABSTRACT

Due to myocardial infarction (MI) a loss of viable cardiomyocytes significantly reduces cardiac function and patients' quality of life. This loss is caused partly by definitive stressors as a result of ischemia. The Yap signalling pathway is a regulator of fetal heart development—its role in adult cardiomyocytes after MI remains to be defined. Using differentiated rat cardiomyotubules (H9c2) we independently screened stressors associated with ischemia as: hypoxia, oxidative stress, inflammation, autophagy, and nutrient deprivation. We found Yap was most sensitive to nutrient deprivation. We then created a nutrient deprivation model as media deprived of the nutrient substrates. Our data suggest that the translocation of phosphorylated Yap is affected under this metabolic stress. Additionally, we found isoleucine could play an important role in cytoplasmic retention of phospho-Yap S397 and contributes to the upregulation of structural integrity-related genes.

## LIST OF ABBREVIATIONS AND SYMBOLS USED

ACE	angiotensin-converting-enzyme
AKT	protein kinase B
AMI	acute myocardial infarction
ANOVA	analysis of variance
ARB	angiotensin II receptor blocker
ATCC	American type culture collection
ATP	adenosine triphosphate
BCAA	branched chain amino acid
BSA	bovine serum albumin
CCL24	c-c motif chemokine ligand 24
CT	computerized tomography
CTGF	connective tissue growth factor
cTn	cardiac troponin
CYR61	cysteine-rich angiogenic inducer 61
DAMPs	danger-associated molecular patterns
DMEM	Dulbecco's Modified Eagle Medium
DTT	dithiothreitol
EBSS	Earle's Balanced Salt Solution
ECG	echocardiogram
ECM	extra-cellular matrix
eNOS	endothelial nitric oxide synthase
FBS	fetal bovine serum
FCCP	carbonyl cyanide-p-trifluoromethoxyphenylhydrazone
GAPDH	glyceraldehyde 3-phosphate dehydrogenase
GEO	gene expression omnibus
GPCR	G protein coupled receptor
GSK3 $\beta$	glycogen synthase kinase 3 $\beta$
IGF	insulin-like growth factor
IR	ischemic reperfusion
LAD	left anterior descending coronary artery
LATS1/2	large tumor suppressor homologue 1/2
LEF	lymphoid enhancer factor
LV	left ventricle
MAP4K	mitogen-activated protein kinase kinase kinase kinase
MI	myocardial infarction
MIAME	minimum information about a microarray experiment
MLKL	mixed lineage kinase-like
MOB1	MOB kinase activator 1A
mPTP	mitochondrial permeability transition pore
MST1/2	mammalian serine/threonine protein kinases1/2
NCBI	national center for biotechnology information
NF2	neurofibromin 2
NO	nitric oxide
NSTEMI	non-ST-segment elevation myocardial infarction



NTC	no template control
OD	optical density
PBS	phosphate-buffered saline
PCI	percutaneous coronary intervention
PHI	phosphatase inhibitor
PI	protease inhibitor
PI3K	phosphoinositide 3-kinase
qPCR	quantitative polymerase chain reaction
RIPK3	receptor interacting protein kinase 3
ROS	reactive oxygen species
SAV1	salvador homologue 1
STEMI	ST-segment elevation myocardial infarction
TAE	tris-acetate-1mM ethylenediaminetetraacetic acid
TAZ	transcriptional coactivator with PDZ-binding motif
TBST	tris-buffered-saline-tween
TCF	T cell factor
TEAD	transcriptional enhanced associate domain
TGF- $\beta$	transforming growth factor $\beta$
TLR	toll-like receptors
TNF $\alpha$	tumor necrosis factor alpha
TNFR1	tumor necrosis factor receptor 1
UPLC	ultra-performance liquid chromatography
VEGF	vascular growth factor
WNT	wingless-related integration site
YAP	yes associated protein

## ACKNOWLEDGEMENTS

First and foremost, I would like to say a huge thank you to my mom and brother for their never-ending support, constantly reminding me I can do anything I put my mind too and to do things that bring me joy. I would not be where I am today without both of your encouragement and love. Endlessly grateful to have you both by my side. Love you.

Thank you to all my lab members, committee members, faculty, and administrative staff for making my experience at DMNB so positive. I would not have made it through this MSc without your continuous support and guidance.

To Maggie Pickard, I will be forever grateful for the lifelong friendship we have developed throughout our MSc. I am endlessly appreciative of your support both in and out of the lab and can't wait to see what the future has in store for you.

Dr. Keith Brunt, I am eternally thankful to you for making my research experience so positive. Your passion for research is contagious and admirable. I look forward to learning more from you through my PhD journey.

Lastly, I would like to dedicate this work to my dad who passed suddenly when I was nine. You inspired me to pursue cardiac research in hopes of one day making a difference, so another family wouldn't have to experience the loss we have. I miss you every day but know you are watching over and are so proud. I love you always.

Disclaimer: The ideas conceived, experimental directions/protocols and hypotheses presented in the current work are the result of a collaboration between Victoria L. Nelson and Dr. Keith R. Brunt. Unless otherwise stated, Victoria L. Nelson designed and performed all experiments and analyzed results. Dr. Jason Huber and Dr. Mathew Platt performed rodent surgeries at the University of Guelph. Ashley L. Eadie and Malav Madu received, processed, and analyzed tissue samples (Figure 3.1). Kyle Wells processed and stained tissue, Victoria L. Nelson imaged and analyzed the data (Figure 3.1). Dr. Lester Perez and Michael Connolly ran the experiments and Victoria L. Nelson performed the analysis (Figure 3.2). Dr. Lester Perez ran the experiment, Angella Mercer processed and ran the samples through ULPC, Victoria L. Nelson analyzed the data (3.11).

## **Chapter 1: Introduction**

Despite extensive research, myocardial infarction (MI) remains a leading cause of mortality and morbidity globally [1]. Without effective treatment, or compensation through adaptive remodelling, an MI damages and eliminates irreplaceable cardiomyocytes responsible for cardiac output. Thus, what follows is often a progressive decline into heart failure, decreasing quality of life, and severe future complications for patients.

Through an exploration of a developmental pathway that regulates cardiac development it is plausible that an opportunity will present itself to rescue or improve adaptation to MI injury. Yap signalling, the downstream signalling cascade of the Hippo signalling pathway, has a direct role in the size regulation of a developing heart. Upregulation of Yap is associated with overgrowth of the heart (hyperplasia) [2] in neonatal mice, while downregulation of Yap causes lethal underdevelopment of the heart (hypoplasia) [3]. As a transcriptional co-factor, Yap plays an important role in tissue formation and repair after injury in several organs, satellite muscle cells and liver cells. The role of Yap in the adult heart for repair after MI injury remains to be fully characterized, particularly in regard to upstream stimuli and downstream gene regulation of most cardiac cell types, including cardiomyocytes. Regeneration after an MI is still possible after injury in neonatal mice but such regenerative capacity is lost by 7 days postnatally [4]. After an AMI, during the progressive phases of remodelling and attempted compensation the adult heart relies on reactivation of developmental transcriptional regulatory patterns [5]. Here, we sought to investigate the role Yap signalling plays in the adult heart after MI by investigating MI-associated stressors and associated drivers of injury and heart failure.

### **1.1 Clinical Characteristics and Management of Myocardial infarction (MI)**

Risk factors associated with MI include high blood pressure, high levels of cholesterol, smoking, diabetes, and being overweight [6]. MI occurs when coronary blood flow is reduced or stopped, causing injury to the myocardium as a result of decreased oxygen and nutrient supply with the accumulation of metabolic waste by-products [7]. Cardiac ischemia can arise by many causes including build-up of atherosclerosis coronary plaques, their rupture/erosion, coronary vasospasm, or cardiac microvascular dysfunction and rarefaction (loss or extinction of small blood vessels). When a blockage occurs in one of the main coronary arteries that supply blood to the heart the myocardium becomes severely ischemic with lethal consequences unless

reperfusion is elicited. Even with reperfusion, injury can compromise cardiac function, elicit arrhythmias, and progress to maladaptive remodelling heart failure.

MI results in a wide range of symptoms that vary from person to person. Chest pain, which can be diffuse down the left arm or neck, shortness of breath, sweating, nausea, vomiting, fatigue, and abnormal heart rate are the most common symptoms[6,8]. Chest pain is a common symptom associated with MI, yet over 60% of patients do not experience chest pain as a symptom [9]. This 60% may be explained by the fact that symptoms differ greatly based on sex. Most females experience less severe/more variable symptoms than males. Females are more likely to have nausea or vomiting as symptoms and less likely to experience chest pain [10–13]. The differences in symptom presentation cause delays in females seeking treatment and additionally make diagnosis more challenging, leading to a delay in treatment. Given the danger of ischemic events, immediate diagnosis and treatment are required to reduce damage to the heart.

There are different classifications of MIs categorized based on pathology, prognosis, and clinical outcomes. The evaluation of symptoms and diagnosis often begins with a history, physical exam, echocardiogram (ECG) and cardiac troponin (cTn), testing if MI is suspected [7]. ECG leads are used to examine whether there is an increase in the ST-segment, the isoelectric point between depolarization and repolarization of the ventricles. If there are changes in the ST-segment and other cardiac injuries are ruled out, a diagnosis of ST-elevation MI (STEMI) is made [14]. Secondary to ECG testing cTn, part of the contractile mechanism of the heart, levels are detected in the blood and used to confirm diagnosis especially for a patient who does not have changes in the ST-segment. If cTn levels rise and there are no changes in the ST-segment these patients would be diagnosed with a non-ST-segment elevation MI (NSTEMI) once unstable angina has been ruled out [14]. cTn levels increase after MI as a result of the death of the heart tissue that the release of cTn to the bloodstream[15].

### 1.1.1 Clinical treatment of ST-elevation MI and non-ST-elevation MI

Accurate and rapid diagnosis is critical for patients with MI as treatment strategies differ depending on the severity and whether it is STEMI or NSTEMI variety. For most

patients suffering from STEMI prompt reperfusion therapy is required, which can consist of percutaneous coronary intervention (PCI) and/or fibrinolytic therapy [14]. Drug therapy is required during PCI including administering anti-platelets (e.g., aspirin or Clopidogrel) to prevent clot formation, in addition to anti-coagulants, such as unfractionated heparin or bivalirudin, a thrombin inhibitor, may be used. If PCI is not possible due to lack of resources or timing (within 90–120-minute window) fibrinolytic therapy is used [16]. Fibrinolysis therapy causes intravascular clots to breakdown using medications such as alteplase or reteplase thereby improving blood flow [17]. Additionally, patients could be administered an anti-thrombin (reduce fibrin formation) and/or an anti-platelet (prevents the clumping of platelets) and monitored for 60-90 minutes, and an ECG can confirm the success of fibrinolysis therapy.

Medical management of patients diagnosed with NSTEMI relies heavily on the assessment of mortality risk within 6 months or further cardiovascular events. For those in the low-risk group (<3% 6-month mortality rate predicted), management with anti-platelets and anti-thrombins with ongoing cardiac monitoring of patients is the first line of treatment [18]. Ischemia testing, such as stress test, ECG and/or cardiac computerized tomography (CT) scan, may be performed before the patient is discharged, and if symptoms and elevated troponin persist angiography may be needed. For patients in the intermediate and higher risk group (>3% 6-month mortality rate predicted) immediate angiography is required if the patient is unstable, if the patient is stable angiography with follow-on PCI can be performed with 72 hours of diagnosis [18]. Patients receive anti-platelet and anti-thrombin medications to prevent further clot formation, dose, and choice of medications changes based on bleeding risk and contraindications with other medications [16]. As with STEMI, consistent assessment of left ventricular function is expected to monitor patient progress. Once a patient is stable cardiac rehabilitation begins, varying based on the outcome and/or severity of the MI.

Cardiac rehabilitation should be initiated prior to hospital discharge and follow-up appointments scheduled in the community [16]. Rehabilitation varies from patient to patient but includes exercise, lifestyle advice, decrease in stress and lifestyle modification, such as changes in diet, smoking cessation, and limiting alcohol consumption. While these changes can decrease the risk of a secondary MI and further deleterious cardiac remodelling, drug therapy is usually required as a means of secondary prevention and decreased stress on the heart long term [16].

Angiotensin-converting-enzyme (ACE) inhibitors or angiotensin II receptor blockers (ARBs) where patients are ACE intolerant are widely prescribed after MI and are continued indefinitely in most cases. ACE inhibitors and ARBs work by causing vasodilation and reducing blood volume and pressure. Beta-blockers, decrease heart rate by inhibiting the sympathetic system, and are typically administered in addition to ACE inhibitors or ARBs for up to 12 months, if the ejection fraction of the left ventricle (LV) is reduced at this time they will be continued indefinitely as well [7]. Titration of both ACE inhibitors and beta-blockers is crucial for determining the most effective dose and will be continuously monitored if changes in dose are required [16].

## **1.2 Preclinical Models of Myocardial Infarction**

There are significant challenges and risks of taking cardiac biopsies to evaluate the heart after MI and this would also be limited to a brief snapshot of the multifaceted molecular mechanisms involved in MI and MI recovery. Additionally, it is hard to specify what would be MI specific mechanisms from comorbidities, physiological stress mechanisms and/or pharmacological treatments. Some insights have been gathered from time-specific mechanisms assessed from human MI sampling, but we cannot solely rely on biopsies and/ or patient samples to study underlying molecular mechanisms. This highlights the important need to utilize preclinical models. Although preclinical models also have limitations, they allow for a progressive study of cardiac and systemic remodelling of MI and the molecular mechanisms involved from the initial event, the recovery and remodelling process after injury. Moreover, these models can be studied in background comorbidities with variations of standard care medications or not depending on the study design. Using the appropriate preclinical model can allow for effective translation from animal models to clinical trials.

### **1.2.1 Myocardial Infarction by Surgical Ligation**

Permanent occlusion of the left anterior descending coronary artery by surgical ligation is the primary method for modeling MI [19–21]. Ligation results in increased oxidative stress markers and cardiomyocyte death as a result of decreased bloodflow, which causes decreased ejection fraction and subsequently increases volume in the left ventricle as a result of ineffective blood clearing [22]. These outcomes are consistent with the characteristics seen in

human patients after MI. This ligation model also allows for the modelling of ischemia reperfusion (IR)- injury whereby removal of the ligation mimics those patients who are eligible for reperfusion compared to permanent ligation where patients are unable to receive reperfusion. While ligation is an effective model of MI it requires surgical expertise and does not emulate all components/types of MI (e.g., plaque rupture) but allows for better understanding of the molecular mechanisms involved [23], as well as determining the effects of pharmacological interventions.

### **1.3 Molecular Mechanisms of Myocardial Infarction**

Numerous cell types and various molecular mechanisms are activated in response to cardiac injury such as MI (Fig 1.1). Each cell type and their respective mechanisms play a critical role in aiding recovery with the remodeling of the myocardium post-MI. They work in concert to decrease initial damage and adapt cardiac work. Each mechanism modulates various steps in the repair and healing process. These complex cell and molecular mechanisms must work cohesively with time to maintain structural integrity and contractile capacity to meet the metabolic demands required by the body.

At the same time, cardiac metabolism which is responsible for the production of energy in the form of adenosine triphosphate (ATP) is needed to maintain proper heart function[24]. Primarily, the heart uses fatty acids as the main fuel source to maintain ATP levels under normal conditions with glucose and lactate used to a lesser extent[25]. However, during an ischemic event such as MI, cardiac metabolism adapts rapidly to the decrease in nutrient and oxygen supply. Metabolic remodelling occurs in the remaining healthy myocardium to compensate for the infarcted area, which includes a shift from fatty acid metabolism to glucose. Glucose metabolism is less efficient, however, it requires less oxygen than fatty acid metabolism[26].

#### **1.3.1 Necrosis and apoptosis after Myocardial Infarction**

Many molecular mechanisms are involved in response to the ischemia caused by myocardial infarction. The first is cardiac cell death, most obviously cardiomyocyte death, which can occur by various mechanisms with the most common being necrosis and apoptosis. Whereby apoptosis and necrosis can be triggered both extrinsically (initiated outside of the cell) through

death toll receptors and intrinsically (initiated signals from within the cell) by mitochondrial pathways [27]. In terms of apoptosis, intrinsic mitochondrial release of cytochrome-c or extrinsic activation of the death receptors activate the caspase pathway. Caspases are a subclass of cysteine-dependent proteases that work by hydrolyzing peptide bonds, resulting in characteristic apoptotic cell shrinkage, membrane blebbing, and chromatin condensation [28]. Apoptosis is a form of regulated cell death and is energy-dependent, meaning it requires ATP for many of its steps including forming the apoptosome, caspase activation, and kinase signalling[29]. In contrast, necrosis is unregulated and a passive process where cell membrane integrity is compromised. Necrosis is considered the earliest form of cell death after myocardial infarction in response to severe physiochemical stress [30]. The mitochondrial necroptosis pathway is the opening of the mitochondrial permeability transition pore (mPTP), which disrupts the proton gradient across the mitochondrial membrane that in turn disturbs ATP synthesis. This results in cell and organelle swelling and loss of cellular structure [31]. The necroptosis death receptor pathway is initiated by tumor necrosis factor receptor 1 (TNFR1) that activates receptor interacting protein kinase 3 (RIPK3), which in turn activates mixed lineage kinase-like domain (MLKL), triggering the permeabilization of the plasma membrane [32]. Though necroptosis shares similar morphology to necrosis, and it is considered a partially regulated form of cell death as it coincides with early activation of apoptosis pathways in a partially regulated manner prior to loss of membrane integrity [33]. After MI the initial cell death is by necrosis, then cardiomyocytes begin a pattern of regulated death by means of apoptosis and necroptosis. While these cell death pathways are the most common and the most heavily studied there are other cell death mechanisms that contribute to cell loss after MI, such as ferroptosis (iron related cell death) [34], pyroptosis (intracellular pathogen cell death) [35] and autosis (autophagy-dependent cell death) [36].

### 1.3.2 Cardiac Hypertrophy After Myocardial Infarction

As cardiomyocyte cell death occurs initially after MI, the heart must compensate for the mechanical and physiological stress cell loss to maintain cardiac output. A compensatory, adaptive response to the dilatation and thinning of the infarct zone by cardiomyocytes is cardiac hypertrophy [37,38]. Hypertrophy can be eccentric (increased cell length) and/or concentric



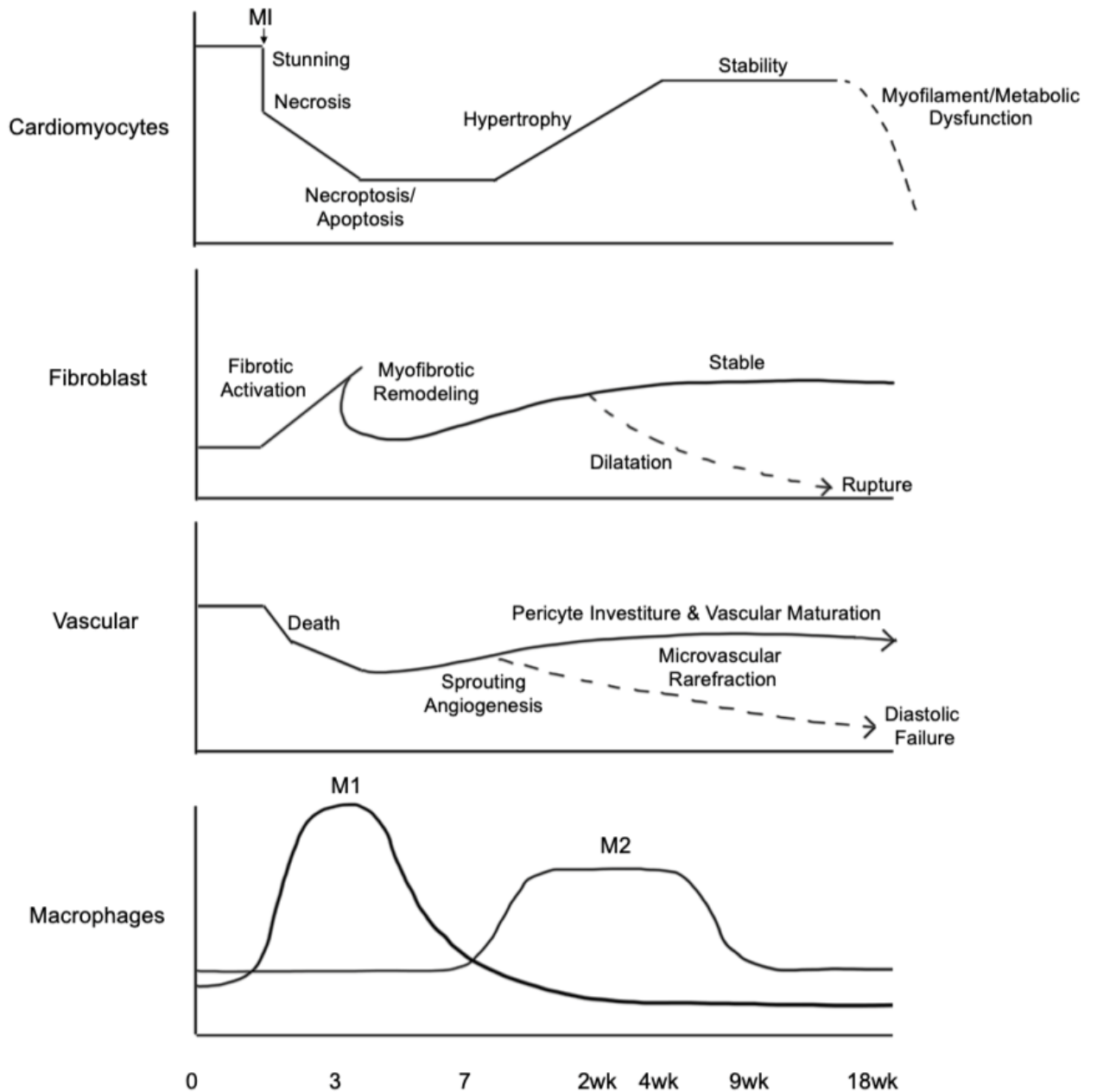


**Figure 1.1: Cell Progression After MI**

Major cell types of the heart as they progress, adapt and compensate in response to myocardial infarction. Initially there is significant cardiomyocyte death, followed by hypertrophy of existing cardiomyocytes to restore function. The ischemic conditions cause activation of fibroblast to myofibroblast resulting in scar formation of the injured myocardium. Death of vascular cells initiates angiogenesis that mature to increase blood supply. Macrophages initially act pro-inflammatory with their M1 phenotype, however transition to their anti-inflammatory phenotype (M2).

(increase in cell thickness) in nature [37,39] and is initiated by volume or pressure overload that is usually referred to as pathological hypertrophy in the context of MI [40]. In response to hemodynamic load, hypertrophy occurs to reduce wall stress, and to maintain function and efficiency of the heart. Hypertrophy is the result of a combination of cellular and molecular mechanisms that include myocyte growth without proliferation, changes in metabolic state, re-expression of fetal genes patterns, dysregulation of calcium handling, and changes in protein expression [40]. MI initiates hypertrophy by mechanical force, neuroendocrine hormones (angiotensin II, endothelin 1, and catecholamines), and downstream signalling pathways (mTOR, AKT, ANP or BNP) [38]. Though adaptation through cardiac hypertrophy is initially beneficial, without appropriate regulation the hypertrophy can lead to changes in chamber shape and loss of contractile force, which ultimately leads to maladaptive remodeling post-MI [38]. This maladaptation results in poor outcomes for MI patients and can eventually lead to heart failure.

### 1.3.3. Fibrotic Response After Myocardial Infarction

Hypertrophy is often flanked by fibrosis [41], which is extra cellular matrix (ECM) cross-linking combined with deposition of collagen (both type I and III) that aids in myocardial repair after MI [42]. Fibroblasts are the cells that contribute to the formation of connective tissue that is responsible for the framework and structure of the extra cellular matrix, which is rich in type I and III collagen and maintains the structural integrity of tissues [43]. After cardiac injury such as MI, fibroblasts are essential for the repair of the myocardium to maintain the structure of the LV wall under pressure from blood volume. During the repair process, cardiac fibroblasts undergo several phenotypic transitions [44]. Initially after injury fibroblasts in the ischemic region attain a pro-inflammatory phenotype that stimulates the secretion of cytokines [45]. Stimulation of cytokines results in activation of specific matrix-degrading proteases responsible for degrading the extracellular matrix. After degradation and clearance of dead cardiomyocytes, fibroblasts within the infarct zone initiate proliferation and recruit resident fibroblasts from the non-infarcted zone as part of their anti-inflammatory phenotype. At the same time, several infarct zone fibroblasts become myofibroblasts, which produce ECM related proteins and express contractile proteins contributing to passive tensile strength and elastance in the LV wall (alpha-smooth muscle actin) [46–48]. Lastly, fibroblasts undergo maturation by

disassembling their stress fibres and convert to specialized cells, which aid in scar formation and maintenance. This scar formation, mainly driven by fibroblasts with the recruitment of inflammatory and other cells, is termed fibrosis. While initially fibrosis is beneficial for maintaining structural integrity of the myocardium, it can result in decreased contractile capacity through stiffening of the chamber walls and altered mechanosensing that can be detrimental to cardiac function and lead to arrhythmias or heart failure [49].

#### 1.3.4 Vascular Remodelling After Myocardial Infarction

The decreased blood supply through cell death of cardiomyocytes and vascular cells from ischemia results in remodelling and collateralization of the vasculature to increase blood supply needed for nutrients and wound healing after MI [50,51]. The main mechanism of neovascularization in the adult heart after MI is angiogenesis [52–54]. Angiogenesis is the process of forming new blood vessels from pre-existing vessels. Specifically, sprouting angiogenesis in the case of MI where the oxygen levels are detected to be low by hypoxia-inducible factors (HIF). In response to the hypoxic environment cells secrete vascular growth factor (VEGF- $\alpha$ ), which initiates endothelial tip cells that control the development of the sprouting capillary through the ECM towards the cells that are releasing VEGF- $\alpha$  [55–57]. Once the filopodia of the tip cells, which consist of numerous VEGF- $\alpha$  receptors, reach the source of VEGF- $\alpha$  being secreted, fusion of the tip cells occurs that results in the formation of a continuous lumen with help from stalk cells that allow for elongation of the capillary sprouts. The creation of the lumen allows for blood flow of oxygenated blood to an otherwise hypoxic environment, which results in the return to normal oxygen levels, HIF degradation and reduction of VEGF- $\alpha$  secretion levels back to normal [58]. Once the new capillary is formed pericytes are recruited to aid with maturation and stabilization of the capillaries [59]. However, if angiogenesis is unsuccessful because of oxidative stress, inflammation and endothelial dysfunction, a reduction in capillary density can lead to microvasculature rarefaction that causes cardiomyocyte stiffness, hypertrophy through decreased endothelial nitric oxide synthase (eNOS) and lower nitric oxide (NO) bioavailability. Altogether, this leads to diastolic heart failure in many patients [60].

### 1.3. 5 Inflammatory Response After Myocardial Infarction

Damage to the myocardium caused by MI results in a sterile inflammatory response driven by damage associated molecular patterns (DAMPs) [61]. Inflammatory responses can be classified into two states pro-inflammatory and anti-inflammatory, where the first response to MI is pro-inflammatory. Initially in the pro-inflammatory state necrotic cell death caused by MI results in the release of DAMPs that stimulate an acute response of immune cells to clear cellular debris, as well as ECM tissue that is degraded by fibroblasts [62–64]. DAMPs bind to pattern recognition receptors (e.g., Toll-like receptors (TLRs)) and release chemokines and cytokines that are secreted from M1 macrophages as part of the pro-inflammatory response [36,63,65,66]. After the “clean up” around the myocardium is completed, M1 macrophages extravasate and additional monocytes intravasate that are polarized to a M2 phenotype, which is considered the start of the anti-inflammatory phase response. Polarization to M2 macrophages results in the release of anti-inflammatory cytokines that promote the repair of myocardial tissues, inhibiting apoptosis, promoting angiogenesis and ECM production that helps with fibrotic scar formation [63]. While there are many cell types and organs involved in the immune response post MI, macrophages of the myocardium are the main contributors to the pro- and anti-inflammatory response [67,68]. Finding the correct balance between both inflammatory states is a challenge in itself, as a longer pro-inflammatory state can result in the death of healthy cardiomyocytes from cytokine stress causing an expansion of the infarct zone, while a protracted anti-inflammatory response can result in a large/more dense and stiff scar formation limiting the hearts contractile capacity [69].

Regulating the molecular mechanisms involved in remodelling after MI is a very complex process that is regulated by various pathways and signals. Determining ways in which we could improve remodelling and adaptation after MI could improve outcomes for patients’ long term. Therefore, considering a development pathway that is known to control cardiomyocyte growth/proliferation in development could aid in adaptive remodelling after MI in adult hearts.

## 1.4 Yap Signalling Pathway

The Hippo signalling pathway and its downstream signalling Yap kinase cascade are evolutionarily conserved pathways that are responsible for controlling organ size including the heart by regulating apoptosis and cell proliferation. The pathway was originally discovered in *Drosophila* over 20 years ago [70]. The core components of Yap signalling include mammalian serine/threonine protein kinases 1/2 (MST1/2), scaffold protein salvador homologue 1 (SAV1), large tumor suppressor homologue 1/2 (LATS1/2), MOB domain kinase activator 1 A/B (MOB1A/B) and the two transcriptional coactivators Yes-associated protein (YAP), and its paralog transcriptional coactivator with PDZ-binding motif (TAZ) [71,72]. The pathway can be regulated by various extrinsic factors that results in the phosphorylation of MST1/2, which phosphorylates LATS1/2 and MOB1 causing them to form a complex. Phosphorylation of LATS1/2 happens in two steps, the first being phosphorylation from MST1/2 in the hydrophobic motif at a conserved threonine residue that initiates autophosphorylation of LATS1/2 T-loop; both phosphorylations are required for LATS1/2 stimulation. Where SAV1 complexes with MST1/2 and acts as a scaffold protein by binding to it, SAV1 C-terminal domain and helps recruit LATS1/2 with the help of MOB1 [73,74]. More recently, the mitogen-activated protein kinase kinase kinase kinase (MAP4K) protein family have been implicated in activation of LATS1/2 without the involvement of SAV1 [75]. Once LATS1/2 has been phosphorylated, it subsequently phosphorylates YAP and TAZ. There are five key phosphorylation sites where LATS1/2 phosphorylates YAP [76]. Of the five, serine/threonine phosphorylation sites Ser127 and Ser397 play an important role in regulating YAP activity. When Yap is phosphorylated at Ser127 by LATS1/2 it forms a consensus site that allows for binding of 14-3-3 leading to cytoplasmic retention [77]. However, phosphorylation at Ser397 is believed to result in proteasomal degradation of YAP [78]. The phosphorylation of YAP and its paralog TAZ inhibits their transcriptional activity. However, when YAP and TAZ are dephosphorylated, they translocate into the nucleus where they bind to transcription factors, such as TEA domain family member 1-4 (TEAD 1-4) (Fig1.2). While there is evidence that YAP/TAZ bind to other transcription factors e.g., ERBB4, EGR-1, RUNXs, p73, CTNNB1, and SMADs [79], it predominately binds to TEAD 1-4. Since YAP/TAZ cannot bind to DNA itself, all transcription factors are DNA-binding allowing for the transcription of YAP-associated genes such as connective tissue growth factor (CTGF), cysteine-rich angiogenic

inducer 61 (CYR61 or CCN1) and C-C motif chemokine ligand 24 (CCL24).

#### 1.4.1 Regulation of the Yap Signalling

The Yap signalling cascade is affected by several intrinsic and extrinsic stimuli that initiate the phosphorylation (inhibition) or dephosphorylation (activation) of the downstream targets Yap/Taz [80]. Unlike other signalling pathways Yap is controlled by an ever-expanding web of mechanisms and factors instead of a singular ligand (Fig 1.3). The pathway can be regulated by mechanical cues, such as cell density, which has been implicated with preventing the translocation of Yap/Taz to the nucleus (inhibition of Yap) caused by cell-cell contact. Increased stiffness of the ECM has been linked to inducing the nuclear translocation (activation of Yap) and decreased stiffness favors the phosphorylation of Yap [81,82]. Additionally, stretching and/or shearing of cells has also been implicated with regulating Yap [80] by interaction with integrins that act on myosin and formins that stimulate F-actin. Stimulation of F-actin results in its bundling that acts on adaptor proteins to regulate translocation of Yap to the nucleus and subsequently its activation [80,83]. Many G protein coupled receptors (GPCRs) have also been identified as regulators of Yap signalling by acting through various G proteins consisting of  $G\alpha$ ,  $G\beta$ , and  $G\gamma$  subunits [74]. While Yap can be activated (unphosphorylated) by certain GPCRs stimulated by thrombin and lipoprotein a (LPA), it can be inactivated by other GPCRs such as ones involved with epinephrine and glucagon [84–87]. Additionally, stress signals play an important role in regulation. For example, oxidative stress caused by increased reactive oxygen species (ROS) activates neurofibromin 2 (NF2), which activates phosphorylated Mst1/2 that results in the inactivation of Yap [88]. Hypoxia on the other hand activates Yap by inhibiting Lats1/2 [89]. Osmotic stress and endoplasmic reticulum stress cause a biphasic response, initially both leading to activation of Yap acutely; however, this later leads to phosphorylation and inactivation [77,90,91]. While there are many other factors linked to Yap regulation, all mechanisms of regulation vary on cellular environment and cell type itself. Inflammation has been linked to increased Yap activity specifically in gut, but others suggest that inflammation leads to phosphorylation of Yap leaving it inactive [92].

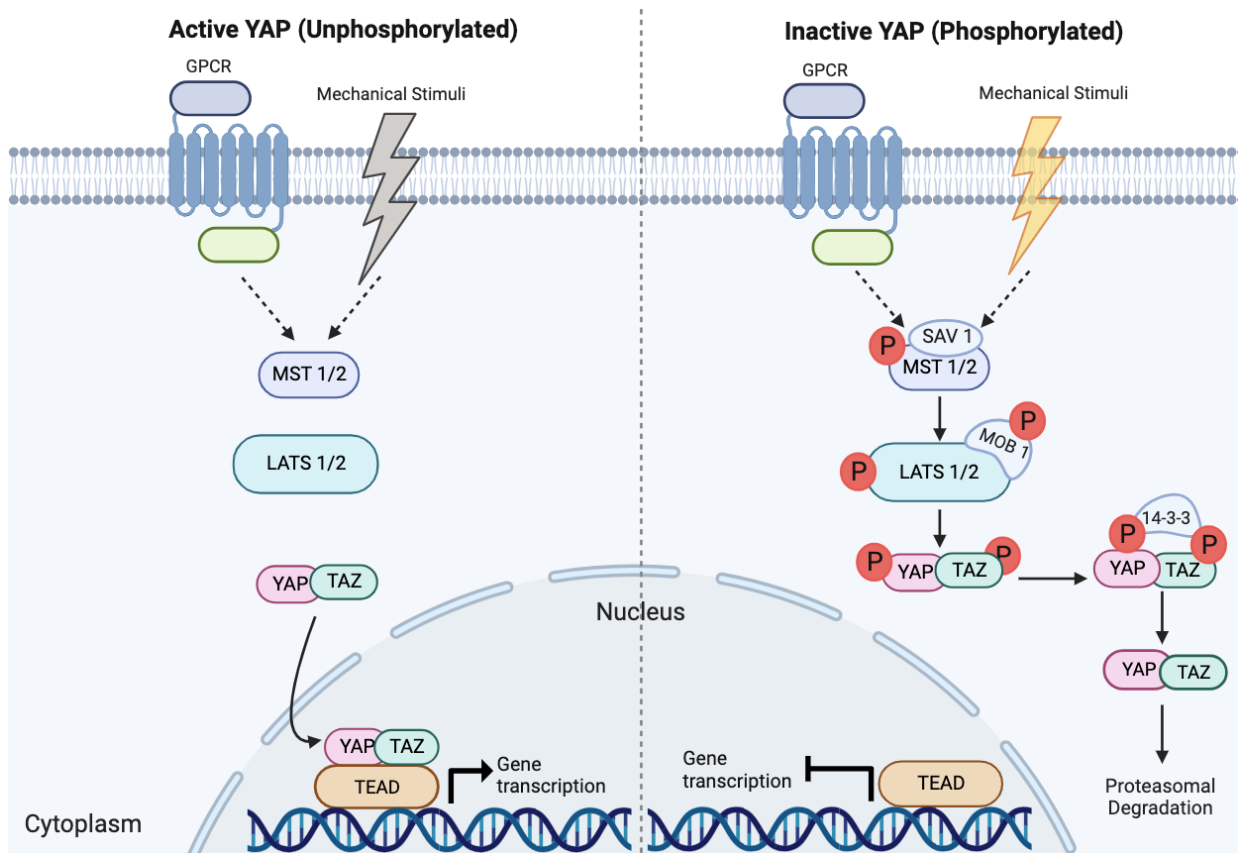


**Figure 1.2 Simplified Yap Signalling Pathway**

Yap signalling consist of two states, the first being active YAP, where stimulation from various stimuli results in the translocation of YAP into the nucleus which allows for binding to its transcription factor, predominately TEAD that leads to gene transcription. The second being inactive Yap where stimulation leads to phosphorylation of MST1/2 that results in the phosphorylation of LATS1/2 and MOB1 with help from its scaffold protein SAV1. Subsequently, LATS1/2 phosphorylates YAP at various sites which leads to cytoplasmic retention and in some cases causes proteasomal degradation.

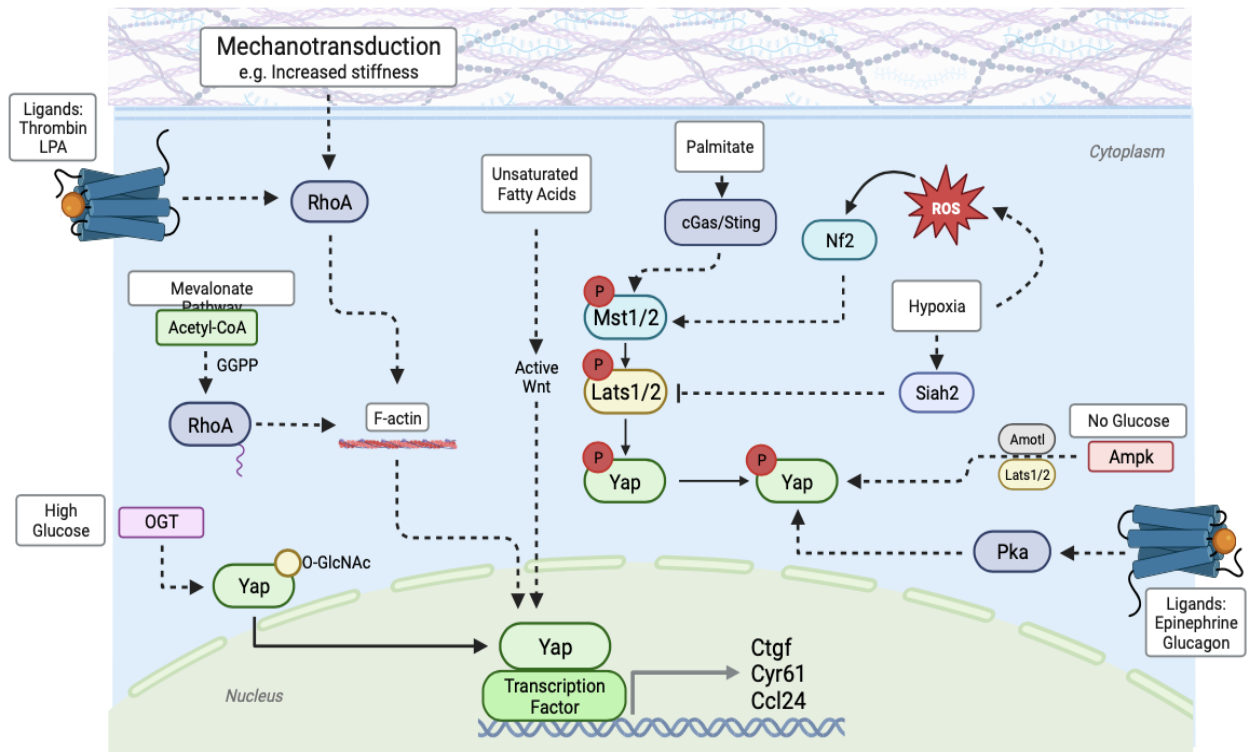


**Figure 1.3 Regulation of Yap Signalling**

Yap signalling can be regulated by various intrinsic and extrinsic factors. Mechanotransduction such as increased ECM stiffness, and/or stretching or shearing can activate Yap by acting on RhoA, which leads to bundling of f-actin causing translocation of Yap to the nucleus leading to transcription of Yap associated genes such as Ctgf, Cyr61 and Ccl24. The mevalonate pathway produces GGPP when Acetyl-CoA is converted, which leads to the prenylation of RhoA that also acts on f-actin to activate Yap. GPCRs that bind thrombin and LPA act through the same RhoA pathway as mechotransduction to activate Yap. Other GPCRs that bind epinephrine and glucagon act on Pka that causes phosphorylation of Yap leaving Yap inactive. High levels of glucose initiate OGT, which o-GlcNAcs Yap with the help of UDP-GlcNAc leading to its translocation and activation in the nucleus. While the absence of glucose activates Ampk that can directly or indirectly through Amotl or Lats1/2 cause phosphorylation and inhibition of Yap. Fatty acids such as palmitate act upon cGas and Sting to initiate phosphorylation of Mst1/2 leading to phosphorylation and inactivation of Yap. While unsaturated fatty acids active Wnt signalling to activate Yap. Oxidative stress caused by increased ROS production acts on Nf2 to phosphorylate Mst1/2 leading to inactivation of Yap. Hypoxia acts on Siah2 that leads to the inhibition of Lats1/2 phosphorylation, which dephosphorylates Yap allowing it to translocate and initiate transcription.



More recently, the role of nutrient sensing and metabolic pathways with Yap signalling have been explored [87]. The first being the mevalonate pathway which converts acetyl-coenzyme A to biochemical precursors of the isoprenoids including cholesterol, heme, steroid hormones, and bile acids [91,93]. The production of geranyl-geranyl-pyrophosphate (GGPP) from the mevalonate pathway results in RHO prenylation and membrane association [87] that results in inhibition of the phosphorylation of Yap leaving Yap active. Other nutrients considered to play a role in Yap regulation are fatty acids and glucose. Fatty acids such as palmitate can increase Mst1/2 activity resulting in the inhibition (phosphorylation) of Yap [94], while unsaturated fatty acids have been shown to activate Yap [91,95]. Levels of high glucose are associated with O-GlcNAcylation of Yap, leading to its activation [96], while removal of glucose resulted in Yap phosphorylation and inactivation [97]. This highlights the role of nutrients and metabolism in Yap regulation; however, like many of the other regulators, these mechanisms can vary dependent on cell types and environment, specifically since most research currently involving nutrients has been in the cancer field where metabolism is pathological.

#### 1.4.2 Yap Signalling in Cardiac Development

While much is known about the cell-extrinsic signalling involved in proliferation of cardiomyocytes during cardiac development, the cell-intrinsic mechanisms were less understood until about 10 years ago when Yap signalling was identified as a potential intrinsic mechanism [82]. Sav1 knockout mice had larger myocardial layers in their ventricles with no change in the size of the cardiomyocyte itself, suggesting increased proliferation of cardiomyocytes [82,98]. These results were confirmed using knockout models of various core components of the Yap signalling pathway.

Extrinsically, insulin-like growth factor (IGF), and Wingless-related integration site (WnT) growth factor signalling control proliferation of cardiomyocytes during cardiac development [99,100]. When Yap is unphosphorylated it enters the nucleus and allows for crosstalk with Wnt/ $\beta$ -catenin signalling pathway. Both Yap and  $\beta$ -catenin enter the nucleus and form a complex with themselves and their respective DNA-binding transcription factor TEAD and T cell factor/lymphoid enhancer factor (TCF/LEF) [98]. Once the complex is formed each

co-activator acts through its respective transcription factor to activate downstream proliferation-related genes. This suggests that activation of Yap signalling would promote the proliferation of cardiomyocytes by enhancing the interaction between YAP and Wnt/ $\beta$ -catenin [99]. Another signalling cascade that may mediate the Wnt and Yap signalling interaction is the IGF pathway. Increased IGF signalling in response to Yap- $\beta$ -catenin results in phosphorylation of protein kinase B (AKT) and glycogen synthase kinase 3 $\beta$  (GSK3 $\beta$ ) by phosphoinositide 3-kinase (PI3K). Phosphorylation of the GSK3 $\beta$  complex by Akt inactivates Gsk3 $\beta$ , which is responsible for the destruction of  $\beta$ -catenin, results in increased levels of  $\beta$ -catenin, which then interacts with YAP in the nucleus to promote cell proliferation through the Yap/  $\beta$ -catenin pathway [82,99,101].

#### 1.4.3 Yap Signalling in Cardiac Regeneration

Mammalian hearts unlike those of fish and amphibians lose their capacity to regenerate postnatally. The main reason for poor regenerative abilities in the adult heart is the inability of the heart to efficiently make new cardiomyocytes after injury. Because Yap signalling plays such an important role in the proliferation of cardiomyocytes in cardiac development, many have wondered what role it may play in the adult heart. Several studies have indicated that inhibiting Yap signalling in postnatal cardiomyocytes causes inhibition of cell-cycle re-entry, while activation leads to progression of cardiomyocytes from S phase, through mitosis and cytokinesis [102]. Studies also suggest that the exit of cardiomyocytes from the cell cycle as the heart ages causes a large decline in Yap activity. Thus, finding ways of manipulating the activation of YAP after cardiac injury in an adult heart has become of particular interest [82]. Studies have attempted to knockout Yap and/or Taz postnatally; however, it resulted in decreased cardiomyocyte proliferation and hypoplasia of the myocardium [3], while on the other hand overexpression of Yap initiated proliferation of cardiomyocytes [2,103]. Moreover, some studies have shown that inhibition of Yap leads to cardiac dysfunction and apoptosis, where others have shown that the activation of Yap was beneficial after MI, which was believed to be through the downregulation of pro-inflammatory cytokines [104]. Furthermore, active Yap is associated with reduced cardiac scar formation and improved cardiac function after MI, while inhibition was linked to exacerbated functional decline and the formation of thick scars, thus emphasizing the importance of Yap in homeostasis of adult cardiomyocytes

[82,99,102]. Much of these Yap effects may be age, time, or cell-dependent and should be interpreted with caution as they may have direct or indirect effects on cardiomyocytes and are not certain to be relevant to drivers of stress after MI.

## **1.5 Summary and Rationale**

MI is of large concern for our population as it affects nearly 805,000 people in the United States alone each year [105] and a comparable proportion in Canada. The reduced and/or stopped blood flow caused by MI results in ischemia in the myocardium that leads to the activation of numerous different molecular mechanisms, progressively with time after MI. While early diagnosis and treatment can limit damage, the loss of cardiomyocytes ultimately leads to heart failure for a large number of patients and MI remains a primary cause of heart failure. Heart failure is a lifelong condition which decreases an individual's quality of life. Because of the loss of regenerative capacity of cardiomyocytes in the adult heart, the human heart relies on many molecular mechanisms to compensate for the cardiac workload needed to sustain life. Although these mechanisms work together to effectively remodel the heart after injury to counteract the cell loss, they do not guarantee that the function of the heart will return to normal, and in most cases do not. Yap signalling plays an important role in the regulation of organ size and growth in cardiac development. More recently, Yap signalling has been explored in the adult heart after MI for regeneration or adaptive remodelling. However, the mechanisms remain undefined leading to our main research question: what are the molecular mechanisms in ischemic myocardium that regulate Yap signalling and why?

## **Chapter 2: Materials and Methods**

### **2.1 *In Silico* Microarray Analyses of Myocardial Infarction in Rats**

The Gene Expression Omnibus (GEO) created by the National Center for Biotechnology Information (NCBI) is a resource of high throughput datasets of research that are in compliance with NCBI's guidelines for Minimum Information About a Microarray Experiment (MIAME) [106]. Myocardial infarction (MI) related microarray data sets were found using the GEO. YAP associated gene expressions were investigated in the left ventricle (LV) of male Wistar rats that received either small, moderate, or large MIs by proximal left coronary artery ligation (Series Accession GDS4907). All expression was compared to sham animals who underwent the same surgery without ligation. Data is represented as relative mRNA (log<sub>2</sub>-transformed) [107].

### **2.2 Animal Care and Preclinical Models**

All experimental procedures and animal care were done in accordance with Canadian Council on Animal Care guidelines and approved by the University of Guelphs Animal Care Committee. Animals were provided with food and water *ad libitum* and maintained on a 12:12 hour light:dark cycle.

#### **2.2.1 Volume Overload Heart Failure (AMI)**

Acute myocardial infarction was achieved by permanent ligation of the left anterior descending coronary artery (LAD) in adult male C57BL/6 mice (8 weeks of age). Animals were anesthetized (2%:100% isoflurane:O<sub>2</sub>), intubated and ventilated (Harvard Apparatus) at 200 breaths/minute. Para-sternal thoracotomy was performed under sterile surgical conditions, next a 7-0 Surgipro™ II polypropylene suture (Covidien) was used to ligate the LAD below the atrioventricular border; confirmed with blanching of the wall below the ligation. The incision was closed by 7-0 Prolene™ (Covidien). The same operation was performed for Sham animals; but no ligation was performed. Post-surgery the animals were checked twice daily for any complications and provided with analgesia. AMI animals and respective shams were humanely harvested under anesthesia at 28 days post-injury.

## **2.3 Tissue Collection and Preparation**

Hearts were removed and flash frozen immediately in liquid nitrogen then stored at -80°C until use. Samples were ground using a porcelain mortar and pestle while submerged in liquid nitrogen. 10-15mg of sample in 120µl NP-40-based lysis buffer (1% NP-40) was homogenized for 30 seconds while on ice using a stainless-steel tissue homogenizer (Omni-International) then placed on ice for 30 minutes. Fresh lysis buffer was made by adding 10µL of phosphatase inhibitor (PHI) cocktail (524628, EMD millipore), 10 µL protease inhibitor (PI) (m250, VWR International) and activated sodium orthovanadate (Calbiochem) per 100µl of lysis buffer. Samples were centrifuged at 4°C for 2 minutes at 2000 rcf, and supernatant was transferred to a new 1.5mL tube, then centrifuged at 4°C for 30 minutes at 1200 rcf. Using a 28 ½-gauge insulin syringe (Becton Dickinson) the supernatant was transferred to a fresh 1.5mL tube.

### **2.3.1 Fixing Tissue and Sectioning**

Hearts were removed and flash frozen immediately in liquid nitrogen then stored at -80°C until use. Then the hearts were fixed using 1xPBS, 50mmol KCL and 10% neutral buffered formalin (VWR International) overnight. After being placed in a tissue cassette were dehydrated in 70,80, and 100% ethanol sequentially, cleared in Xylene, and infiltrated with paraffin wax using an automated tissue processor. Then samples were blocked using paraffin wax until hardened, positioned to allow from cross sectional cuts. Blocks were then sectioned at 4µm using a microtome.

## **2.4 Immunohistochemistry Chromogen Staining**

Paraffin sections were deparaffinized and rehydrated using xylene and xylene 2, along with 100%, 95%, and 70% ethanol. The sections were washed in tap water for 5 minutes and incubated in Tris-EDTA (pH 9) in a steamer for 15 minutes for the purpose of antigen retrieval. They were then incubated in BLOXALL (Vector Labs) Blocking Solution for 10 minutes. Sections were washed in 1XPBS for 5 minutes and incubated for 20 minutes with prediluted normal blocking serum (Vector Labs). The sections were incubated for 30 minutes with 60µl Yap/Taz primary antibody (8418, Cell Signaling Technologies); diluted (1:200) in a PBS-T/

bovine serum albumin (BSA) (1X PBS, 0.1% Tween 20, and 1% BSA solution). Sections were then washed in PBS for 5 minutes. Prediluted biotinylated secondary antibody (Horse Anti-Mouse/Rabbit IgG; VectorBioLabs) were incubated for 30 minutes. The sections were washed in PBS for 5 minutes and incubated for 30 minutes in R.T.U. VECTASTAIN Elite ABC Reagent (Vector Labs,). The sections were then washed for 5 minutes in PBS and stained with DAB Peroxidase Substrate Solution (Vector), for 3 minutes under the microscope. The sections were quickly rinsed in tap water, counterstained in Hematoxylin (Vector) for 1 minute, and washed in tap water for 5 minutes. Sections were dehydrated in reverse sequential ethanol and xylene solutions and then mounted using DPX Mountant for Histology (Sigma-Aldrich) and allowed to dry overnight.

## **2.5 Cell Culture**

H9c2 embryonic rat cardiomyoblasts from American Type Culture Collection (ATCC), were expanded from a cryostock, using pre-warmed plating media, Dulbecco's Modified Eagle Medium (DMEM; Gibco®) supplemented with 10% Fetal Bovine Serum (12483020; FBS, Gibco), on a 10cm culture plate in 37°C, 95% air, and 5% CO<sub>2</sub> incubation. The following day, media was aspirated off the plate; the cells were washed in 5mL of 1X Phosphate-Buffered Saline (PBS; VWR; CA45000-426) which was then aspirated and replaced with 10mL of fresh plating media. Cells were cultured to 80% confluency before next passage and did not surpass 18 passages from initiating cryostock. For experiments, cells were seeded at 500,000 cells/60mm plate.

### **2.5.1 Cell Treatments**

#### ***2.5.1.1 Serum Deprivation (Differentiation)***

H9c2 cells were differentiated to quiescent myotubes with the removal of FBS for 6 days, with media changes every 72 hours (DMEM-HG, no FBS). Cells were seeded at 500,000 cells/ 60mm plate before serum deprivation and experimentation began on day 6.

### *2.5.1.2 MI Stressors*

**Nutrient Deprivation:** A 10nM Hepes (Ambresco) was made in Earle's Balanced Salt Solution (EBSS, Gibco) followed by 60 minutes in the water bath sonicator. Solution was kept at 4°C for up to a year.

**Cytokine Stress:** Tumor necrosis factor alpha (TNF $\alpha$ ) was supplemented (20mg/mL) into DMEM and cells were placed in the incubator for 12 hours at in 37°C, 95% air, and 5% CO<sub>2</sub> before harvest.

**Mitophagic Stress:** Carbonyl cyanide-p-trifluoromethoxyphenylhydrazone (FCCP) [2 $\mu$ M] was made in DMEM and cells were treated for 12 hours in 37°C, 95% air, and 5% CO<sub>2</sub> incubation before harvest.

**Hypoxia:** Hypoxia experiments were carried out using a HERAcell 150.i CO<sub>2</sub> incubator (Thermo Scientific) that allows for adjustments in atmospheric O<sub>2</sub> and N<sub>2</sub>. Cells were incubated in DMEM at 1% O<sub>2</sub> for 24 hours before harvest.

**Oxidative Stress:** Hydrogen peroxide [450 $\mu$ M] was made in DMEM and cells were treated for 24 hours 37°C, 95% air, and 5% CO<sub>2</sub> incubation before harvest.

**Ischemia:** Cells were incubated at 1% O<sub>2</sub> in DMEM no glucose (11966025, Gibco) for 24 hours before harvest.

### *2.5.1.3 L-isoleucine Solution*

L-Isoleucine (105.0 mg/L) powder was added to our nutrient deprivation media, vortexed and water bath sonicated for 60 minutes. L-isoleucine solution was kept for up to a month at 4°C.

### *2.5.1.4 Palmitate*

20% Bovine serum albumin BSA was prepared by adding 25 $\mu$ l of DMEM-1X media to a 50mL tube (Falcon) in a biosafety cabinet. Media was warmed for 5 minutes in a 50°C rotor. 5g of BSA was added to the tube containing the media and centrifuged at 1,200xg for 5 minutes. The mixture was warmed for 5 minutes on the 50°C rotor and then transferred to another 50mL tube. 10X BSA Control was prepared by adding 10.8mL of 20% BSA to 1.2mL of 1X DMEM in the biosafety cabinet and sterile filtered using a 0.22 $\mu$ m syringe and filter

(VWR International). 10X BSA Control was stored at  $-80^{\circ}\text{C}$ . 5% sodium palmitate was prepared by adding 500mg of sodium-palmitate to 15mL of pre-warmed 1X DMEM media in a 50mL falcon tube. The tube was placed into a boiling water bath for 30 minutes and then vortexed to disperse the sodium palmitate. When the solution was clear, the falcon tube was removed from the water bath and aliquoted into 1.5mL tubes. 5% sodium palmitate was stored at  $-80^{\circ}\text{C}$ . To prepare 10X BSA-bound palmitate, frozen 5% sodium palmitate and 20% BSA aliquots were thawed in the thermocycler at  $75^{\circ}\text{C}$  for 5 minutes. The solutions were then sterile filtered (0.22um) in the biosafety cabinet. A 50mL tube was pre-warmed on the  $50^{\circ}\text{C}$  rotor, to which 9mL of 20% BSA and 1mL of sodium palmitate was added (Palmitate to BSA complexation ratio 1.5:1). The tube was vortexed between additions and then sterile filtered. The BSA-bound palmitate solution was aliquoted into 1mL aliquots and then stored at  $-80^{\circ}\text{C}$ .

#### *2.5.1.5 D-glucose*

50mL of nutrient deprivation solution was aliquoted to a 50mL falcon tube along with D-glucose powder to a final concentration of 4.5g/L. This D-glucose solution was then sterile-filtered through a 0.22um filter in the biosafety cabinet, added back to the remaining 450mL nutrient deprivation media, and stored in  $4^{\circ}\text{C}$ .

## **2.6 Resazurin Metabolic Assay**

PrestoBlue (Invitrogen) was used to determine metabolic activity. H9c2 cells were seeded to 15,000 cells/well with 100 $\mu\text{l}$  media/well. Following treatment, cells were rinsed twice with sterile 1X PBS and fresh media and treatments, along with 10 $\mu\text{l}$  10% PrestoBlue Cell Viability Reagent, was added to each well of the plate as per Invitrogen PrestoBlue instructions. The cells were incubated at  $37^{\circ}\text{C}$  for 1 hour. Fluorescence was measured using Synergy H4 Hybrid Reader (Biotek) with excitation (560nm) and emission (590nm) wavelengths. The 560/590nm control was subtracted from its respective treatment group when calculating metabolic activity.

## **2.7 Immunoblotting**

### **2.7.1 Cell Collection and Whole Cell Lysate Preparation**

Cells were harvested in a biosafety cabinet by aspirating off media, rinsing thoroughly with 600 $\mu\text{l}$  1X non-sterile PBS, and scraped in a NP-40 based lysis buffer (60 $\mu\text{l}$ /60mm plate)



containing 10µl of PI, PHI and sodium orthovanadate (Calbiochem) per 1000µl lysis buffer. Lysates were pipetted into 1.5mL tubes and stored at -80°C. The lysates were then sonicated on ice for 10 seconds at 20kHz and 30% amplitude using a QSonicator.

### 2.7.2 Nuclear and Cytoplasmic Protein Extraction

After serum deprivation protocol and 1 hour of respective treatment, media was aspirated off all plates and cells were washed in PBS for 1 minute. 45-60µl of hypotonic buffer (10mM Hepes, 10mM KCl, 0.1mM EDTA, 0.1mM EGTA, 1mM DTT at pH7.9) that is supplemented to a 1:100 ratio with PHI, PI, and sodium orthovanadate cocktails was added to the cells and plates were scraped, with lysates being collected into a 1.5mL tube (Eppendorf). The tubes were stored on ice for 20 minutes and were flicked to resuspend the lysates in 5-minute increments. The lysates were centrifuged at 20,000xg for 5 minutes and the supernatant was collected into a 1.5mL tube as Cytosolic. 120µl of hypotonic buffer was then added to the lysates which were resuspended by briefly flicking the tubes. The tubes were immediately centrifuged at 20,000xg for 5 minutes and supernatant was collected in a 1.5mL tube as Wash. 30µl of hypertonic buffer (20mM Hepes, 0.4M NaCl, 1mM EDTA, 1mM EGTA, 1mM DTT) supplemented to a 1:100 ratio with PHI, PI, and sodium orthovanadate cocktails was added to the lysates and tubes were placed on ice for 30-45 minutes while being flicked again in 5-minute increments. Lysates were centrifuged once more at 10,000xg for 5 minutes and supernatant was collected in a 1.5mL tube as Nuclear; then lysates were all stored at -80°C until further use.

### 2.7.3 Bicinchoninic Acid (BCA) Assay

Whole cell protein concentration was quantified using BCA protein assay kit (Thermo). Lysates were diluted 1 in 10 with ddH<sub>2</sub>O, 9µL sample with 81µL ddH<sub>2</sub>O. Diluted samples (25µl) were loaded in triplicate to a 96 well non-culture plate (82050-760, VWR) along with BSA standards (Invitrogen) (2000-0µg/ml) for standard curve. 200µl of BCA solution (Pierce) was added to each well and incubated at 50°C for 10-15 minutes. The plate was placed in a Synergy H4 Hybrid Reader at room temperature and the optical density (OD)/Absorbance at 562 nm was taken.

#### 2.7.4 Bradford Assay

Nuclear and cytoplasmic concentrations were quantified using Bradford reagent (Biorad), as chelating agents in the buffers are incompatible with BCA assays. Lysates were diluted 1 in 2 with ddH<sub>2</sub>O, 5µL of diluted samples were loaded in singlet to a 96 well non-culture plate (VWR International) with respective BSA standards (1000-0µg/ml), hypotonic buffer for cytosolic and hypertonic buffer for nuclear fraction. 250µL of room temperature 1X Bradford reagent (BioRad) was added to each well and incubated at room temperature for 5 minutes. The plate was placed in a Synergy H4 Hybrid Reader at room temperature and the optical density (OD)/Absorbance at 595 nm was taken.

#### 2.7.5 Western Blotting

Using the mean assay concentrations, samples were prepared with 4X SDS and 10% dithiothreitol (DTT) and boiled at 99°C for 5 minutes. The boiling samples were loaded, following 3µl Precision Plus Protein Standards Kaleidoscope™ ladder (BioRad), into a 3.5% 1X stacking gel causing separation by molecular size. They were resolved in a 10% Mini-Protean Gel. Running occurred at a constant voltage (90V) in 1X Tris/Glycine/SDS Electrophoresis Buffer (1610772; Biorad) and continued until the dye was propelled to the edge of the gel (approximately 1 hour 45 minutes). The samples were transferred to nitrocellulose membrane (0.2µM, 1620112; BioRad) at 100V and 4°C in 1X Tris/Glycine Transfer Buffer (1610771EDU; BioRad) for 75 minutes. After rinsing with ddH<sub>2</sub>O, the membranes were stained with Reversible Protein Stain (Thermo). The stained membranes were then labeled and imaged using the ChemiDoc MP Imaging System (BioRad). The stain was removed using Memcode Eraser (Thermo). Membranes were thoroughly rinsed in ddH<sub>2</sub>O and 1X Tris-Buffered-Saline-Tween 20 (TBST) and blocked in 5% skim-milk/1X TBST for 1 hour. Following blocking, membranes were incubated overnight at 4°C in primary antibody (1% skim-milk/1X TBST and 4% Sodium Azide) p-Yap S127 (1:1000, #13008, Cell Signaling), p-Yap S397 (1:1000, 13619, Cell Signaling) Yap/Taz (1:1000, 8418, Cell Signaling) Lamin A/C (1:1000, 2032, Cell Signaling Technologies), GAPDH (1:1000, TA802519, Origene), Cleaved Caspase 3 (1:1000, 9664, Cell Signaling Technologies), Caspase 3 (1:1000, 9662, Cell Signaling Technologies), Hmox1 (1:1000, H4535, Milipore Sigma). After membranes were washed thoroughly with TBST, they were then incubated in horseradish peroxidase-conjugated

secondary antibody anti-rabbit (1:1000-1:2000, 31460, Invitrogen) or anti-mouse (1:1000-1:2000, Biorad) with 5% milk for 2 hours at room temperature. Using Clarity Western ECL Substrate (1705060S; BioRad) Luminol/enhancer and Peroxide solutions, membranes were imaged with the ChemiDoc MP Imaging System (BioRad). The blots were stripped in 25mL of 0.5M Tris-HCl/SDS buffer, supplemented with 125 $\mu$ l  $\beta$ -mercaptoethanol for 45 minutes. The membranes were then blocked and reprobed.

#### 2.7.6 Densitometry

Densitometric calculations were performed using ImageLab Software v5.0 (BioRad). The density of the target protein was normalized to the total protein density, determined by the respective Memcode-stained lane, to find the relative integrated density.

### 2.8 Isolation and Measurement of Free Amino Acids

A cell pellet containing 1 million cells was suspended in 60  $\mu$ L of MilliQ water and 60 $\mu$ L of 2M perchloric acid (CA71007-908, VWR) with 120 $\mu$ L of internal standard (4  $\mu$ g/mL) containing arginine-d7, glycine-d5, lysine-d4, and leucine-d3 (made from: CDN Isotopes, D-7786, D-0277, D-2554, and D-1973 respectively) then vortexed and lysed using an ultrasonicator two times for 10 seconds. The protein was precipitated by repeating two minutes of sonication at room temperature followed by 5 minutes in an ice bath twice. Cells were then centrifuged at 4°C for 15 minutes at 13,000rpm and the supernatant was transferred to a clean tube and the cell pellet was washed with 60 $\mu$ L MilliQ water. Supernatant (150 $\mu$ L) was neutralized with 120-150 $\mu$ L of potassium hydroxide [2M] (CABH9262, VWR) then centrifuged at 13,000 rpm. Supernatant was transferred to a new tube and the extract was freeze dried for two to four hours, before being resuspended in 60 $\mu$ L of 50:50 Methanol: MilliQ water. Resuspended extract (10 $\mu$ L) was transferred to an autosampler vial and combined with 70  $\mu$ L of Borate Buffer (186003836, Waters) for 5 minutes as per the Waters AccQTag Derivatization Kit. Samples were vortexed then 20 $\mu$ L AccQTag Derivatization Agent (186003836, Waters) was added followed by another vortex and left to sit for one minute before being placed in the heating block at 55°C for 10 minutes then vortexed to remove any air bubbles. Samples were run using the Waters Acquity ultra-performance liquid chromatography

(UPLC), Xevo-TQS-micro-Tandem Mass Spectrometer using Multiple Reaction monitoring for each BCAA with respective internal standards. Quantification was done using TargetLynx (Waters) software, and samples were corrected by milligrams of protein and quality control blank and spike blanks were run.

## **2.9 Quantitative Polymerase Chain Reaction (qPCR)**

### **2.9.1 Extraction of RNA from Tissue**

Ambion TRIzol (1mL) reagent (Life Technologies) was added to a 2mL analyzer tube for every 50-100mg of tissue. Samples were removed from liquid nitrogen and placed in analyzer tube which are pre-filled with homogenizer beads and left to incubate for 10 minutes. After incubation, the tube was placed into the MP TissueLyser, and appropriate tissue program was run. Then samples were centrifuged for 10 minutes at 12,000xg. Supernatant was transferred to a fresh 1.5mL tube and samples were left for 5 minutes at room temperature to incubate. For every 1mL of TRIzol, 200uL of chloroform was added to each sample tube, then vortexed for 10-15 seconds followed by a 15-minute incubation at room temperature. Lastly, samples were centrifuged at 12,000xg again for 15 minutes and the top upper phase (clear) which contains the RNA was moved to another clean 1.5mL tube and stored at -80°C until use.

### **2.9.2 RNA Isolation from H9c2 Cells**

In the biosafety cabinet, cells were harvested using 600µL lysis buffer from the Qiagen RNeasy Mini kit with 6µL β-mercaptoethanol for each plate. Lysate was scraped using a cell scraper then collected and placed into a clean labelled 1.5mL Eppendorf tube. Samples were stored at -80°C until use. 500µL of ethanol was added to each thawed sample and briefly inverted to mix. 700µl of the sample was added onto a Qiagen spin column (RNeasy Kit, Qiagen), which was then centrifuged at 12000xg for 30 seconds. This was repeated until the entire sample had been transferred to the column tube and centrifuged. All flow-through was discarded. 350µl of Wash Buffer RW1 was added to the column and it was centrifuged at 12000xg for 30 seconds. The flow-through was discarded. 10µl DNase 1 stock solution was added to 70µl RDD Buffer, mixed gently, and 80µl was added directly onto the spin column membrane. The samples were left for 15 minutes at room temperature. 350µl of Wash Buffer RW1 was added onto the spin column and it was centrifuged at 12000xg for 1 minute. The spin

column was then transferred to a new 2mL collection tube and washed with 500µl of RPE Buffer. The sample was centrifuged at 12000xg for 1 minute and flow-through was discarded. The spin column was washed again with 500µl of RPE Buffer and centrifuged twice at 12000xg for 1 minute. The spin column was then transferred to a new 1.5mL collection tube. 30-50µl of RNase-free H<sub>2</sub>O was added to the spin column and left to incubate for 1 minute at room temperature. The sample was centrifuged at 12000xg for 1 minute. The flow-through was pipetted back into the spin column and left to incubate for 2 minutes. The tube was centrifuged at 12000xg for 1 minute. The RNA was stored at -80°C until use.

### 2.9.3 Complementary DNA (cDNA) Synthesis

A 20µl cDNA reaction mixture, prepared by loading the sample-specific volume equivalency of 4µg RNA and topped up to the 20µl volume with Nuclease-free H<sub>2</sub>O, was loaded into RNase/DNase-free strip-tubes along with 20µl 2X Master Mix. One tube was designated No RT where Reverse Transcriptase was left out of the Master Mix. The reaction mixture was centrifuged (<1 minute) and then incubated in the Mastercycler Nexus Gradient Thermocycler (Eppendorf) at 25°C for 10 minutes, 37°C for 120 minutes, 85°C for 5 minutes and then held at 4°C and cDNA was stored at -80°C.

### 2.9.4 SYBRGreen Quantitative Polymerase Chain Reaction (qPCR)

Primer-pairs (Table 1) were designed using OLIGO Primer Analysis Software V6.31 (Molecular Biology Insights, Inc.). For each primer set, a qPCR Master Mix, consisting of 5µl Platinum SYBR Green qPCR Supermix-UDG (Invitrogen), 0.2µl 10mM forward primer, 0.2µl 10mM reverse primer, 0.02µl ROX reference dye, and 2.58µl Nuclease-free H<sub>2</sub>O, and then

**Table 1. Primer Sequences and Annealing Temperatures of Oligonucleotides used in qPCR**

Target		Primer Sequence (5'-3')
RtAng2	F1	TCAGCACTATGATGCCAAGCC
	R1	TTGATGCTGCCCTTATTGCCAT
RtAnkrd1	F1	GGCCAGCTCCAGGGGTTTCAGC

	R1	GCTGAACCCCTGGAGCTGGCC
<u>RtBirc5</u>	F1	TTCCTTACAGTCAAGAAGCAGGT
	R1	TTCTTGGCTCTTTGTTTGTCCA
<u>RtB2m</u>	F1	ACATCCTGGCTCACATGAA
	R1	ATGTCTTCGGTCCCAGGTG
<u>RtCcl24</u>	F1	CTCTAAGAAGCAGTTCAAGGCTA
	R1	ACCTCAAATTTTCTATGTGGCTA
<u>RtCtgf</u>	F1	CGCTGACATTCTGATTCCAGT
	R1	CTGATCCATTGCTTTACCGTCT
<u>RtCyr61</u>	F1	CCCTTGAGGCTACTACCTG
	R1	ATTACATTTCCCCATCCCTCC
<u>RtFgf21</u>	F1	CACAGCACACCGCAGTCCA
	R1	AGAAACCTAGAGGCTTTGACACC
<u>RtGapdh</u>	F1	GGCCGAAGGGCCCACTA
	R1	TGTTGAAGTCACAGGAGACAACCT
<u>RtGdf15</u>	F1	AACTCAGAACCAACCCCTGACC
	R1	GACCCCAATCGCACCTCTGGAC
<u>RtHprt1</u>	F1	CCCAGCGTCGTGATTAGTGATG
	R1	TTCAGTCCTGTCCATAATCAGTC
<u>RtIgf2bp3</u>	F1	ATCCCCTTGAAGATTTTAGCTC
	R1	ATTTTAGTGTCCGTGTCTTGC
<u>RtLamb1</u>	F1	ACAGATACTTCGCCTACGACT
	R1	CACATTCGCTGGCATGACC
<u>RtMlc2</u>	F1	TCAAAGTCTGTTCCGTCCCT
	R1	AACTTGGCGTCCATAATTGCT

<u>RtNppa</u>	F1	CGGACAAAGGCTGAGAGAGAA
	R1	TTCTCTCTCAGCCTTTGTCCG
<u>RtPkm2</u>	F1	AATGCAGGATTGGAAACCCTC
	R1	AGATAATGCTGCCCTTCTGTGA
<u>RtU6</u>	F1	GCTTCGGCAGCACATATACTAA
	R1	AACGCTTCACGAATTTGCGT
<u>RtVegf<math>\alpha</math></u>	F1	TGGTGCTACTGTTTATCCGTA
	R1	ATTATCTCGGAAAACCTGCTCT
<u>Rt<math>\beta</math>-actin</u>	F1	CGAGTACAACCTTCTTGCAGC
	R1	ACCCATACCCACCATCACAC
<u>Rt18s</u>	F1	GAGCTGGAATTACCGCGGCT
	R1	AAACGGCTACCACATCCAAG

pooled into a 1.5mL Micro Centrifuge tube (Eppendorf). The mixture was briefly vortexed and then split in equal volume and loaded into a strip-tube; 8 $\mu$ l of the Master Mix was pipetted from each tube into a 96-well qPCR plate. 2 $\mu$ l cDNA was added to rows A-G of the plate; row H served as a no-template control (NTC) containing master mixture only. The qPCR plate was sealed and centrifuged at 2500 rpm for 3 minutes. The reaction mixture was incubated at 50°C for 120s, 95°C for 120s, and 35-40 cycles of incubation at 95°C for 3s and 60°C for 30s (Applied Biosystems Viia 7).

### 2.9.5 qPCR Gradient

For each primer set, 5 $\mu$ l of previously synthesized cDNA was pooled and pipetted into a tube in a RNase/DNase-free strip-tube along with a PCR Master Mix containing 17.495 $\mu$ l RNase-free H<sub>2</sub>O, 37.55 $\mu$ l Platinum SYBR Green qPCR Supermix-UDG (Invitrogen), 7.5 $\mu$ l of 10mM forward and reverse primers, and 0.15 $\mu$ l ROX reference dye. The strip-tube containing this reaction mixture was centrifuged (<1 minute) and then incubated in the Mastercycler

Nexus Gradient Thermocycler (Eppendorf) at 50°C for 2 minutes, 95°C for 2 minutes, 35 cycles of 95°C for 15 seconds and 60°C for 30 seconds, and 60°C for 1 minute. An initial testing of qPCR primers was performed by making a 40µl dilution series (1:10) using the PCR product, to visualize where CT values fall in the measurable range. 2µl of this diluted reaction mixture containing cDNA was added to a qPCR plate along with 8µl qPCR Master Mix. A no-template control containing only master mixture was present for each plated primer set. The qPCR plate was sealed and centrifuged at 2500 rpm for 3 minutes to remove air bubbles. Once all air bubbles were removed the plate was placed on the thermocycler for qPCR, 50°C for 120s, 95°C for 120s, and 35-40 cycles of incubation at 95°C for 3s and 60°C for 30s (Applied Biosystems Viia 7).

#### 2.9.6 Primer Validation - Agarose DNA Electrophoresis

A 2% Agarose Gel was prepared by adding 150mL 1X 40mM Tris-acetate-1mM EDTA (TAE) and 3g Agarose to an Erlenmeyer flask. The mixture was heated in a microwave in 45 second intervals, swirling in between, until it was boiling and in solution. The flask was then briefly cooled under tap water. 1µl SYBR™ Safe DNA Gel Stain (Invitrogen) was added to the flask for each mL of molten agarose (15µl SYBR Safe:150mL agarose). The contents of the flask were then poured into the gel tray in the casting apparatus. Air bubbles were removed from the gel. The agarose was left to set at room temperature for 20 minutes. Once the gel had solidified, the comb was removed, and the tray was placed into the gel box. 10µl samples and ladder were mixed with 1.6µl bromophenol blue loading dye and loaded into the wells of the gel. 1X TAE running buffer was added to the gel box, covering the surface of the gel. Running occurred at 120V and continued until the dye front from loading dye had migrated two-thirds of the way through the gel (approximately 1 hour 20 mins). The gel was then removed from the box and loaded into the ChemiDoc MP Imaging System (BioRad) where it was imaged. Primers were validated by the presence of a singular band and by confirmation of molecular weight using ladder.

#### 2.10 Immunocytochemistry

H9c2 cells were seeded at 600,000/plate on a glass coverslip in a 60mm dish and were differentiated using the protocol from section 2.5.1.1. Once the cells were differentiated, they



were treated with nutrient deprivation media for one hour followed by being washed with PBS and fixed with warmed formaldehyde (4% in PBS) for 5 minutes. Then washed three times with ice-cold PBS before being permeabilized in 0.1% Triton-X-100 for 15 mins, followed by another three rounds of washes with ice cold PBS. Followed by being blocked using a 1% BSA in 1XPBS 0.1% Tween 20 solution for 15 minutes. After another wash cells were incubated and protected from light in AlexaFluor 488 Phalloidin (Thermo Scientific) stain diluted 1:1000 in 1XPBS for 30 minutes, followed by a wash and incubation in primary antibodies diluted 1:400 at 4°C for 24 hours. After another wash cells were incubated in a fluorophore-conjugated secondary antibody (Alexa Fluor 647 donkey-anti-rabbit) diluted 1:400 for 30 minutes at room temperature. Cells were washed again then stained with Hoechst 33342 which was diluted 1:3000 in 1XPBS for 1 minute at room temperature followed by a final wash before the coverslip was mounted on to a glass slide using a 1:1 glycerol and PBS and shealed using clear nail polish around the coverslip edges and allowed to dry overnight at 4°C before being imaged.

## **2.11 Statistical Analysis**

Results are representative of mean  $\pm$  standard deviation unless otherwise specified. All statistical analysis were done using GraphPad Prism 9 (GraphPad Software Inc.). A pairwise comparisons that involve two groups was determined using a Student's two-tail t-Test. For results that included three or more groups were analyzed using one-way or two-way analysis of variance (ANOVA). Statistical significances between groups were measured by Tukey's post-hoc test. P-values lower than 0.05 were considered statistically significant.

## **Chapter 3: Results**

### **3.1 Yap Signalling in Mice After Myocardial Infarction**

To determine the effect of MI on Yap levels in the heart we performed immunohistochemistry on 28-day post-MI mouse hearts compared to sham. Positive Yap-staining was observed compared to negative control (secondary antibody control) using Zeiss Observer. Z1 (Fig.3.1). To determine where Yap was localized, we used a Panoramic MIDI slide scanner and found that Yap-staining was elevated in post-MI tissue; most noticeably in the peri-infarct zone (Fig.3.2A/B) and to a lesser extent in the left ventricular wall (Fig.3.2C) and comparatively no discernible differences in the remote region of the right ventricle (Fig.3.2D). The elevation in Yap levels in the peri-infarct region was detectable by western blot as early as 1-week post-MI when inflammatory remodeling due to ischemic injury is dominant (Fig.3.2II). The peri-infarct but not the infarct showed significantly higher Yap level, suggesting cellularity and time are relevant to molecular drivers of Yap levels. Taz levels did not change compared to sham in either the infarct or peri-infarct zone (Fig.3.2II). The increase in Yap levels occurs in early and late remodeling stages and is consistently elevated in the peri-infarct zone predominated by stressed cardiomyocytes adapting to volume overload and ischemic injury.

### **3.2 Effects of Ischemic Stressors on Yap Signalling in H9c2 Rat Cardiomyotubes**

To clarify the role of Yap in cardiomyocyte-like cells from specific stimuli encountered during MI, we screened salient forms of stress drivers that are independent of mechanical load typically associated with Yap levels. Firstly, we compared differentiated to proliferative H9c2 cells, where we determined that Yap levels were increased in differentiated cells compared to proliferative (Fig. 3.3-I). However, there were no changes in Yap levels between differentiated cells and all other ischemic stressors/stimuli conditions. All stimuli conditions were compared to the differentiated state, which is the primary state of cardiomyocytes in a developed heart, and all stimuli were tested on differentiated cells. Since phosphorylation plays an important role in Yap signalling, we examined one of the major Yap phosphorylation sites (p-S397) in our conditions.

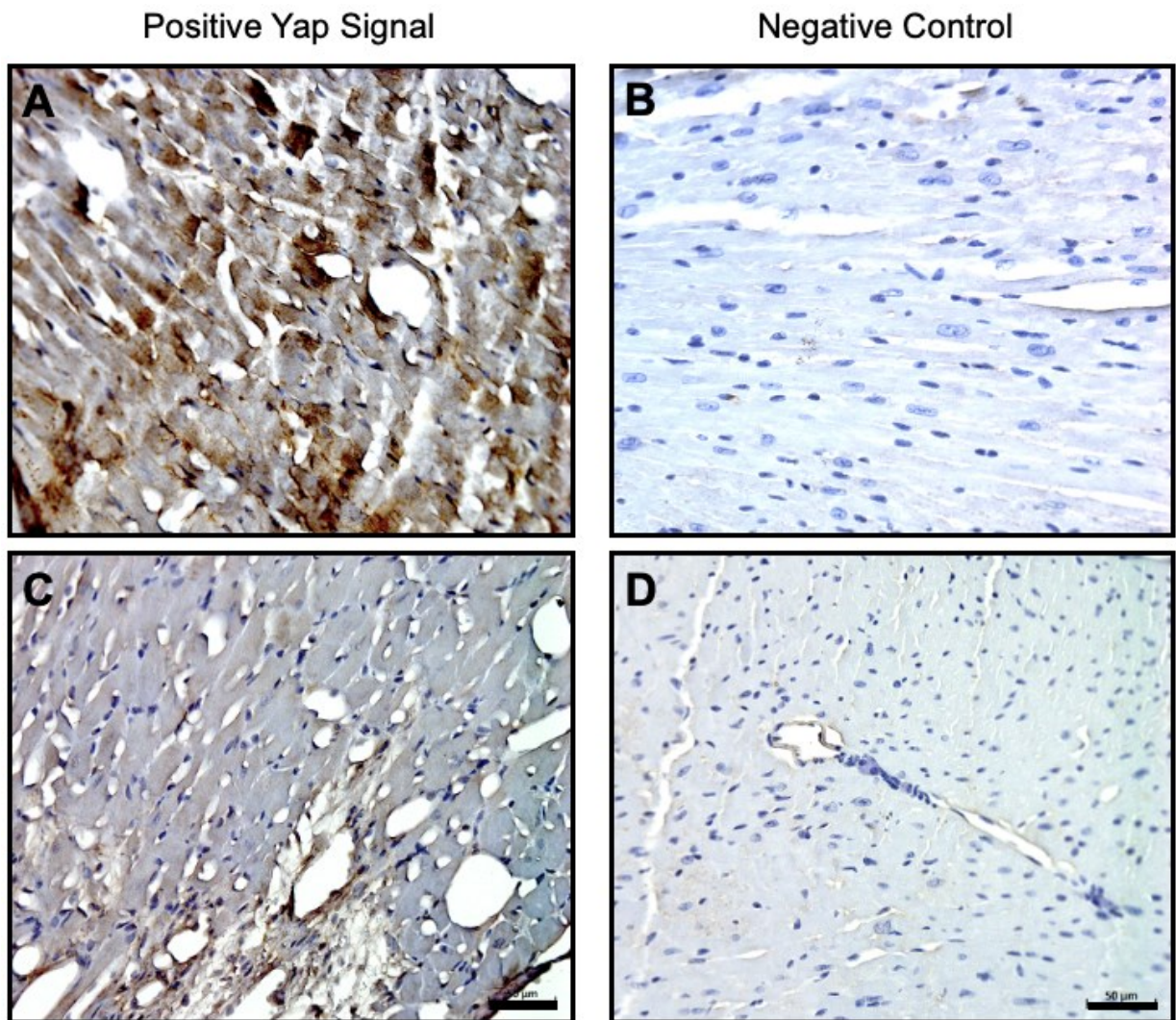


**Figure 3.1: Positive Yap Signalling 28-day Post MI in Mice**

Yap immunohistochemistry using 28-day post MI mouse tissue visualized using Zeiss Observer. Z1 microscope. Positive Yap signal seen by the brown staining (**A, C**) compared to secondary antibody only negative control (**B, D**) at 20x. Scale bars demonstrate 50µm.

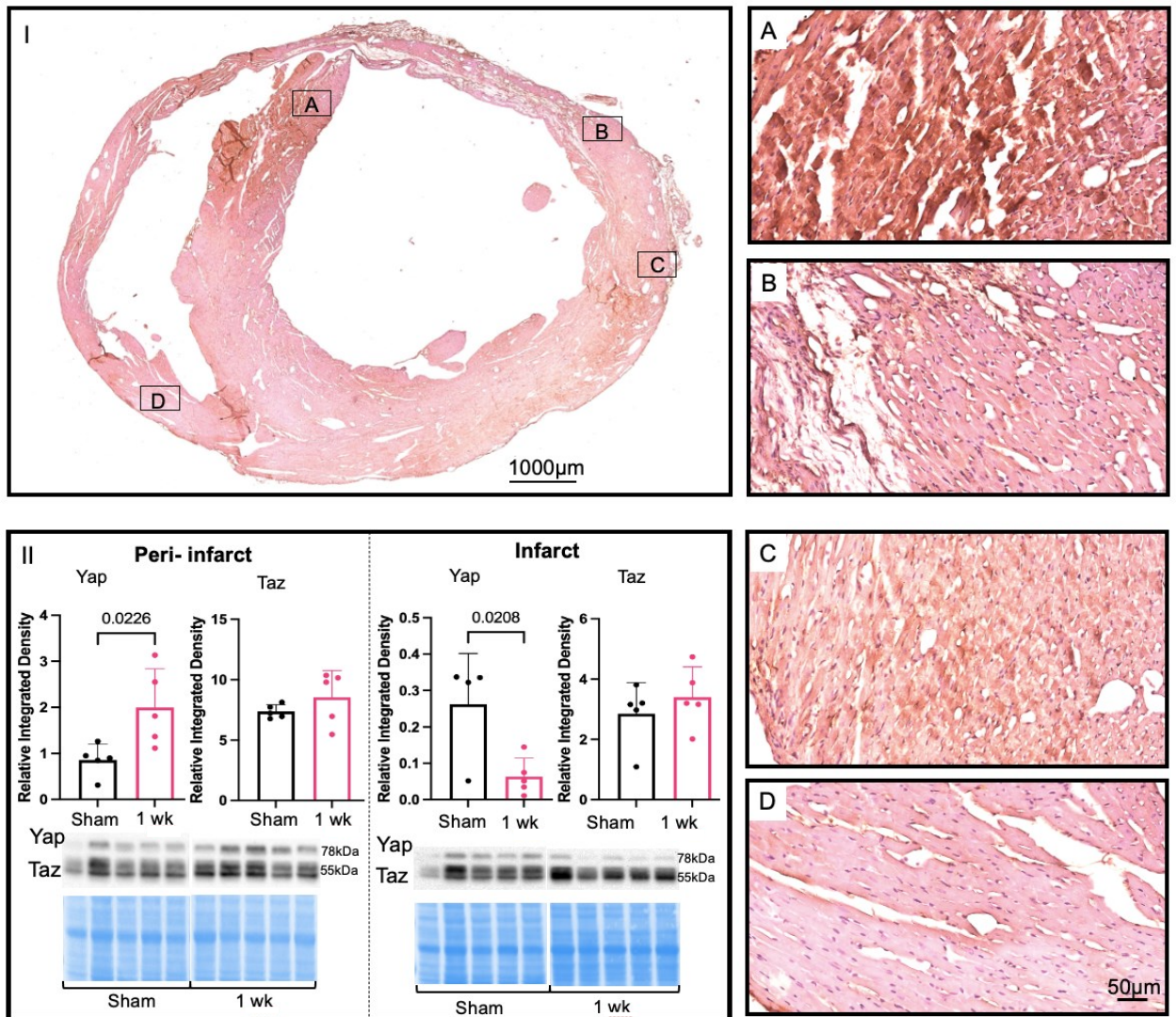


**Figure 3.2: Increase in peri-infarct Yap Levels after MI.**

**(I)** Yap immunohistochemistry of a 28-day post MI mouse heart scanned using a Panoramic MIDI slide scanner at 43x and viewed at 1.3x. Peri-infarct zone **(A-C)** had higher Yap expression seen by the brown positive Yap signal, compared to remote region **(D)** mostly pink and controls (not shown) observed at 25x. **(II)** Yap expression was increased in the peri-infarct zone and decreased in the infarct zone of 1 week post MI mice compared to shams. Immunoblot and densitometric analysis of Yap and Taz peri-infarct and infarct zone of sham compared to 1 week post MI mice.

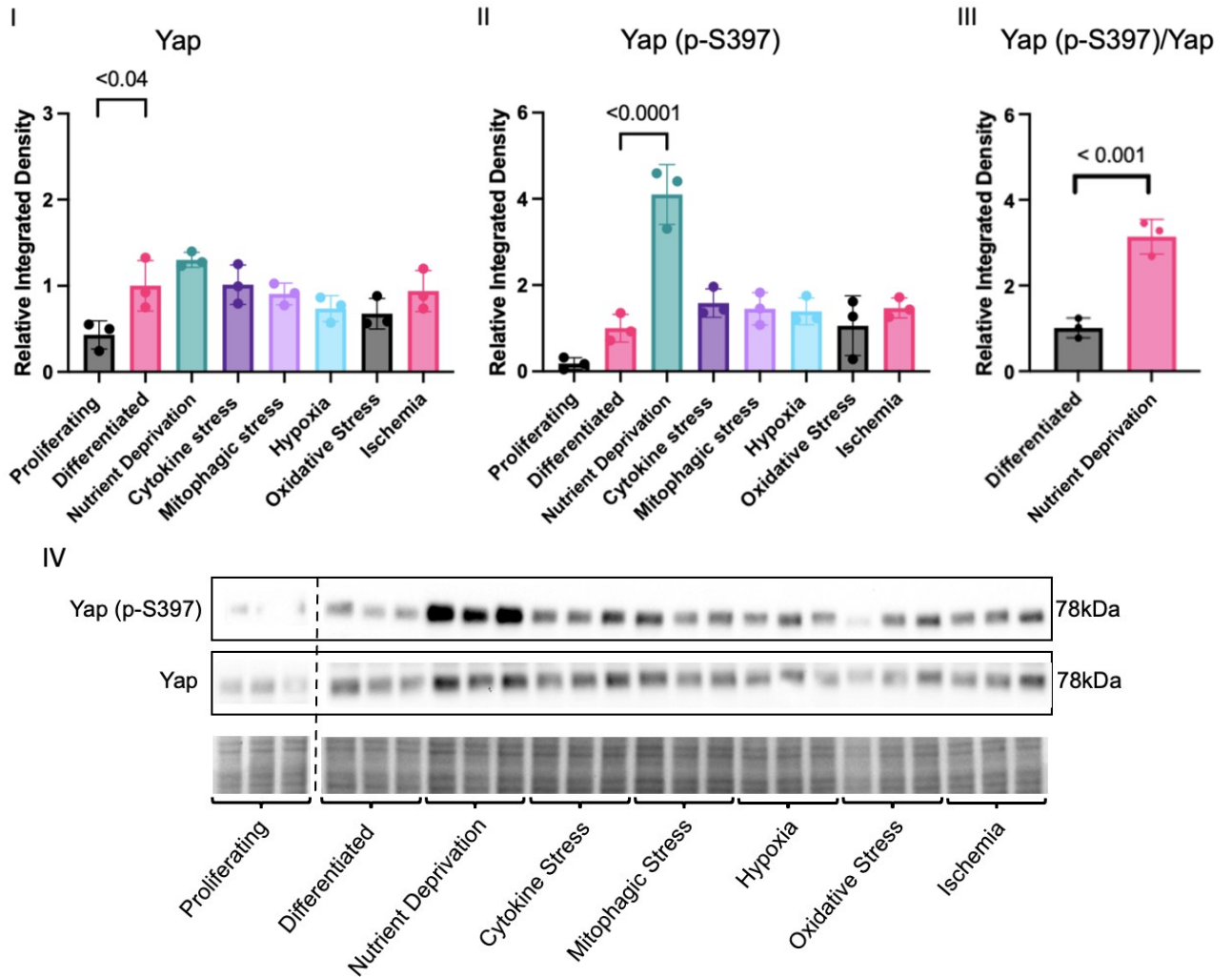


**Figure 3.3: Screen of ischemic stressors experienced during an MI effect on Yap signalling.**

**(I)** Analysis of Yap in screen of proliferating (DMEM+10% FBS), differentiated (DMEM), nutrient deprivation (EBSS, 1h), cytokine stress (TNF $\alpha$  20ng/mL, 12h), mitophagic stress (FCCP 2 $\mu$ M, 12h), hypoxia (O $_2$  1%, 24h), oxidative stress (H $_2$ O $_2$  450 $\mu$ M, 24h), ischemia (O $_2$  1%, + 0% glucose, 24h) in H9c2 cells where expression was increased in differentiated cells compared to proliferating. **(II)** Yap (p-S397) was significantly increased under nutrient deprivation conditions compared to all other ischemic stressors. **(III)** Significant increase in ratioed Yap (p-S397) to total Yap in nutrient deprivation conditions. **(IV)** Corresponding relative blots and Pierce® Memcode to demonstrate uniform loading.

We determined that while Yap (p-S397) phosphorylation in the presence of other ischemic stressors did not change compared to proliferative or differentiated cells, the nutrient deprivation condition (acute) significantly increased Yap (p-S397) phosphorylation compared to differentiated and proliferative H9c2 (Fig3.3II). This increase was confirmed by ratio of the Yap (p-S397) to total Yap levels (3.3III). This suggests that though there are various stimuli associated with MI, deprivation of essential nutrients has the greatest impact on Yap phosphorylation.

There are many phosphorylation sites involved in the Yap signalling cascade, which ultimately determine the degradation or intracellular localization of the protein; either Yap transactivation (de-phosphorylated) or Yap cytoplasmic retention and/or degradation (phosphorylated). Based on the increased levels observed in nutrient deprivation conditions at Yap serine 397 we wanted to validate our previous findings and determine whether the same effects were seen at important another phosphorylation site, Yap (p-S127). There were no changes in total Yap levels (Fig3.4I) with the increased Yap (p-S397) as expected (Fig3.4II), in addition to an increase in Yap (p-S127) under nutrient deprivation conditions compared to control (DMEM)-treated H9c2 cells (Fig3.4III). Collectively, these results demonstrate that Yap phosphorylation is sensitive to acute nutrient deprived conditions.

To investigate whether the acute nutrient deprivation of the nutrient deprivation conditions impacted cellular stress and cell death, particularly, apoptosis cleaved and total caspase 3 were measured as late apoptosis markers and Hmox1 as an early marker of cellular stress. No significant difference between DMEM controls and nutrient deprivation were observed in cleaved or total caspase-3 levels (Fig3.5I-III) and Hmox1 levels was also unchanged between DMEM controls and nutrient deprivation conditions (Fig3.5IV). Together this confirms no apoptosis or signs of cell stress after one hour of nutrient deprivation occurs, which is not unexpected in a short timeframe.

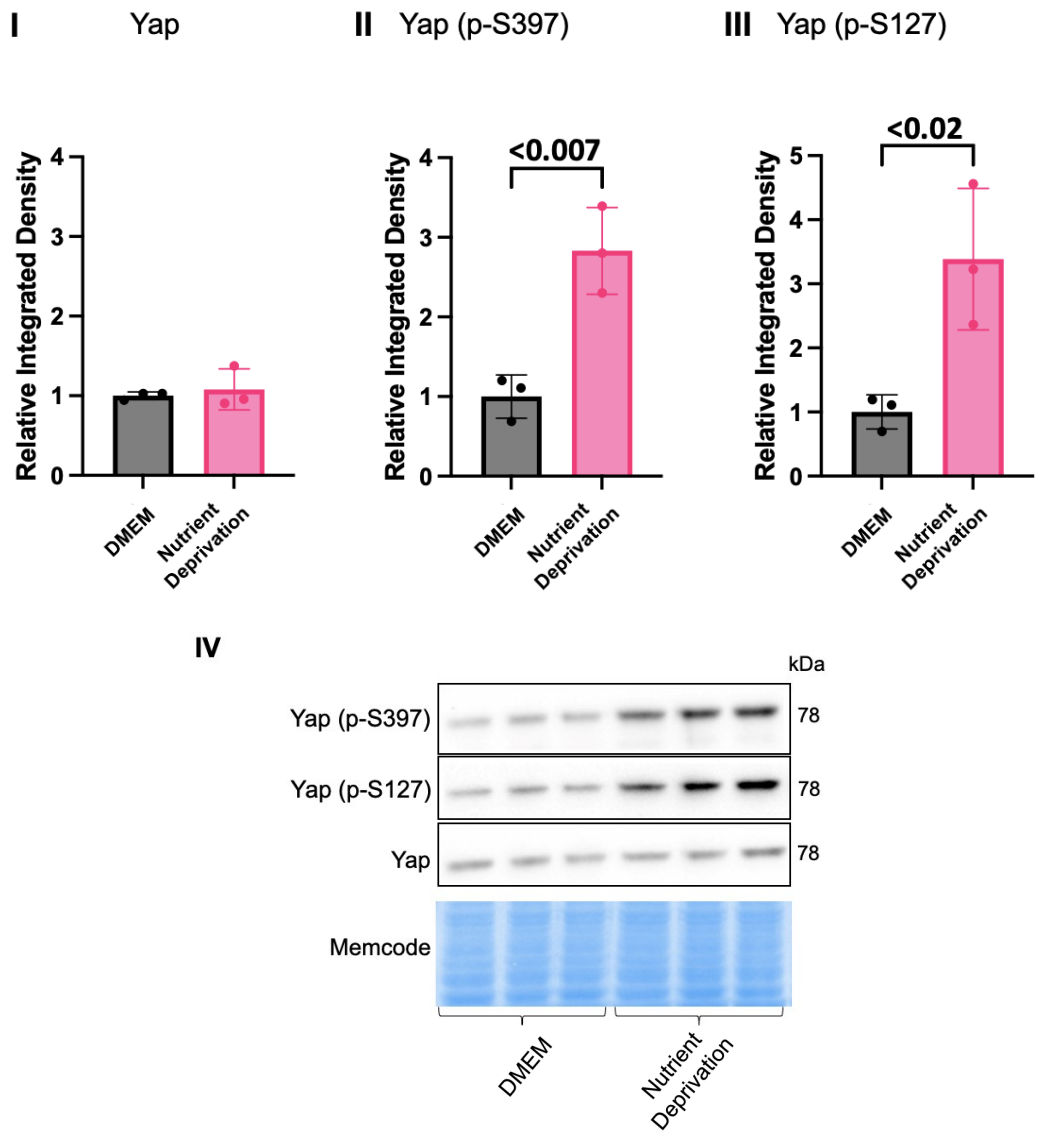


**Figure 3.4: Increased Phosphorylation at Two Key Sites in Nutrient Deprivation Conditions**

H9c2 cells were differentiated for 6 days in the absence of FBS, on the day of the experiment controls received a media change and our treatment groups received nutrient deprivation solution for 1 hour before harvest. (I) Yap expression was unchanged compared to controls. (II) Yap (p-S397) was significantly increased in nutrient deprivation conditions compared to controls. (III) Yap (p-S127) was also significantly increased under nutrient deprivation conditions compared to controls. (IV) Representative Yap, Yap (p-S397), and Yap (p-S127) blots with respective Pierce® Memcode stain demonstrating uniform protein loading.





### **3.3 Yap Signalling Related Protein Levels Changes in Sub-Cellular Fractionation**

To investigate whether the translocation of Yap or phospho-Yap was affected by nutrient deprivation, we first used immunocytochemistry with Phalloidin to stain f-actin on the cellular membrane (green), Hoechst to stain the nucleus (red) and Yap fluorescence antibody (red). There were no changes in total Yap levels and little evidence of translocation to the nuclei (Fig3.6I). However, both Yap (p-S397) and Yap (p-S127) appeared to cluster proximally to, and colocalize in, the nuclei in nutrient deprivation conditions compared to controls (Fig3.6II-III). This can be confirmed by the speckling and purplish color of nuclei (blue) and Yap antibody (red) overlap in nutrient deprivation compared to controls. This suggests that nutrient deprivation conditions likely cause Yap (p-S397) and Yap (p-S127) to translocate to the nucleus.

To confirm changes in translocation patterns of Yap and phospho-Yap, we performed nuclear and cytoplasmic fractionation of H9c2 myotubules. In agreement with the immunocytochemistry results (Fig.3.6), there were no changes in total Yap levels in either the nuclear or cytoplasmic fractions compared to DMEM controls (Fig3.7I, IV). Yet, cytoplasmic Yap (p-S397) was increased compared to controls (Fig.3.7II), with no change in the Yap (p-S127) cytoplasmic fraction in nutrient deprivation conditions (Fig.3.7III). There was an increase in both Yap (p-S397) and Yap (p-S127) levels in the nuclear fraction in nutrient deprivation conditions compared to controls (Fig.3.7V-VI). To confirm a clean separation of prepared cytoplasm and nucleus protein fractions glyceraldehyde 3-phosphate dehydrogenase (GAPDH) and Lamin A/C levels, respectively were used to confirm compartmentation (Fig.3.7VII). Collectively, these changes in sub-cellular fractions indicate that translocation patterns of Yap signalling are sensitive to acute nutrient deprivation.

### **3.4 The Effect of Fatty acids and Glucose on Yap Signalling Protein Levels**

Nutrient deprivation is an acute state, meaning that the cells are deprived of three macro essential nutrients: amino acids, glucose, and fatty acids (Fig.3.8) for one hour. To determine which of the three major components is responsible for the changes in phosphorylated Yap in nutrient deprivation compared to controls. Firstly, from figure 3.3 we determined that there were no changes in Yap (p-S397) levels between

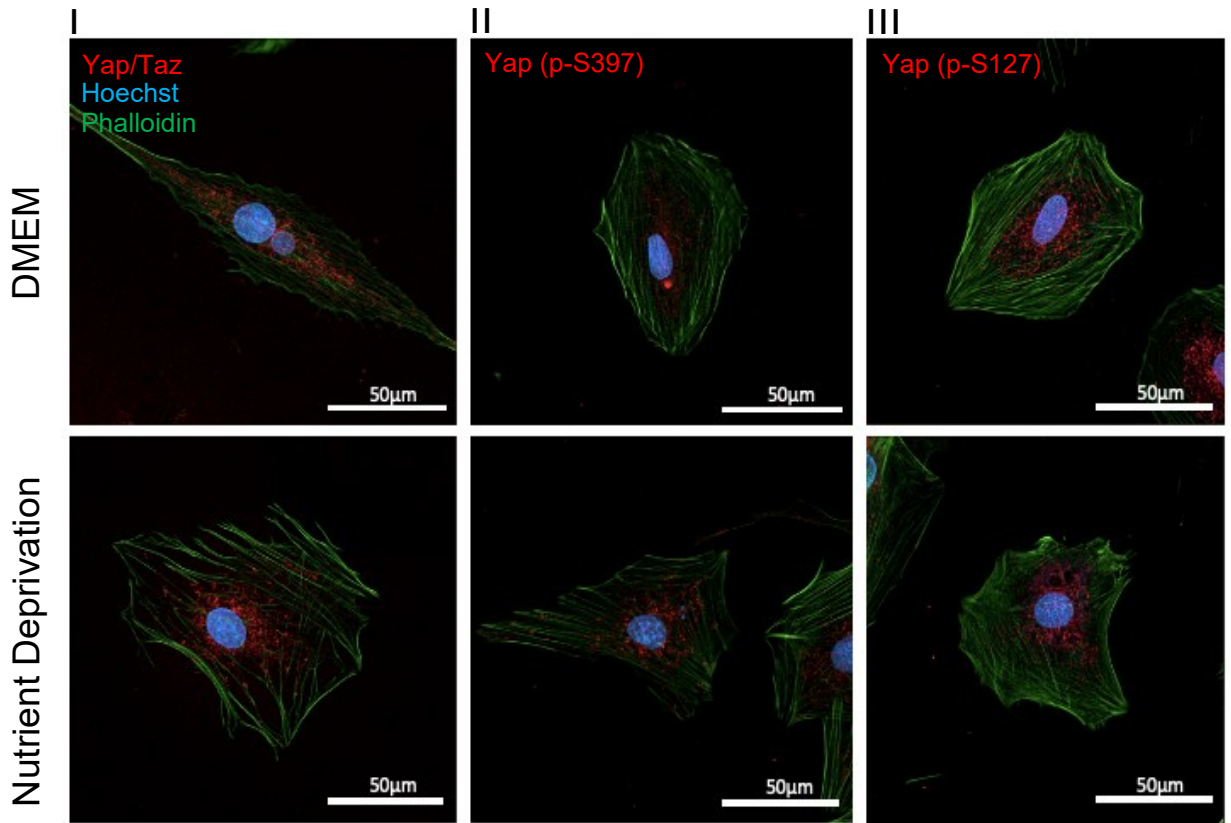


**Figure 3.6: Evidence of Nuclear Compartmentalization in Nutrient Deprivation Conditions.**

H9c2 cells were differentiated for 6 days in the absence of FBS, on the day of the experiment controls received a media change and our treatment groups received nutrient deprivation solution for 1 hour. Cells were permeabilized and blocked followed by staining with Phalloidin, Hoechst and incubated with respective fluorescent antibody for immunofluorescent. **(I)** No changes in Yap compartmentalization (nuclear and cytoplasmic) compared to controls. **(II-III)** Yap (p-S397) and Yap (p-S127) were increased in the nucleus of nutrient deprivation conditions compared to controls.



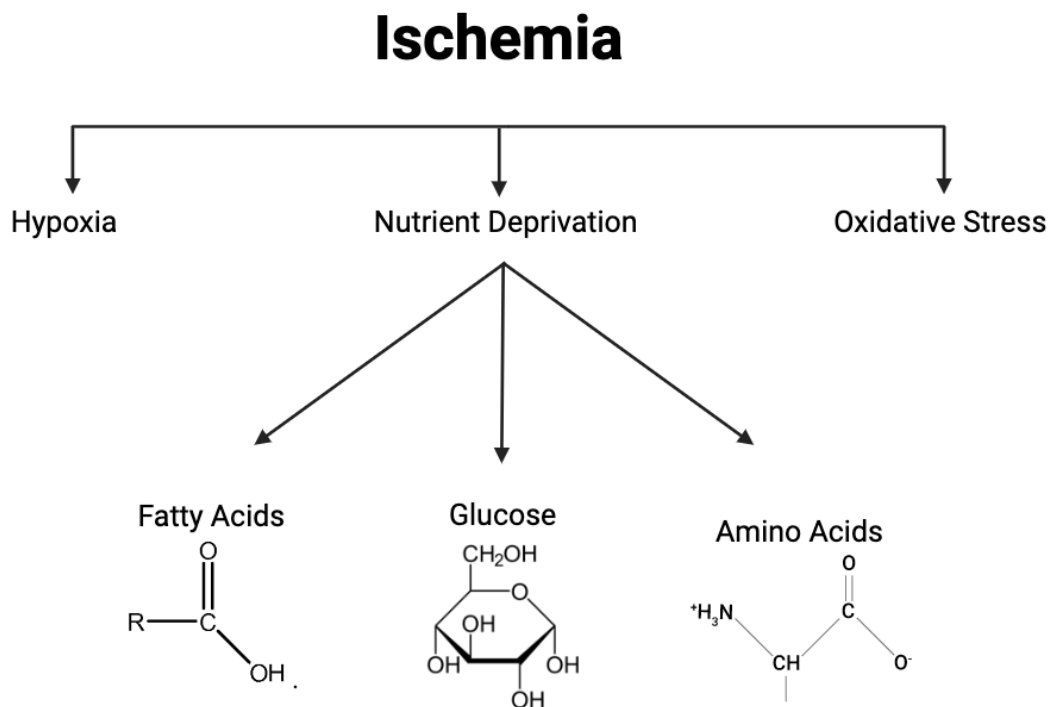


**Figure 3.8: Schematic of ischemic components.**

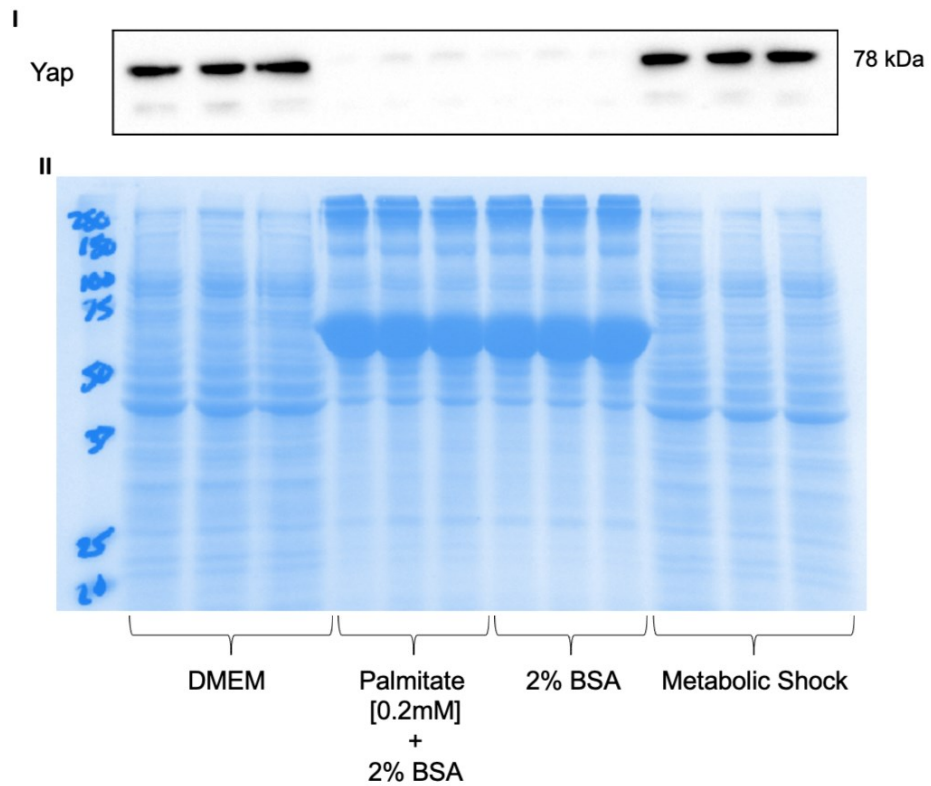
Ischemia is complex and has many components, three major components are hypoxia, oxidative stress, and nutrient deprivation. We had previously ruled out hypoxia and oxidative stress for changes in phosphorylation patterns for Yap, therefore, nutrient deprivation was left to test. Nutrient deprivation consist of deprivation of three essential nutrients, fatty acids, glucose, and amino acids and each component will be tested separately to determine their effects on Yap signalling.

proliferative and differentiated H9c2, with the only difference being that proliferative cells are cultured with 10% FBS. FBS has significant fatty acids as a macronutrient, therefore, we assumed fatty acids are not the nutrient responsible for the changes in Yap levels and phosphorylation by the nutrient deprivation conditions. In an attempt to confirm this, we added 2 $\mu$ M palmitate, the most abundant fatty acid [93], to our nutrient deprivation media. However, the albumin needed to serve as a carrier interfered with the western blotting and could not be cleared within the hour of our shock analysis of Yap. This also affected the protein concentration values of BCA assay, therefore resulting in too low of protein in treatment groups compared to controls for accurate detection and/or comparison (Fig3.9I). Even with multiple washes, we were not able to remove enough albumin for the detection of Yap and/or phosphorylated yap with direct fatty acid reconstitution.

Next, we wanted to determine whether glucose was the nutrient driving the changes in phosphorylated Yap. As such, D-glucose was supplemented into our nutrient deprivation media to 4.5g/L, which is equivalent to the glucose levels of DMEM (control). Supplementation of D-glucose resulted in a decrease in total Yap levels compared to DMEM controls (Fig.3.10I). Additionally, Yap (p-S397) was increased with D-glucose supplementation, while Yap (p-S127) was unchanged compared to controls (Fig3.10II-III). Because total Yap levels was decreased, and Yap (p-S397) was increased in the presence of glucose, while only Yap (p-S127) was unchanged, D-glucose alone was not able to attenuate the increases in both phosphorylation sites (S397&S127) and rather decreased Yap levels which was previously unaffected under nutrient deprivation conditions. Therefore D-glucose alone is not responsible for changes in the Yap signalling patterns in nutrient deprivation conditions. Through reduction and deduction methods we can conclude that neither fatty acids nor glucose alone are responsible for the increases in phosphorylation at S397 and S127 of Yap (Fig.3.11) due to nutrient deprivation of total nutrient deprivation.

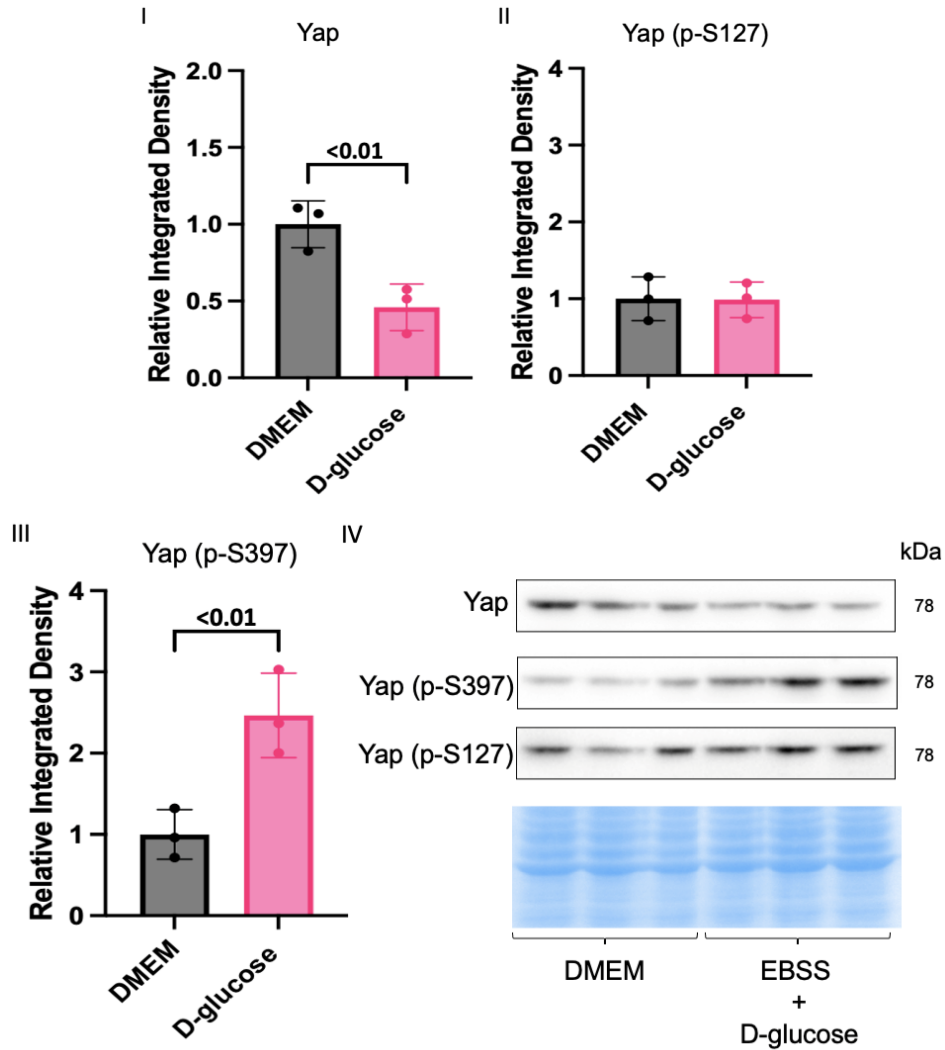
### **3.5 Changes in Amino Acids Impact Yap Signalling in H9c2 Rat Cardiomyotubes**

Since fatty acids and glucose were not the sole cause of the increased phosphorylation of Yap (S397&S127), amino acids are indicated to be the essential nutrient likely responsible for the changes under nutrient deprivation conditions compared to control.



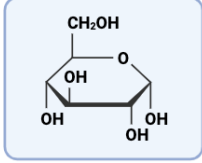
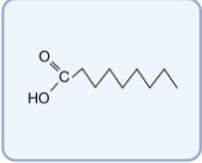
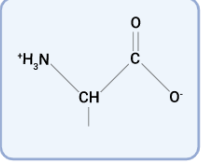
**Figure 3.9: Unsuccessful Fatty Acid Supplementation in Nutrient Deprivation Conditions.**

H9c2 cells were differentiated for 6 days in the absence of FBS, on the day of the experiment controls received a media change and our treatment groups received nutrient deprivation, with 0.2mM palmitate or 2% BSA for 1 hour. **I)** Unequal Yap levels at 50seconds. **II)** Pierce® Memcode demonstrating uneven protein loading due to high concentration of albumin at 60kDa compared to DMEM controls and nutrient deprivation alone.



**Figure 3.10: Effects of D-glucose Supplementation on Yap Signalling.**

H9c2 cells were differentiated for 6 days in the absence of FBS, on the day of the experiment controls received a media change and our treatment groups received nutrient deprivation solution supplement with 4.5g/L D-glucose for 1 hour. **(I)** D-glucose supplementation decreased Yap levels compared to DMEM. **(II)** There were no changes in Yap (p-S127) compared to DMEM. **(III)** Yap (p-S397) was increased in D-glucose groups compared to DMEM. **(IV)** Respective Yap, Yap (p-S127) and Yap (p-S397) blots with Pierce® Memcode as protein loading control.

	Glucose 	Fatty Acids 	Amino Acids 	Yap	Yap (p-S397)	Yap (p-S127)
Serum (FBS)	✓	✓	✓	↑	No change	—
DMEM only	✓	—	✓	No change	No change	—
----- Ergo changes not driven by fatty acids -----						
EBSS	—	—	—	No change	↑	↑
EBSS + Glucose	✓	—	—	↓	↑	No change
----- Ergo changes not driven by glucose -----						

**Figure 3.11 Deduction and Reduction Approach to Focus on Amino Acids.**

Schematic depicting the changes or lack thereof in Yap, Yap (p-S397) and Yap (p-S127) caused by FBS (fatty acids) which allowed us to determine that changes in Yap phosphorylation was likely not caused by fatty acids. Both Yap S397 and S127 were increased in nutrient deprivation (EBSS) while there were no changes in total Yap levels. Supplementation with D-glucose decreased total Yap levels compared to DMEM controls, while Yap (p-S397) was increased with no change in Yap (p-S127).



Firstly, to characterize whether there were changes in free amino acid levels between controls and nutrient deprivation, UPLC was performed (Fig.3.12). Interestingly, all non-essential free amino acid levels were increased in nutrient deprivation conditions compared to controls, while all free essential amino acid levels were decreased. Additionally, all branched-chain amino acids (BCAA); valine, isoleucine and leucine were decreased to the same extent. These results suggest a potential shift in amino acid utilization under acute nutrient deprivation stress conditions, that could be either beneficial and/or detrimental to the fate of the cells. Given the observed results from the UPLC data, to determine if one or more amino acids were able to attenuate the changes in phospho-Yap in nutrient deprivation conditions compared to controls. We first tested the three amino acids that were decreased most significantly compared to controls from Fig.3.12 for supplementation: L-threonine, L-valine, and L-isoleucine. L-Leucine supplementation was not available at the time of experiments and was therefore not tested. Concentrations equivalent to DMEM media (0.8mM) of all three amino acids were added to nutrient deprivation media separately and compared directly to DMEM control. Both L-threonine and L-isoleucine supplementation resulted in an increase in Yap levels (Fig. 3.13I), however, Yap levels after treatment with L-valine was unchanged compared to DMEM controls (dashed line). Conversely, phospho-Yap levels at both S397 and S127 was increased with L-valine supplementation but was unchanged with both L-threonine and L-isoleucine compared to controls (Fig.3.13II-III). The attenuation of both phospho-Yap sites to control levels demonstrates the effects of L-threonine and L-isoleucine supplementation on the increase seen in nutrient deprivation conditions. Thus, confirming that amino acids, or lack thereof, are a cause of the increase in phospho-Yap in nutrient deprivation conditions. Together the results suggest that either L-threonine or/and L-isoleucine are responsible for regulating the phosphorylation of Yap S397&S127 under nutrient deprivation conditions compared to controls. Threonine is catabolized to isoleucine and is regulated by an inhibitory feedback loop (Fig.3.14), where isoleucine binds to the allosteric active site on the threonine deaminase when isoleucine levels are high, which inhibits the binding of threonine. However, when levels of isoleucine are low, threonine can bind, and catabolism can continue. As such, given that threonine is catabolized to isoleucine by the inhibitory feedback loop it highlights the importance of isoleucine as the limiting factor [108].

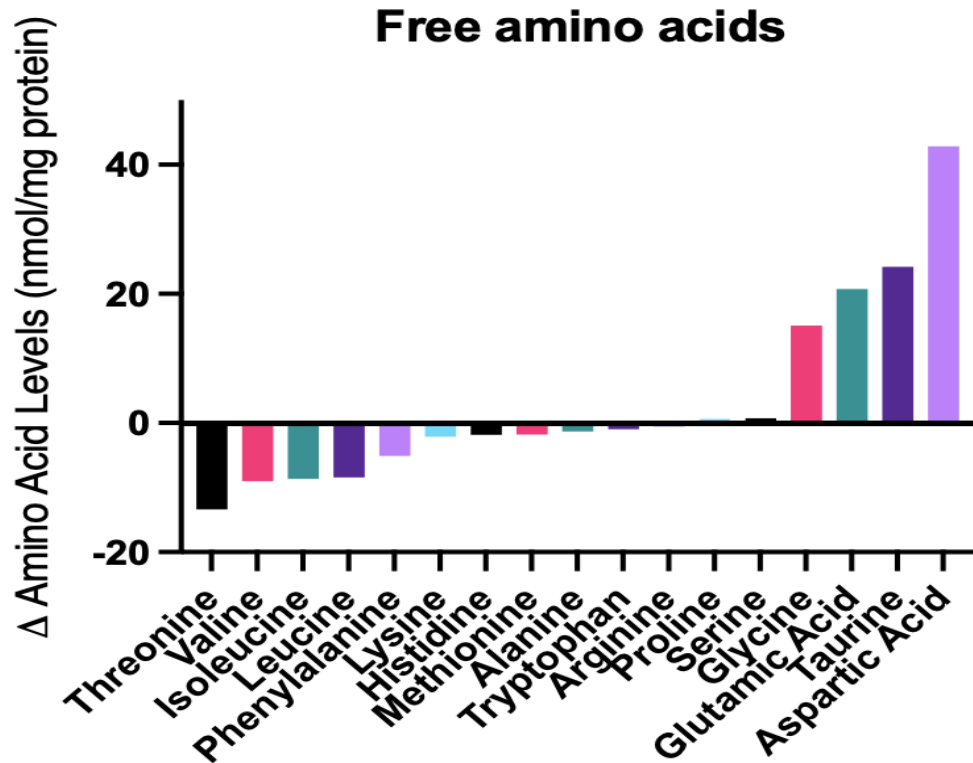


**Figure 3.12: Effects on Free Amino Acids in Nutrient Deprivation Conditions.**

H9c2 cells were differentiated for 6 days in the absence of FBS, on the day of the experiment controls received a media change and our treatment groups received nutrient deprivation solution for 1 hour. UPLC free amino acid levels differences between controls and nutrient deprivation conditions. All non-essential amino acid levels were increased where all essential amino acid levels were decreased in nutrient deprivation compared to controls. All three branched chain amino acids were decreased to the same extent.

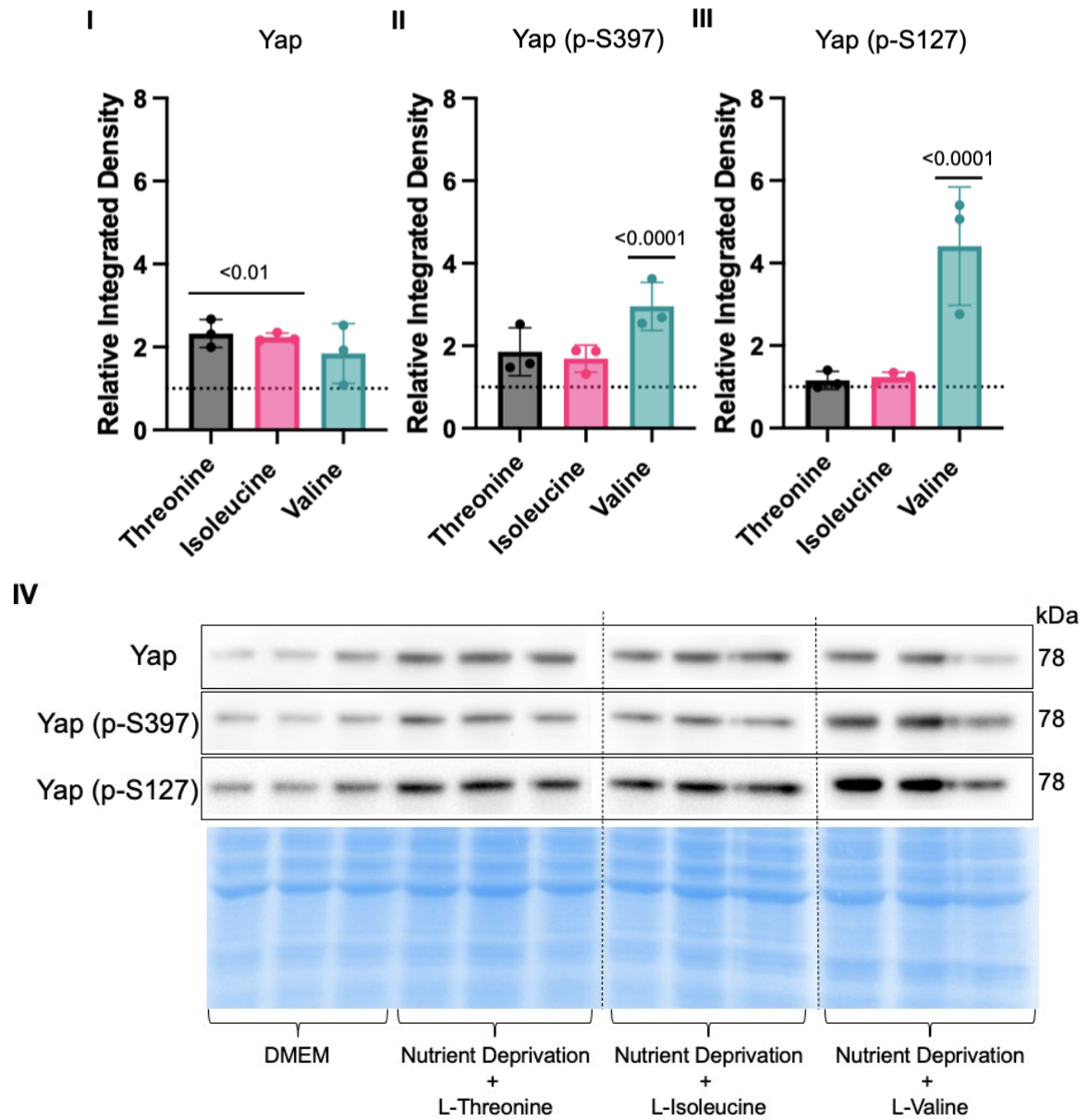


**Figure 3.13: Effects of Amino Acid Supplementation in Nutrient Deprivation Conditions.**

H9c2 cells were differentiated for 6 days in the absence of FBS, on the day of the experiment controls received a media change and our treatment groups received nutrient deprivation solution with respective amino acid supplemented for 1 hour prior to harvest. **(I)** Total Yap levels were increased in threonine and isoleucine groups compared to DMEM controls (dashed line) while there was no change between controls and valine supplementation. **(II)** Supplementation of threonine and isoleucine caused no changes in Yap (p-S397) levels compared to DMEM controls. Yap (p-S397) levels was increased in the Valine group compared to controls. **(III)** Yap (p-S127) levels were unchanged between threonine and isoleucine groups and controls and increased in the valine treatment compared to controls. **(IV)** Representative blots for Yap, Yap (p-S397) and Yap (p-S127) and Pierce® Memcode demonstrating uniform protein loading.

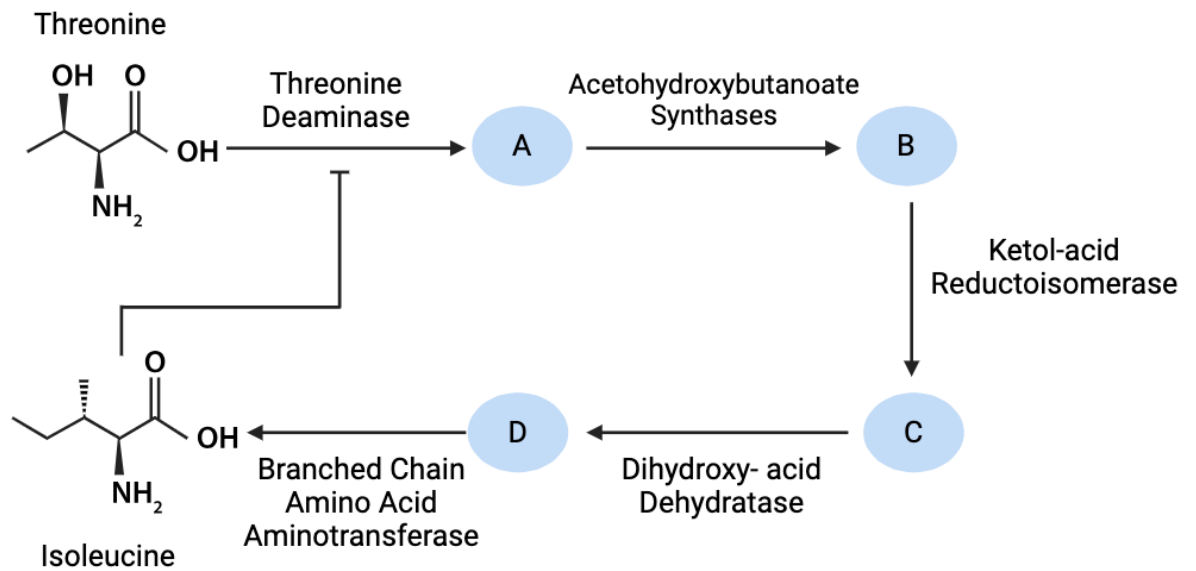


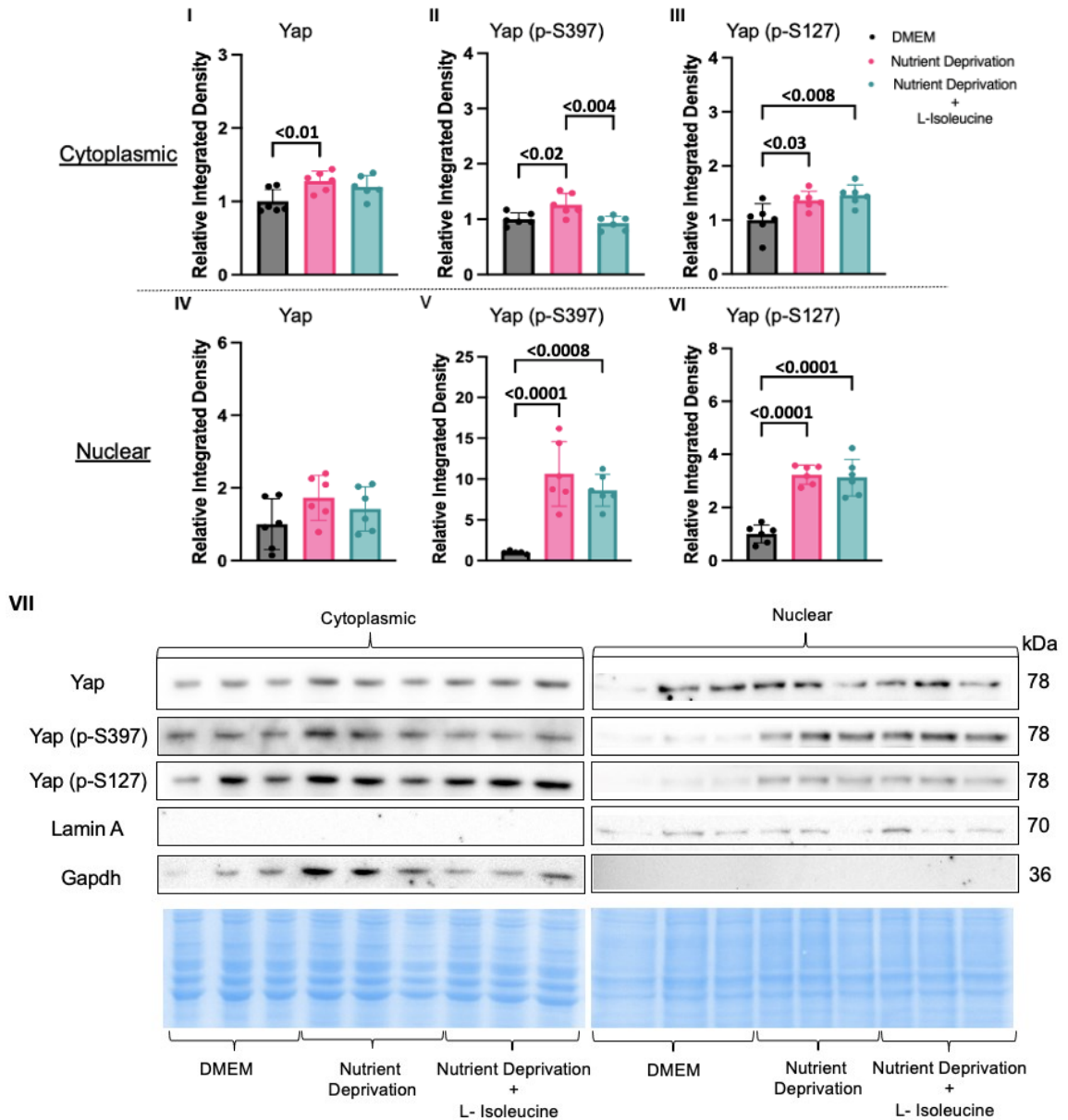
**Figure 3.14: Threonine and Isoleucine Feedback Inhibition.**

Threonine is catabolized to isoleucine through five various steps with the first enzyme being threonine deaminase, followed by acetoxybutanoate synthase then ketol-acid reductoisomerase and dihydroxyl-acid dehydratase which are enzymes shared in many branch chain pathways, followed by the last step which involves branch chain amino acid transferase or more specifically isoleucine transaminase. When isoleucine levels are high, isoleucine can bind to an allosteric site on threonine deaminase which inhibits threonine from binding, though when isoleucine levels are low threonine can bind and catabolize to isoleucine.

To establish whether L-isoleucine supplementation alone affected the phosphorylation patterns of Yap (S397&S127), we performed cellular fractionation of DMEM, nutrient deprivation conditions and nutrient deprivation conditions with L-isoleucine supplementation. L-isoleucine supplementation was able to attenuate the increase in cytoplasmic Yap (p-S397) seen in nutrient deprivation conditions (Fig.3.15II). However, nuclear phosphorylation of both Yap (p-S397) and Yap (p-S127), and cytoplasmic Yap (p-127) was unchanged compared to nutrient deprivation conditions (Fig.3.15III, V-VI). It required additional data points to see an increase of total Yap levels in the cytoplasm in nutrient deprivation conditions compared to DMEM controls suggesting the effect size is small (Fig.3.15I) and remained increased with L-isoleucine supplementation which is consistent with figure 3.13. These results suggest that isoleucine alone does not reverse all the effects of nutrient deprivation conditions but does play a role in phosphorylation patterns of Yap (p-S397).

### **3.6 Hepes Supplementation Does Not Impact the Response to Nutrient Deprivation in Rat Cardiomyocytes**

To exclude any effects of the Hepes supplementation which is added to the nutrient deprivation conditions to maintain pH and has previously shown influences on cell signalling [109,110], Yap levels was compared with EBSS alone, EBSS with 10mM Hepes and EBSS with 25mM Hepes. With 25mM Hepes being the highest recommended concentration to use in cell culture and 10mM being the concentration that was supplemented into our nutrient deprivation conditions. There was no difference in total Yap, Yap (p-S397) or Yap (p-S127) levels with 10mM Hepes compared to EBSS alone. However, 25mM Hepes decreased total Yap, and Yap (p-S127) levels compared to EBSS alone, while Yap (p-S397) was unchanged (Fig.3.16I-III). Hence, 10mM Hepes supplementation in our nutrient deprivation conditions does not affect Yap signalling but at higher doses could be a confounding variable. Whether the changes in phosphorylated Yap levels caused by nutrient deprivation conditions could be reversed was unclear, therefore we refeed the cells using DMEM media for one hour following one hour in nutrient deprivation conditions. We found that one hour of refeeding with all essential nutrients of DMEM media after nutrient deprivation for one hour decreased total Yap levels compared to controls, while Yap (p-S397) and Yap (p-S127) were unchanged (Fig.3.17I-III).



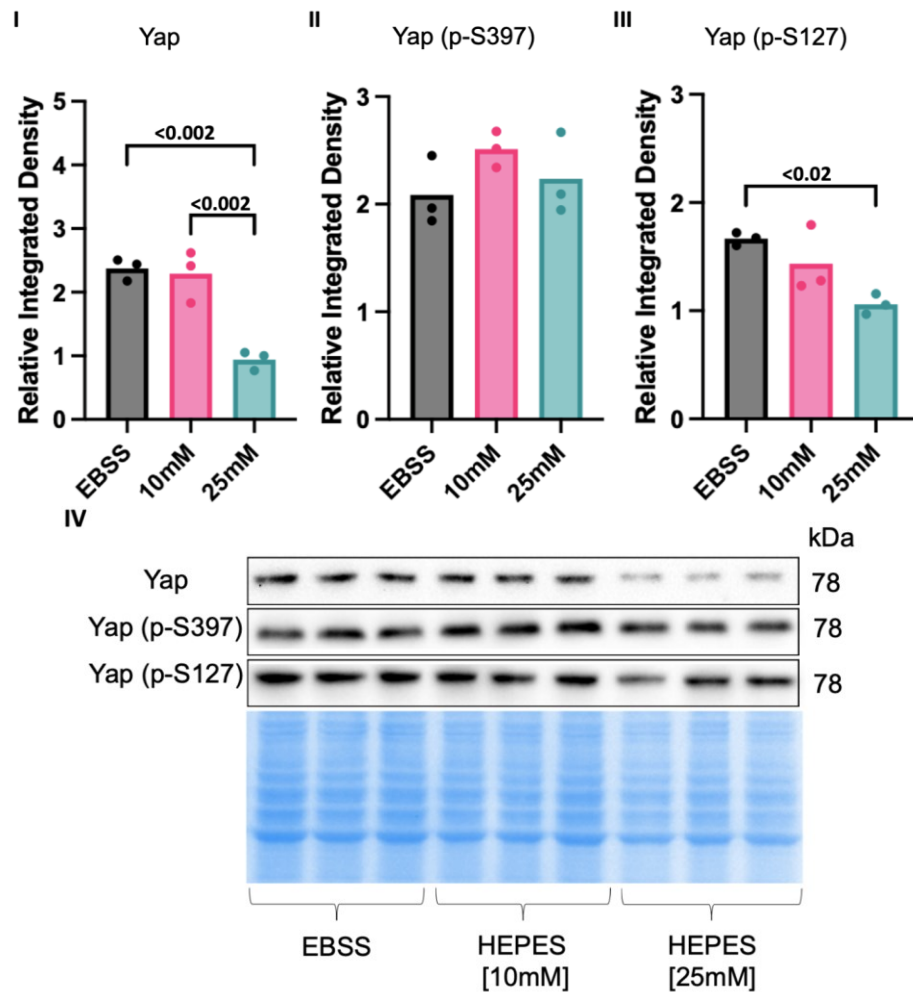


**Figure 3.16: Validation That HEPES Supplementation at Utilized Concentration Does Not Affect Yap Levels.**

H9c2 cells were differentiated for 6 days in the absence of FBS, on the day of the experiment cells were incubated with EBSS, EBSS with 10mM or 25mM for 1 hour. **I**) Yap levels were unchanged between EBSS and EBSS with 10mM HEPES while it was decreased at 25mM HEPES. **II**) HEPES had no effect on Yap (p-S127) levels. **III**) Yap (p-S127) was unaffected by 10mM HEPES but was decreased by 25mM compared to EBSS alone. Representative blots for Yap, Yap (p-S397) and Yap (p-S127) and Pierce® Memcode demonstrating uniform protein loading (**IV**).

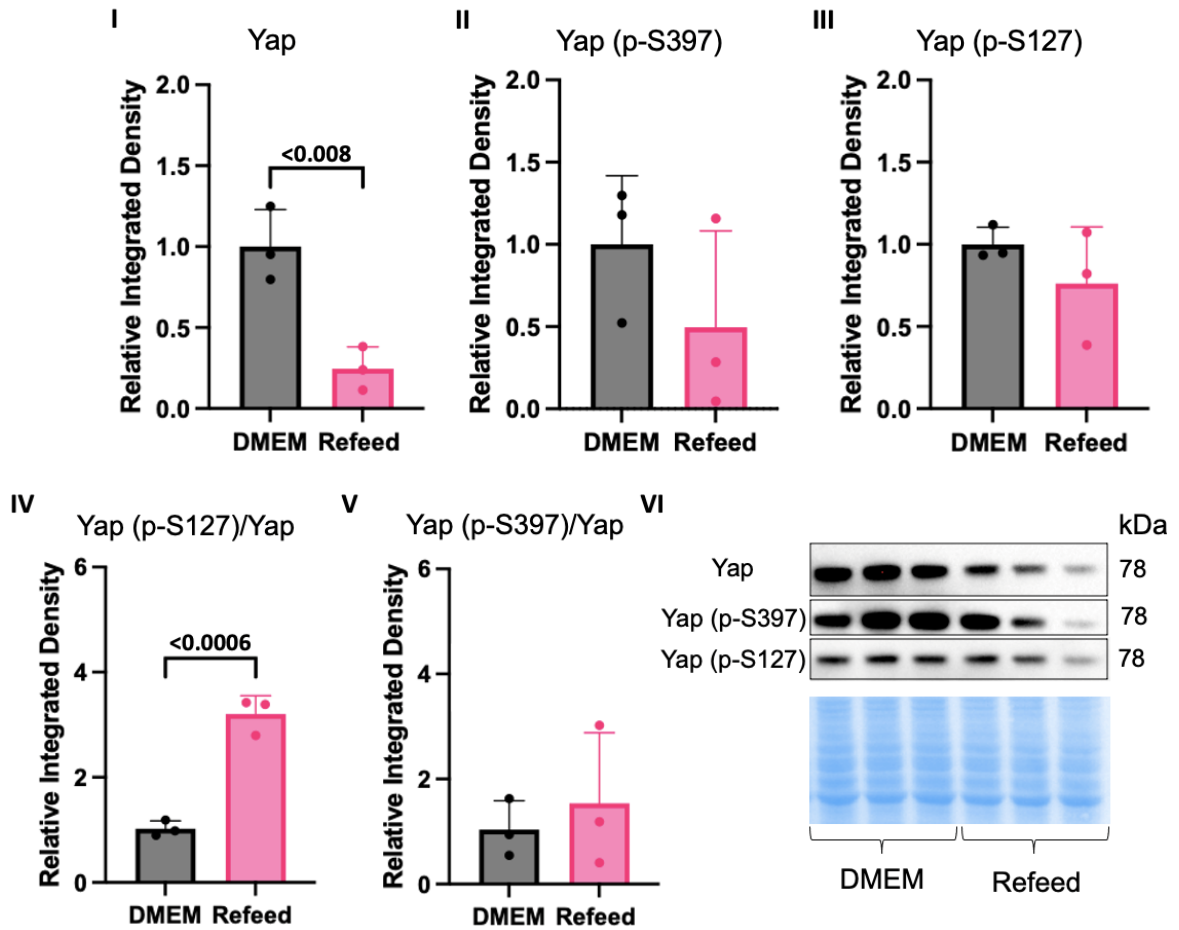


**Figure 3.17: The Effects of Re-addition of DMEM After One Hour of Nutrient Deprivation.**

H9c2 cells were differentiated for 6 days in the absence of FBS, on the day of the experiment controls received a media change and our treatment groups received nutrient deprivation solution for one hour, followed by re addition of DMEM control media for one hour. Refeeding with DMEM decreased total Yap levels after one hour (**I**) but had no effect on Yap (p-S397) and Yap (p-S127) alone (**II**, **III**). **IV** Ratioed Yap (p-S127) to total Yap levels were increased in the refeed group compared to DMEM controls. Ratioed Yap (p-S397) to total Yap levels had no significant changes compared to controls (**V**). **VI** Representative blots for Yap, Yap (p-S397) and Yap (p-S127) and Pierce® Memcode demonstrating uniform protein loading (**IV**).



However, the ratio of Yap (p-S127) to total Yap levels were increased after a refeed (Fig.3.17IV) but the ratio of Yap (p-S397) to total Yap was unchanged compared to DMEM controls (Fig.3.17V). These data suggest that changes in phosphorylation caused by nutrient deprivation cannot be fully reversed by supplementing back the nutrients with comparable time.

### **3.7 Nutrient Deprivation Conditions Alters Gene Expression**

Changes in Yap levels and phosphorylation patterns could translate to changes in gene expression as a response to the nutrient stress. To establish whether nutrient deprivation or nutrient deprivation with L-isoleucine supplementation had any effect on gene expression, reference (“house-keeping”) genes need to be defined across conditions used for qPCR. Gapdh and Hprt1, are common reference genes used for H9c2’s yet they, along with several other reference genes, were different between one or more group. There were significant differences between nutrient deprivation and nutrient deprivation with L-isoleucine in Gapdh, Hprt1, U6, and beta-actin genes, while there were differences between DMEM controls and nutrient deprivation for the B2m gene and differences between all three groups for the 18s gene. The only gene which remained constant between all three groups was Igf2bp3 which was initially anticipated to be a target gene (Fig.3.18). As per Minimum Information for Publication of Quantitative Real-Time PCR Experiments (MIQE) all qPCR data was analyzed using Igf2bp3 and then confirmed with a second reference gene, Hprt1 for nutrient deprivation compared to DMEM and B2m for nutrient deprivation with isoleucine compared to DMEM.

To determine which Yap-associated genes could be impacted by the changes in phosphorylation patterns caused by nutrient deprivation conditions five main themes of MI recovery were used to identify plausible gene targets. Yap-associated genes that are known to have a role in neovascularization, inflammation, cell survival, cardiac performance, and matrix remodeling (Fig.3.19) and ten genes, two from each MI role were selected. No differences in neo-vascularization, inflammation, cell survival or cardiac performance associated genes were found between any of the three groups, DMEM controls, nutrient deprivation, or nutrient deprivation with L-isoleucine supplementation. Additionally, there were no changes in Fgf21 a gene linked with matrix remodeling, however, Ctgf was significantly increased in nutrient deprivation with L-isoleucine supplemented compared to nutrient deprivation alone or DMEM controls (Fig.3.20).

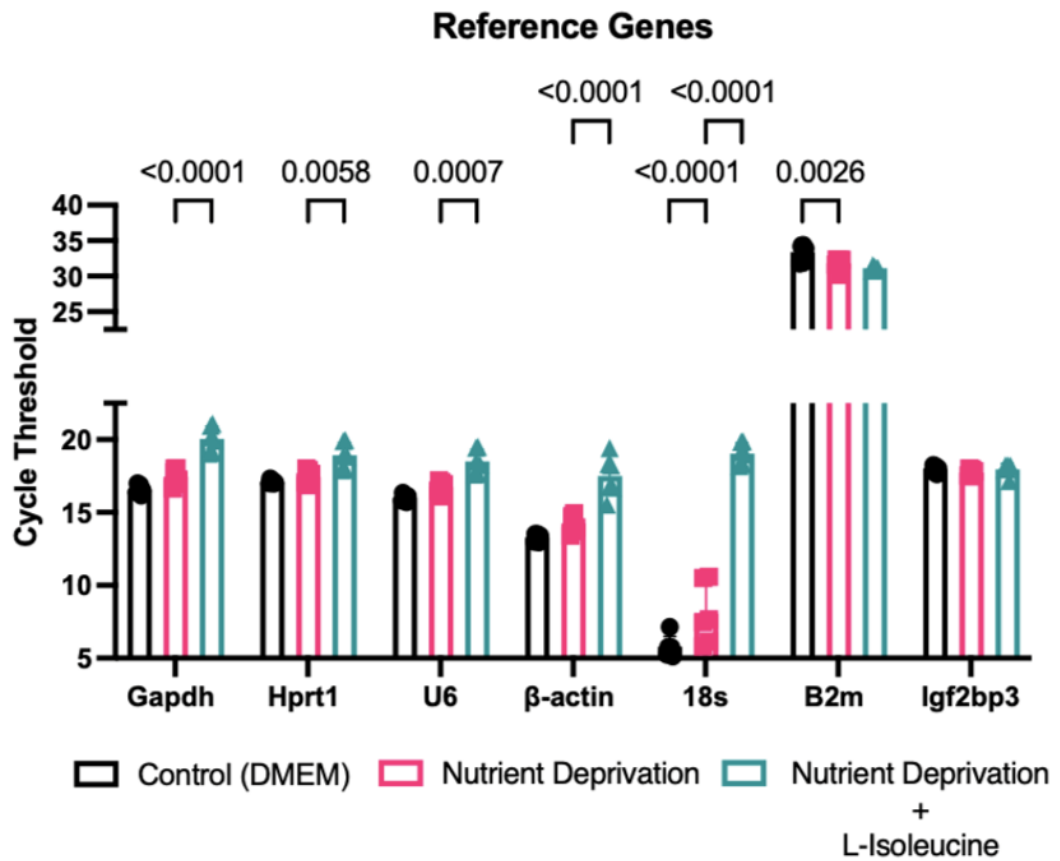


**Figure 3.18: Determination of Reference Genes for qPCR Analysis.**

H9c2 cells were differentiated for 6 days in the absence of FBS, on the day of the experiment controls received a media change and our treatment groups received nutrient deprivation solution or nutrient deprivation with L-isoleucine for 1 hour. RNA was extracted and converted to cDNA which was used for qPCR. Six common reference genes used for H9c2 cells were tested, however all were significantly different between one or more groups. Igf2bp3 was the only gene tested that did not change between all three groups.

## Themes of MI Recovery

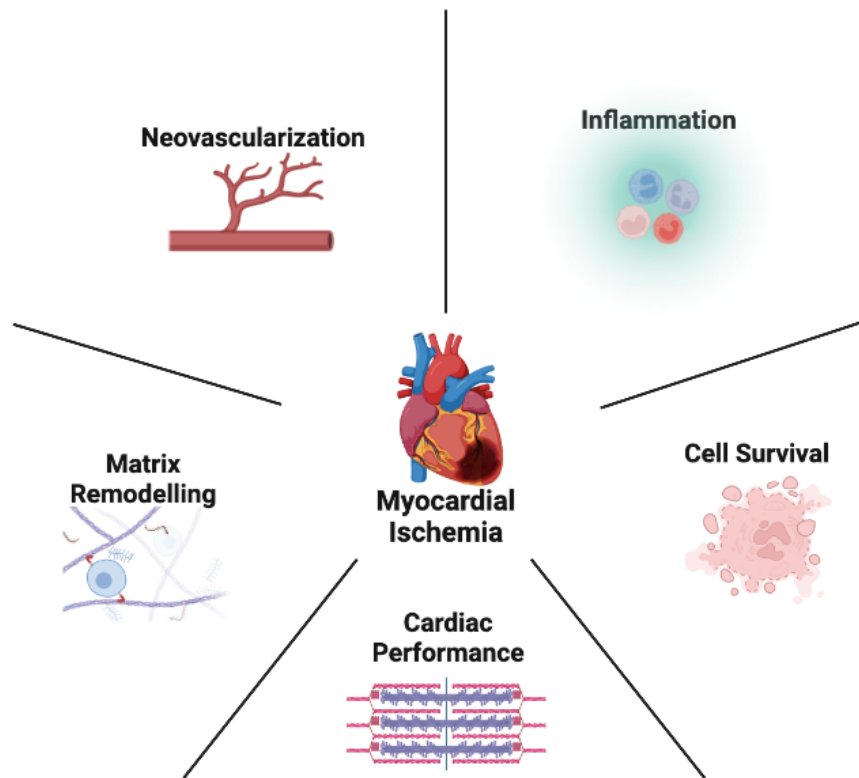


**Figure 3.19: Five Themes Associated with Myocardial Infarction Recovery.**

All methods of recovery and respective areas of research fit into one of the five themes associated with recovery after an MI. The five themes are neo-vascularization, inflammation, cell survival, cardiac performance, and matrix remodelling.

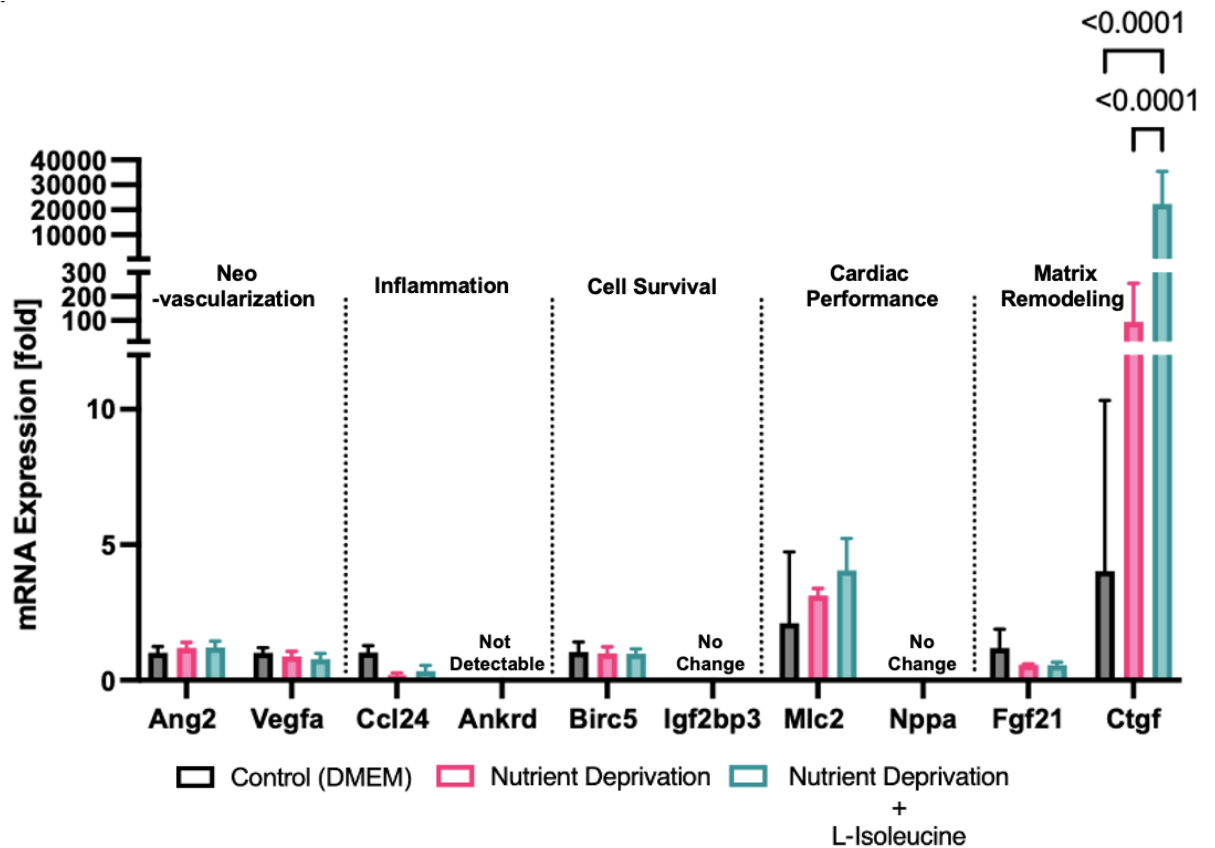


**Figure 3.20: Supplementation of Isoleucine Results in an increase of mRNA Expression of a Matrix Related Gene**

H9c2 cells were differentiated for 6 days in the absence of FBS, on the day of the experiment controls received a media change and our treatment groups received nutrient deprivation solution or nutrient deprivation with L-isoleucine for 1 hour. RNA was extracted and converted to cDNA which was used for qPCR. Two genes from each theme of MI recovery were tested, with no changes in genes associated with neo-vascularization, inflammation, cell survival and cardiac performance. However, Ctgf a gene associated with matrix remodelling was significantly increased in nutrient deprivation with L-isoleucine compared to nutrient deprivation alone.

Ctgf is an important gene of interest in matrix remodeling during MI recovery, suggesting that L-isoleucine may play an important role in matrix remodeling after MI through Yap-signalling.

To determine if Yap-associated genes were similarly affected *in vivo*, we analyzed open-access microarray data set from Entrez Gene Expression Omnibus (GEO) (<http://www.ncbi.nlm.nih.gov/geo/profile/>). A study was identified from GEO that used rats and MI by left coronary artery ligation. Data set GDS4907 included the three genes which are consistently associated with Yap: Ctgf, Cyr61 and Ccl24 and associated with fibrosis and inflammation. The data set included the left ventricle of shams, small, moderate, and large MI groups. Ctgf expression was significantly increased in the large MI group compared to sham and all other sizes of MI (Fig.3.21I). While Cyr61 and Ccl24 were unchanged between all groups including shams (Fig.3.21II-III). These results were consistent with those seen in our qPCR data in the nutrient deprivation supplemented with L-isoleucine, which showed increased Ctgf suggesting that Yap-associated Ctgf expression could be a downstream target in response to severe nutrient deprived conditions of MI.

### **3.8 Nutrient Deprivation Conditions Alters Metabolic Activity**

In order to determine whether nutrient deprivation or nutrient deprivation with L-isoleucine resulted in any changes in cell survival using images of H9c2 cells in nutrient deprivation and nutrient deprivation with L-isoleucine that were taken at one, three, and six hours. At one hour of nutrient deprivation there was loss of cell viability compared to DMEM controls and nutrient deprivation with L-isoleucine, this trend holds true for three and six hours as well. By six hours nutrient deprivation treatment had approximately 20% cell survival, while L-isoleucine supplemented cells had approximately 40% cell survival (Fig3.22). Whether L-isoleucine could prevent the detrimental effects long-term after nutrient deprivation, Presto Blue was added to the plate at one, two-, four-, six- and sixteen-hour time points (Fig.3.23I) to nutrient deprivation solution and nutrient deprivation supplemented with L-isoleucine and compared to DMEM controls. Nutrient deprivation and nutrient deprivation with L-isoleucine both initially increased apparent metabolic activity compared to DMEM controls (dashed line) until six hours where both treatments then showed less metabolic activity compared to controls, which continued to trend downwards until 16 hours (Fig.3.23II).

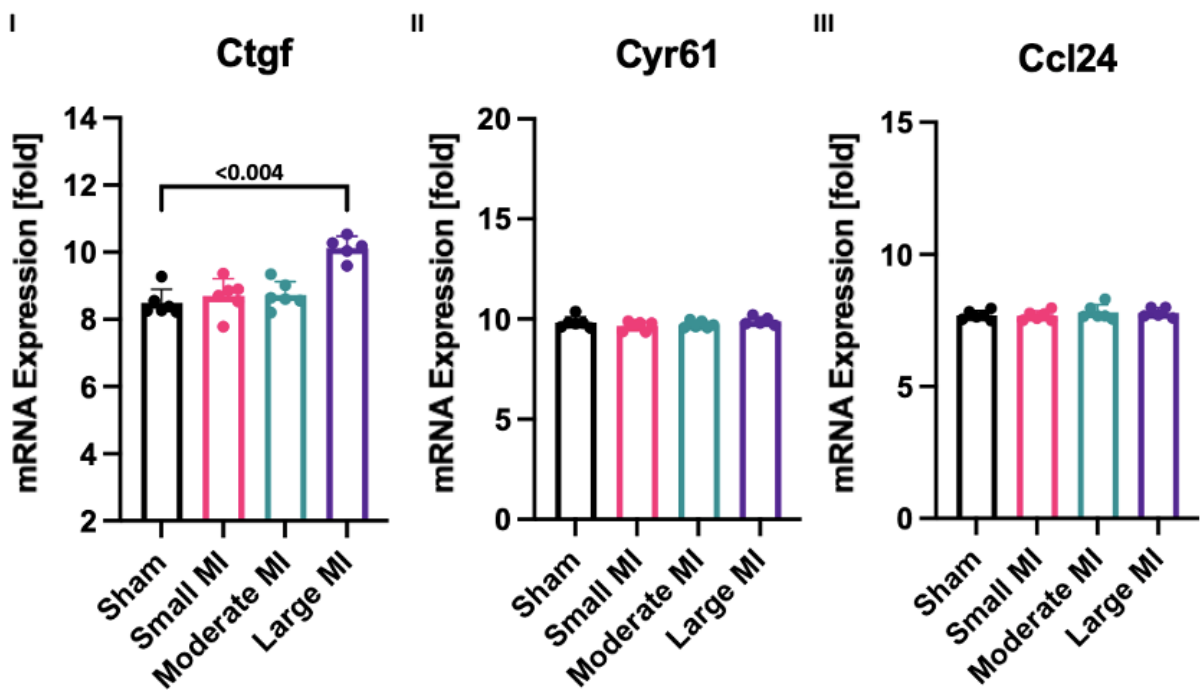


**Figure 3.21: Expression of Known Yap Regulated Genes from a Gene Expression Omnibus (GEO) Data Set.**

mRNA (log<sub>2</sub>-transformed) was analyzed in rat MI model using public microarray datasets. Left ventricles were removed from rats who underwent left coronary artery ligation to induce large, moderate, or small myocardial infarctions. Three genes associated with Yap were tested Ctgf, Cyr61 and Ccl24. **I**) Ctgf was significantly increased in the large MI group compared to all other groups, while Cyr 61 and Ccl24 did not vary between all four group including control shams (**II-III**).

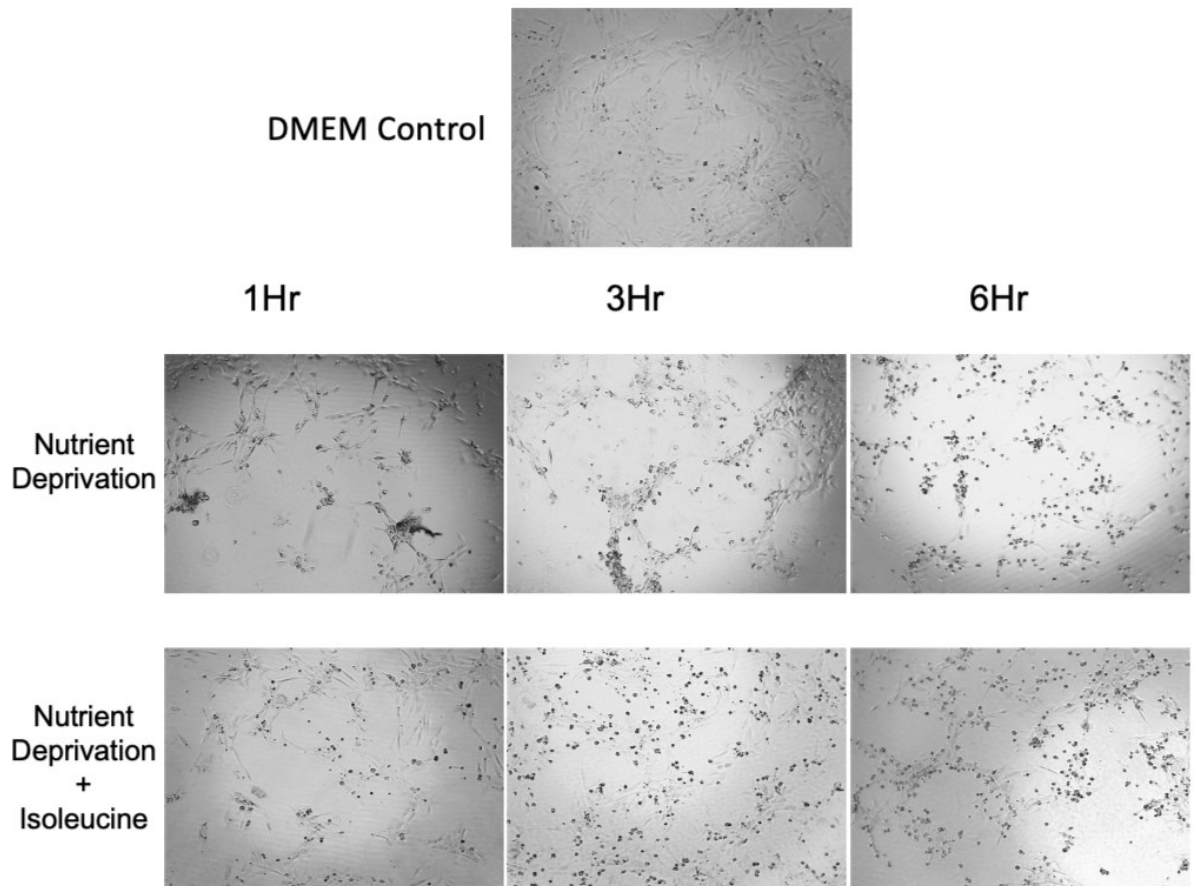


**Figure 3.22: L-isoleucine Supplementation Suggest More Cell Survival/Adhesion Compared to Nutrient Deprivation Alone.**

Photos of H9c2 cells in nutrient deprivation, and nutrient deprivation with isoleucine at one hour, three hours and six hours compared to DMEM controls. Significant cell loss had occurred within one hour of nutrient deprivation compared to DMEM control, while there was significantly less in nutrient deprivation with isoleucine at all three time points, one hour, three hours and six hours.

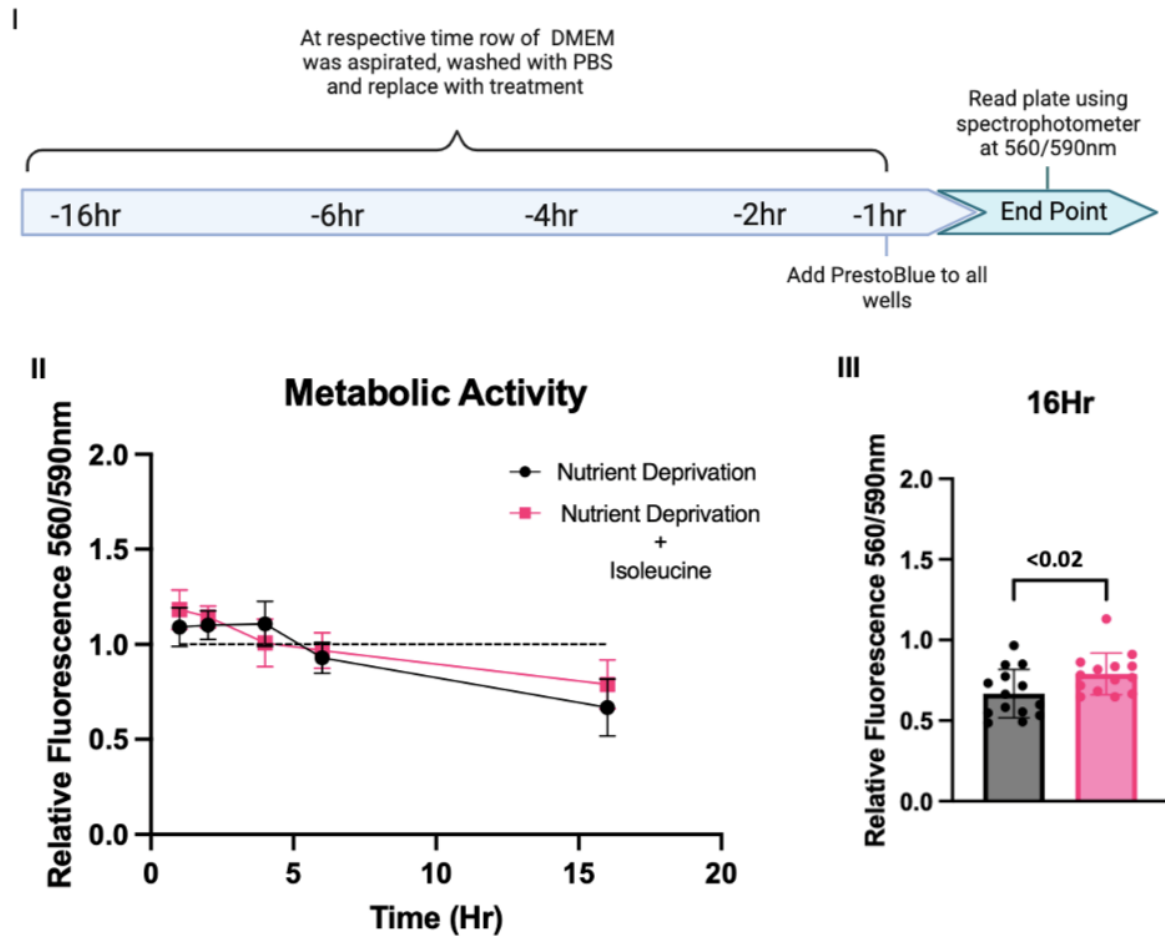


**Figure 3.23: The effects of Nutrient Deprivation and Nutrient Deprivation supplemented with L-isoleucine.**

H9c2 cells were differentiated for 6 days in the absence of FBS, on day 7 the media of one row at a time was aspirated, washed followed by either nutrient deprivation or nutrient deprivation with L-isoleucine, this was repeated for our 16, 6,4,2 and 1 hour time points (I). (II) Nutrient deprivation and nutrient deprivation with L-isoleucine initially increase metabolic activity compared to DMEM control (dashed line) until approximately 4hr, whereby 6hr the metabolic activity starts to decline below DMEM controls and trends downwards until 16hrs. (III) nutrient deprivation with L-isoleucine has more metabolic activity at 16hrs compared to nutrient deprivation alone.



With nutrient deprivation alone trending lower than nutrient deprivation with L-isoleucine. Comparatively, the decreased metabolic activity in the Presto Blue Assay and the images of H9c2 suggest that L-isoleucine supplementation can maintain metabolic activity and cell adhesion compared to nutrient deprivation over time even in the absence of any further nutrients.

## Chapter 4: Discussion

### 4.1 Summary of findings

Much of our understanding of cardiac Yap signalling has been determined in cardiac development as a regulator of organ size and proliferation of cardiomyocytes. However, more recently its potential roles in the adult heart after MI have started to be explored. It was shown that upregulation of Yap signalling by knocking out one of its upstream proteins (Sav1 or Lats1/2) has been linked to cell cardiac regeneration after MI [111]. Lin et al. suggests that Yap activation promotes re-entry of the cell cycle and does not induce cardiomyocyte hypertrophy but rather leads to improved heart function, reduced scar size, and improved survival which was consistent with results from various other studies [102,111,112]. Activation of Yap after MI was well tolerated for up to three months without affecting cardiac performance. While there are several studies suggesting that Yap activation after MI leads to better outcomes, the molecular drivers and downstream mechanisms involved in the regulation of Yap and how it is affecting various cardiac cells after MI is less understood.

Here we sought to determine the stress drivers and molecular mechanisms that may regulate and/or promote Yap signalling after MI. We found that Yap expression was significantly increased specifically in the peri-infarct zone after MI, which may be explained by the fact that Yap expression has been seen to increase in cardiac fibroblasts three to five days after MI [113]. However, the mechanisms of activation and the role of Yap in cardiomyocytes was less understood. Our results suggest that of the variable stressors involved in MI the deprivation of essential nutrients including glucose, fatty acids and amino acids had the greatest effect on Yap signalling in rat cardiomyotubes. Additionally, our results highlight the importance of amino acids in regulating Yap signalling and the regulation of metabolic activity necessary for survival. We also found that changes in Yap signalling caused by the acute nutrient deprivation of our nutrient deprivation conditions affected a previously known Yap-associated gene, *Ctgf*, which has been linked with poor outcomes for patients after MI. These findings collectively improve our understanding of some of the underlying mechanisms that may be involved in Yap signalling in the adult heart after MI. They may also provide insight into potential therapeutic targets which could improve remodelling of the adult heart after MI.

## 4.2 Yap Expression in Response to Acute Nutrient Deprivation

Yap signalling and its methods of regulation have been widely explored through various conditions, stressors, and cell types, however, the specific molecular mechanisms that are attributed to the improvement of outcomes through activation of Yap signalling after MI are less understood. Typically, mechanical stress is thought to be the primary driver regulating cardiac Yap signalling. Here we show the important role of metabolic stress can also be a major driver of altered Yap-signalling. Our investigation into the role of metabolic stressors in cardiomyotubes revealed that acute nutrient deprivation caused by our nutrient deprivation conditions was the only stressor associated with MI that changed the expression of Yap compared to mitophagic stress, cytokine stress, hypoxia, or oxidative stress most often associated as stress determinants after MI. These results are surprising as those other stressors were thought to effect Yap-signalling, but this could be due to a lack of cellular specificity amongst cardiac cells (cardiomyocytes, fibroblasts, vascular cells, et al.). Acute nutrient deprivation did not change total Yap levels yet did increase post translational modification at Yap (p-S397) and Yap (p-S127) in whole cell lysate—consistent with the inactivation of Yap signalling, and therefore, not likely to result in increased gene transcription of downstream targets. In determining which essential nutrient was responsible for the acute changes in Yap, initially either glucose and/or fatty acids were postulated as being responsible since they are major energy sources for cardiomyocytes and have previously been linked to phosphorylation of Yap leading to its inactivation [91]. Our data showed that glucose and fatty acid supplementation alone did not reverse the increase in Yap (p-S397) and Yap (p-S127) expression after nutrient deprivation conditions implicating amino acids as the nutrient responsible for the changes. While glucose supplementation did not attenuate the increase in Yap (p-S397) it did cause a decrease in total Yap levels suggesting that increased Yap (p-S397) could be causing proteasomal degradation of Yap which is consistent with other studies [114–116]. Our results show a shift in amino acid bioavailability, where all non-essential amino acids were increased in nutrient deprivation conditions compared to control, yet all essential amino acid levels were decreased compared to controls. This could be explained as essential amino acids must come from an extrinsic source, where non-essential amino acids can be made by the cell through proteolysis. Therefore, in response to acute nutrient deprivation the cardiomyocytes may be quickly consume the essential amino acids to maintain appropriate

function and dispense with proteins to build up excess non-essential amino acids thereafter. Of the essential amino acids, threonine was decreased to the greatest extent followed by valine, isoleucine, and leucine—three branched-chain amino acids. Supplementation with threonine and L-isoleucine returned phosphorylated Yap signals to control levels in whole-cell lysate. We focused on isoleucine as the likely rate-limiting amino acid. A feedback loop between threonine and isoleucine, allows for threonine deaminase, the enzyme involved in catalyzing the first reaction to be inhibited when isoleucine allosterically binds and inhibits the reaction at high levels of isoleucine [117]. Therefore, increased levels of threonine as seen in our nutrient deprivation conditions can generate by conversion, isoleucine. Additionally, these three branched chain amino acids were decreased to the same extent, which may be explained by the fact that all three are metabolized by the same enzymes. First, they undergo transamination where they are converted to their respective branch chain  $\alpha$ -keto acids, followed by oxidative decarboxylation which is catabolized by branched-chain  $\alpha$ -ketoacid dehydrogenase. From here each amino acid aids in adenosine triphosphate production through distinct pathways [118].

#### **4.3 Compartmentalization of Yap After Nutrient Deprivation in Rat Cardiomyotubes**

Canonically, the translocation of Yap between the nucleus and cytoplasm plays an important role in the regulation of Yap activity. To investigate the effects of acute nutrient deprivation by nutrient deprivation we sub-fractionated the nuclear and cytoplasmic fractions of H9c2 myotubules. In agreement with our whole cell lysate results, an increase in Yap (p-S397) and Yap (p-S127) was shown. Intriguingly expression was increased both in the nucleus and cytoplasm in nutrient deprivation compared to controls (Table 2). This is atypical, as most reports suggest that phosphorylated Yap is cytoplasmically retained or associated with nuclear export to the cytoplasm [81,119]. It has been suggested that there could be a biphasic pattern of localization for Yap signalling once phosphorylated [120] that is time dependent [121]. This might account for the increase in total Yap expression in the cytoplasm under nutrient deprivation conditions compared to controls. It may be a reasonable hypothesis that if the time course were expanded, there would be flux of Yap from the nucleus to cytoplasm. Interestingly, Yap and Taz do not have a nuclear localization signal which is typically responsible for accumulation of proteins to the nucleus, therefore the exact mechanism of nuclear localization

or shuttling is unknown [121]. There is evidence that mechanical forces regulate the translocation of Yap in addition to biochemical cues such as actin specifically in the

**Table 2. Summary of Compartmentalization Patterns Results in Nutrient Deprivation and Nutrient Deprivation with Isoleucine Compared to DMEM Controls**

		Yap	Yap (p-S397)	Yap (p-S127)
Nutrient Deprivation	Cytoplasm	↑	↑	↑
	Nucleus	-/-	↑↑↑	↑↑↑
Nutrient Deprivation + Isoleucine	Cytoplasm	-/-	-/-	↑↑
	Nucleus	-/-	↑↑↑	↑↑↑

absence of cell-cell contact (i.e., after cardiac injury) [122]. Future studies that immunoprecipitated Yap under these conditions could identify key regulatory binding partner proteins necessary for compartmentation or cytoplasmic/nuclear shuttling.

Supplementation with L-isoleucine maintained expression of Yap, Yap (p-S397) and Yap (p-S127) levels comparable to controls in the whole cell lysates, and subcellular fraction showed that phosphorylated Yap was increased in the nucleus at both sites and at Yap (p-S127) in the cytoplasm. Supplementation with L-isoleucine only returned cytoplasmic Yap (p-S397) expression back to that of controls. Typically, phosphorylation at S397 is associated with translocation to the cytoplasm and subsequently leads to proteasomal degradation of Yap [78]. Therefore, one could hypothesize that Yap (p-S397) is being translocated to the nucleus where might then be dephosphorylated to activate Yap or that Yap (p-S397) accumulates in the nucleus after metabolic stress before it is transported to the cytoplasm, which could be confirmed by extending the timeline of the experiments.

#### **4.4 Connective Tissue Growth Factor in Yap Signalling and the Heart.**

The Ctgf gene encodes the Ctgf protein which is also known as cellular communication network factor 2. Regulation of the expression of Ctgf can be done at the transcriptional, post-transcriptional, and translational levels and is controlled by several pathological and physiological cues. As a secreted protein it is involved in initiating signal transduction by binding to various extra cellular constituents and receptors (eg. integrins, heparan sulfate proteoglycans, LRP, and TrkA). The consequences of Ctgf binding are diverse and have been linked with ECM/myofibrosis, endothelial-mesenchymal transition, macrophage polarization (M1>M2), autophagy and senescence-associated metabolic disruption [123]. It is responsible for the direct binding of cytokines and mediates ECM related proteins, in addition to regulating growth factor and cytokine activity by modulating crosstalk between signalling pathways. Ctgf is associated with fibrosis by controlling fibroblast proliferation, angiogenesis, matrix production and ECM deposition. Fibroblasts are fundamental for creating and maintaining the ECM, while the migration, activation, and differentiation to myofibroblasts of fibroblast is a major driver of fibrosis after injury. Transforming growth factor  $\beta$  (TGF- $\beta$ ) regulates myofibroblast differentiation and tissue formation while Ctgf indirectly acts as a downstream mediator of TGF- $\beta$  to trigger proliferation of fibroblast, migration and myofibroblast differentiation. The role of Ctgf is confirmed by deletion of Ctgf that was associated with decreased ECM production in the heart. The release of Ctgf from M2 macrophages is associated with the proliferation, and migration of fibroblast that contribute to the formation of the ECM [124]. In addition to the role of Ctgf in fibroblast and macrophages, it plays a role in endothelial cells function. Endothelial cells are important for angiogenesis, the process of forming new blood vessels from pre-existing ones. Ctgf increases vascular endothelial growth factor (VEGF) production, which is responsible for angiogenesis, through various pathways (e.g., AKT, ERK and Pi3K) that increase miR-210. Upregulation of miR-210 leads to inhibition of prolyl hydroxylase 2 activity that promotes increased VEGF expression and angiogenesis [125]. The regulation of Ctgf expression is controlled by various transcription factors with TEAD and its coactivator YAP being one of several [123]. Of the genes we tested during our study only Ctgf expression was markedly changed in response to nutrient deprivation conditions. When L-isoleucine was supplemented back, Ctgf expression increased further.

While there was no change in total Yap expression with L-isoleucine supplementation, there is a decrease in Yap (p-S397) in the cytoplasm compared to nutrient deprivation alone. Therefore, one could hypothesize that this phosphor-reduction results in activation of Yap, which allows for the transcription of Ctgf countercurrent to the change in total Yap. The activity of Yap/Tead and Ctgf are mutually regulated suggesting that increased activated Yap (unphosphorylated) is correlated with increased Ctgf [126]. The role of Yap in Ctgf associated angiogenesis was confirmed by re-expression of Yap that rescues angiogenesis in Ctgf mutant mice [126]. This suggests that Ctgf itself may be a feedback regulator of Yap-signalling.

As for fibroblasts, activated Yap increases Ctgf expression to promotes fibroblast proliferation [127]. Yap also plays a role in regulating the ECM through Ctgf expression, for example in the heart after MI elevated unphosphorylated Yap coincides with increased ECM production. This was confirmed using verteporfin, a drug which inhibits the binding of Yap to TEAD that stops gene transcription and decreased ECM production and proliferation of fibroblasts. This therefore resulted in decreased fibrosis and stiffness of the heart after MI compared to controls [128]. Inhibition of Ctgf might improve survival and ejection fraction in addition to improving remodelling by increased cross-sectional area of cardiomyocytes, heart weight and fibrotic genes [129]. Upregulation of Ctgf has also been associated with the hypertrophy of cardiomyocytes [130]. The role of Ctgf is likely cell and time dependent and may not be so readily reversed if the goal is to reduce its expression via Yap simply by L-isoleucine supplementation. Its effects are diverse on all cardiac cell types and include both autocrine and paracrine effect likely to influence all major remodelling events after MI but is one of the most rapid responses detected during cardiac stress.

#### **4.5 Clinical Relevance of Yap, Isoleucine, and Ctgf**

Clinically, increased circulating BCAA levels after MI are associated with increased risk of cardiovascular mortality and acute heart failure. Specifically, it has been shown to increase the risk of adverse events for patients with STEMI that require reperfusion[131]. However, not all patients experience elevated circulating BCAA levels after MI. In fact, in mice it was seen that circulating BCAA decreased out to 4 weeks compared to sham animals, yet cardiac BCAA levels were increased as a result of impaired BCAA catabolism after MI.

*Wang et al.* suggest that permanent MI is correlated with increased cardiac BCAA's caused by defective catabolism [132]. In cases where BCAA catabolism is defective there was a progressive loss of contractile capacity of the heart that leads to early death both in zebrafish and in mice [133]. *Gannon et al.* suggest that in conditions where energy is deprived, BCAA might improve the sensitivity to glucose uptake. In conditions where there is excess energy, the catabolism of BCAA is disrupted, which leads to accumulation of BCAA either in circulation or intracellularly [134]. Yap signalling plays an important role in the regulation of amino acids where decreased Yap activity is correlated with lower levels of SLC7A5 (or L-type amino acid transporter 1) which is responsible for the transport of amino acids to initiate protein synthesis [135]. Therefore, decreased SLC7A5 is linked to higher levels of amino acids. This is consistent with our results that show supplementation of L-isoleucine to our nutrient deprivation conditions resulted in decreased Yap (p-S397) in the cytoplasm compared to nutrient deprivation alone and also increased Ctgf expression that has been associated with poor remodelling and increased death after MI. Interestingly, the activation Yap (unphosphorylated) not only caused the upregulation of SLC7A5, and other genes involved in nutrient uptake, it also led to the upregulation of Ctgf [136]. Taken together a possible mechanism between Yap signalling and amino acids may be Yap acting to regulate amino acid metabolism instead of amino acids acting upon Yap signalling, or perhaps it works in both directions. Since increased BCAA amino acids are correlated with poor outcomes, and activating Yap signalling can decrease amino acid levels by increasing SLC7A5 activity, then increasing Yap signalling after MI may promote better outcomes for patients by improving adaptive remodelling. Therefore, these data highlight that Yap signalling could be a potentially beneficial drug targeted effect after MI, should such a possibility be realized.

#### **4.6 Limitations and Future Directions**

There are several limitations to the research performed for this thesis that limit the opportunity to make definitive conclusions as to the benefit/detriment of Yap signalling. Firstly, this study aside from *in vivo* analysis of Yap expression was performed *in vitro* with H9c2 cardiomyotubes. While *in vitro* studies allow for cell specificity and direct modeling of conditions for identification of molecular mechanisms, it lacks the complexity of the humoral, cellular, and molecular mechanisms interacting amongst various cardiac cell types that are fully



matured and functioning to meet physiological demands. Furthermore, our results are demonstrated in a singular rat cell line, these results could be supported by using another cell line to confirm the results, such as human AC16's cardiomyocyte cell lines or isolated primary cardiomyocytes or whole isolated heart perfusion analysis. This would allow for a more complete picture of the mechanisms involved and account for the species differences from human and rodents. An additional limitation to this study is the short timeline of one hour, which provides a snapshot in time, however, this lacks the mechanistic insight of progressive and multiple inputs that drive change in a progressive MI with or without reperfusion. Furthermore, we were not able to directly say that fatty acids don't play a role as the timeline of our study didn't allow for the absorption of palmitate, therefore we are reliant on fetal bovine serum that consists of many other nutrients besides fatty acids. While we were able to mimic many drivers of MI in our study, we lacked a model of waste accumulation that occurs after MI. Therefore, the role of waste accumulation in Yap signalling was not identified by this work. Since we have learned that circulating BCAA and intracellular BCAA play important roles in remodeling after MI, another limitation to our study is that only free amino acids were quantified, however, bound amino acid analysis was not performed. Additionally, our experiments were only carried out testing the supplementation of L-valine, L-threonine, and L-isoleucine. While the role of leucine and other amino acids were evaluated, neither was the combination of various amino acids as they were all supplemented individually. Combinations of amino acids might influence cell signalling in variable ways we have not determined. Leucine could be of particular interest since isoleucine and leucine have the same chemical formula but slightly different chemical structures. Leucine specifically is implicated in the regulation of other pathways, such as mTOR, and there has been an association between mTOR activity and vascular growth that is YAP/TAZ dependent [136].

#### **4.7 Conclusions**

In conclusion, our study characterizes Yap signalling under acute nutrient deprivation conditions and highlights the importance of amino acids involvement in Yap signalling. Further our finding implicates a relationship between isoleucine, Yap and Ctgf as part of very rapid gene expression changes with nutrient deprivation. Further understanding of the crosstalk

between isoleucine and Yap with other signalling pathways will be required before determining the optimal target for therapeutic advancements that might improve outcomes after MI.

## References

- 1 Thygesen K, Alpert JS, Jaffe AS, *et al.* Fourth universal definition of myocardial infarction (2018). *Russ. J. Cardiol.* 2019;**24**. doi:10.15829/1560-4071-2019-3-107-138
- 2 Vite A, Zhang C, Yi R, *et al.*  $\alpha$ -catenin-dependent cytoskeletal tension controls yap activity in the heart. *Dev* 2018;**145**. doi:10.1242/dev.149823
- 3 Agah R, Frenkel PA, French BA, *et al.* Gene recombination in postmitotic cells: Targeted expression of Cre recombinase provokes cardiac-restricted, site-specific rearrangement in adult ventricular muscle in vivo. *J Clin Invest* 1997;**100**. doi:10.1172/JCI119509
- 4 Mia MM, Singh MK. The Hippo Signaling Pathway in Cardiac Development and Diseases. *Front. Cell Dev. Biol.* 2019;**7**. doi:10.3389/fcell.2019.00211
- 5 Oka T, Xu J, Molkenin JD. Re-employment of developmental transcription factors in adult heart disease. *Semin. Cell Dev. Biol.* 2007;**18**. doi:10.1016/j.semcdb.2006.11.012
- 6 Lu L, Liu M, Sun RR, *et al.* Myocardial Infarction: Symptoms and Treatments. *Cell Biochem Biophys* 2015;**72**:865–7. doi:10.1007/s12013-015-0553-4
- 7 Ojha N, Dhamoon AS, Chapagain R. *Myocardial Infarction (Nursing)*. 2021.
- 8 Kosuge M, Kimura K, Ishikawa T, *et al.* Differences between men and women in terms of clinical features of ST-segment elevation acute myocardial infarction. *Circ J* 2006;**70**:222–6. doi:10.1253/circj.70.222
- 9 Valensi P, Lorgis L, Cottin Y. Prevalence, incidence, predictive factors and prognosis of silent myocardial infarction: A review of the literature. *Arch. Cardiovasc. Dis.* 2011;**104**:178–88. doi:10.1016/j.acvd.2010.11.013
- 10 Patel H, Rosengren A, Ekman I. Symptoms in acute coronary syndromes: Does sex make a difference? *Am Heart J* 2004;**148**:27–33. doi:10.1016/j.ahj.2004.03.005
- 11 Goldberg RJ, O'Donnell C, Yarzebski J, *et al.* Sex differences in symptom presentation associated with acute myocardial infarction: A population-based perspective. *Am Heart J* 1998;**136**. doi:10.1053/hj.1998.v136.88874

- 12 Herlitz J, Bang A, Karlson BW, *et al.* Is there a gender difference in aetiology of chest pain and symptoms associated with acute myocardial infarction? *Eur. J. Emerg. Med.* 1999;**6**. doi:10.1097/00063110-199912000-00007
- 13 Goldberg R, Goff D, Cooper L, *et al.* Age and sex differences in presentation of symptoms among patients with acute coronary disease: The REACT trial. *Coron Artery Dis* 2000;**11**. doi:10.1097/00019501-200007000-00004
- 14 Mechanic, O. J., Gavin, M., & Grossman SA. *Acute Myocardial Infarction*. 2022.
- 15 Lim W, Qushmaq I, Cook DJ, *et al.* Elevated troponin and myocardial infarction in the intensive care unit: a prospective study. *Crit Care* 2005;**9**:R636-44. doi:10.1186/cc3816
- 16 Acute Coronary Syndromes. *Natl Inst Heal Care Excell* 2022.
- 17 Ibanez, B., James, S., Agewall, S., Antunes, M. J., Bucciarelli-Ducci, C., Bueno, H., Caforio, A. L. P., Crea, F., Goudevenos, J. A., Halvorsen, S., Hindricks, G., Kastrati, A., Lenzen, M. J., Prescott, E., Roffi, M., Valgimigli, M., Varenhorst, C., Vranckx, P. 2017 ESC Guidelines for the management of acute myocardial infarction in patients presenting with ST-segment elevation: The Task Force for the management of acute myocardial infarction in patients presenting with ST-segment elevation of the European Society of Cardiology. *Eur Heart J*;39:119–177.
- 18 Basit H, Malik A, Huecker MR. Non ST Segment Elevation Myocardial Infarction - StatPearls - NCBI Bookshelf. *StatPearls* 2021.
- 19 Lindsey ML, Brunt KR, Kirk JA, *et al.* Guidelines for in vivo mouse models of myocardial infarction. *Am. J. Physiol. - Hear. Circ. Physiol.* 2021;**321**. doi:10.1152/AJPHEART.00459.2021
- 20 Luginbuhl J, Parapanov R, Krueger T, *et al.* Murine myocardial infarction model using permanent ligation of left anterior descending coronary artery. *J Vis Exp* 2019;**2019**. doi:10.3791/59591
- 21 Kolk MVV, Meyberg D, Deuse T, *et al.* LAD-ligation: A murine model of myocardial infarction. *J Vis Exp* Published Online First: 2009. doi:10.3791/1438

- 22 Pei H, Song X, Peng C, *et al.* TNF- $\alpha$  inhibitor protects against myocardial ischemia/reperfusion injury via Notch1-mediated suppression of oxidative/nitrative stress. *Free Radic Biol Med* 2015;**82**. doi:10.1016/j.freeradbiomed.2015.02.002
- 23 Wang J, Bo H, Meng X, *et al.* A simple and fast experimental model of myocardial infarction in the mouse. *Texas Hear Inst J* 2006;**33**.
- 24 Yehualashet AS, Belachew TF, Kifle ZD, *et al.* Targeting Cardiac Metabolic Pathways: A Role in Ischemic Management. *Vasc Health Risk Manag* 2020;**16**:353–65. doi:10.2147/VHRM.S264130
- 25 Zuurbier CJ, Bertrand L, Beauloye CR, *et al.* Cardiac metabolism as a driver and therapeutic target of myocardial infarction. *J Cell Mol Med* 2020;**24**:5937–54. doi:10.1111/jcmm.15180
- 26 Doenst T, Nguyen TD, Abel ED. Cardiac metabolism in heart failure: implications beyond ATP production. *Circ Res* 2013;**113**:709–24. doi:10.1161/CIRCRESAHA.113.300376
- 27 Del Re DP, Amgalan D, Linkermann A, *et al.* Fundamental mechanisms of regulated cell death and implications for heart disease. *Physiol Rev* 2019;**99**. doi:10.1152/physrev.00022.2018
- 28 Park, M. Y., Ha, S. E., Vetrivel, P., Kim, H. H., Bhosale, P. B., Abusaliya, A., & Kim GS. Differences of Key Proteins between Apoptosis and Necroptosis. *Biomed Res Int* 2021.
- 29 Kushnareva Y, Newmeyer DD. Bioenergetics and cell death. *Ann N Y Acad Sci* 2010;**1201**:50–7. doi:10.1111/j.1749-6632.2010.05633.x
- 30 Orrenius S, Nicotera P, Zhivotovsky B. Cell death mechanisms and their implications in toxicology. *Toxicol Sci* 2011;**119**. doi:10.1093/toxsci/kfq268
- 31 Belizário J, Vieira-Cordeiro L, Enns S. Necroptotic cell death signaling and execution pathway: Lessons from knockout mice. *Mediators Inflamm*. 2015;**2015**. doi:10.1155/2015/128076

- 32 Galluzzi L, Kepp O, Chan FKM, *et al.* Necroptosis: Mechanisms and Relevance to Disease. *Annu. Rev. Pathol. Mech. Dis.* 2017;**12**. doi:10.1146/annurev-pathol-052016-100247
- 33 Dhuriya YK, Sharma D. Necroptosis: A regulated inflammatory mode of cell death. *J. Neuroinflammation.* 2018;**15**. doi:10.1186/s12974-018-1235-0
- 34 Wu X, Li Y, Zhang S, *et al.* Ferroptosis as a novel therapeutic target for cardiovascular disease. *Theranostics.* 2021;**11**. doi:10.7150/THNO.54113
- 35 Popov S V., Maslov LN, Naryzhnaya N V., *et al.* The Role of Pyroptosis in Ischemic and Reperfusion Injury of the Heart. *J. Cardiovasc. Pharmacol. Ther.* 2021;**26**. doi:10.1177/10742484211027405
- 36 Schirone L, Forte M, D'ambrosio L, *et al.* An Overview of the Molecular Mechanisms Associated with Myocardial Ischemic Injury: State of the Art and Translational Perspectives. *Cells.* 2022;**11**. doi:10.3390/cells11071165
- 37 Nauta JF, Hummel YM, Tromp J, *et al.* Concentric vs. eccentric remodelling in heart failure with reduced ejection fraction: clinical characteristics, pathophysiology and response to treatment. *Eur J Heart Fail* 2020;**22**. doi:10.1002/ejhf.1632
- 38 Nakamura M, Sadoshima J. Mechanisms of physiological and pathological cardiac hypertrophy. *Nat. Rev. Cardiol.* 2018;**15**. doi:10.1038/s41569-018-0007-y
- 39 De Simone G. Concentric or Eccentric Hypertrophy: How Clinically Relevant Is the Difference? *Hypertension.* 2004;**43**. doi:10.1161/01.HYP.0000121363.08252.a7
- 40 Kehat I, Molkenin JD. Molecular pathways underlying cardiac remodeling during pathophysiological stimulation. *Circulation* 2010;**122**. doi:10.1161/CIRCULATIONAHA.110.942268
- 41 Schirone L, Forte M, Palmerio S, *et al.* A Review of the Molecular Mechanisms Underlying the Development and Progression of Cardiac Remodeling. *Oxid Med Cell Longev* 2017;**2017**. doi:10.1155/2017/3920195
- 42 Mathis GA, Sirica AE. Effects of medium and substratum conditions on the rates of DNA synthesis in primary cultures of bile ductular epithelial cells. *Vitr Cell Dev Biol* 1990;**26**. doi:10.1007/BF02624101

- 43 Talman V, Ruskoaho H. Cardiac fibrosis in myocardial infarction—from repair and remodeling to regeneration. *Cell Tissue Res.* 2016;**365**. doi:10.1007/s00441-016-2431-9
- 44 Reichardt IM, Robeson KZ, Regnier M, *et al.* Controlling cardiac fibrosis through fibroblast state space modulation. *Cell. Signal.* 2021;**79**. doi:10.1016/j.cellsig.2020.109888
- 45 Venugopal H, Hanna A, Humeres C, *et al.* Properties and Functions of Fibroblasts and Myofibroblasts in Myocardial Infarction. *Cells.* 2022;**11**. doi:10.3390/cells11091386
- 46 Ieda M, Fu JD, Delgado-Olguin P, *et al.* Direct reprogramming of fibroblasts into functional cardiomyocytes by defined factors. *Cell* 2010;**142**:375–86. doi:10.1016/j.cell.2010.07.002
- 47 Frangogiannis NG, Michael LH, Entman ML. Myofibroblasts in reperfused myocardial infarcts express the embryonic form of smooth muscle myosin heavy chain (SMemb). *Cardiovasc Res* 2000;**48**. doi:10.1016/S0008-6363(00)00158-9
- 48 Cleutjens JPM, Verluyten MJA, Smits JFM, *et al.* Collagen remodeling after myocardial infarction in the rat heart. *Am J Pathol* 1995;**147**.
- 49 Segura AM, Frazier OH, Buja LM. Fibrosis and heart failure. *Heart Fail Rev* 2014;**19**. doi:10.1007/s10741-012-9365-4
- 50 Wu X, Reboll MR, Korf-Klingebiel M, *et al.* Angiogenesis after acute myocardial infarction. *Cardiovasc. Res.* 2021;**117**. doi:10.1093/cvr/cvaa287
- 51 Li N, Rignault-Clerc S, Biemann C, *et al.* Increasing heart vascularisation after myocardial infarction using brain natriuretic peptide stimulation of endothelial and WT1+ epicardial cells. *Elife* 2020;**9**. doi:10.7554/eLife.61050
- 52 Shiojima I, Sato K, Izumiya Y, *et al.* Disruption of coordinated cardiac hypertrophy and angiogenesis contributes to the transition to heart failure. *J Clin Invest* 2005;**115**. doi:10.1172/JCI24682
- 53 Friehs, I., Margossian, R. E., Moran, A. M., Cao-Danh, H., Moses, M. A., & del Nido PJ. *Vascular endothelial growth factor delays onset of failure in pressure-overload hypertrophy through matrix metalloproteinase activation and angiogenesis*. Basic research in cardiology

- 54 Tirziu D, Chorianopoulos E, Moodie KL, *et al.* Myocardial hypertrophy in the absence of external stimuli is induced by angiogenesis in mice. *J Clin Invest* 2007;**117**. doi:10.1172/JCI32024
- 55 Gerhardt H. VEGF and endothelial guidance in angiogenic sprouting. *Organogenesis*. 2008;**4**. doi:10.4161/org.4.4.7414
- 56 Carmeliet P, De Smet F, Loges S, *et al.* Branching morphogenesis and antiangiogenesis candidates: Tip cells lead the way. *Nat. Rev. Clin. Oncol.* 2009;**6**. doi:10.1038/nrclinonc.2009.64
- 57 Goodwin, K., & Nelson CM. Branching morphogenesis. *Dev*;**147**.
- 58 Adair, T. H., & Montani JP. *Angiogenesis*. Morgan & Claypool Life Sciences
- 59 Chien S. Mechanotransduction and endothelial cell homeostasis: The wisdom of the cell. In: *American Journal of Physiology - Heart and Circulatory Physiology*. 2007. doi:10.1152/ajpheart.01047.2006
- 60 Mohammed SF, Hussain S, Mirzoyev SA, *et al.* Coronary microvascular rarefaction and myocardial fibrosis in heart failure with preserved ejection fraction. *Circulation* 2015;**131**. doi:10.1161/CIRCULATIONAHA.114.009625
- 61 Silvis MJM, Kaffka genaamd Dengler SE, Odille CA, *et al.* Damage-Associated Molecular Patterns in Myocardial Infarction and Heart Transplantation: The Road to Translational Success. *Front. Immunol.* 2020;**11**. doi:10.3389/fimmu.2020.599511
- 62 Frangogiannis SDP and NG. The Biological Basis for Cardiac Repair After Myocardial Infarction: From Inflammation to Fibrosis. *Physiol Behav* 2017;**176**.
- 63 Ong SB, Hernández-Reséndiz S, Crespo-Avilan GE, *et al.* Inflammation following acute myocardial infarction: Multiple players, dynamic roles, and novel therapeutic opportunities. *Pharmacol. Ther.* 2018;**186**. doi:10.1016/j.pharmthera.2018.01.001
- 64 Wen H, Peng L, Chen Y. The effect of immune cell-derived exosomes in the cardiac tissue repair after myocardial infarction: Molecular mechanisms and pre-clinical evidence. *J. Cell. Mol. Med.* 2021;**25**. doi:10.1111/jcmm.16686



- 65 Arslan F, De Kleijn DP, Pasterkamp G. Innate immune signaling in cardiac ischemia. *Nat. Rev. Cardiol.* 2011;**8**. doi:10.1038/nrcardio.2011.38
- 66 Ghigo A, Franco I, Morello F, *et al.* Myocyte signalling in leucocyte recruitment to the heart. *Cardiovasc. Res.* 2014;**102**. doi:10.1093/cvr/cvu030
- 67 Frangogiannis NG. Inflammation in cardiac injury, repair and regeneration. *Curr. Opin. Cardiol.* 2015;**30**. doi:10.1097/HCO.0000000000000158
- 68 Jung M, Dodsworth M, Thum T. Inflammatory cells and their non-coding RNAs as targets for treating myocardial infarction. *Basic Res. Cardiol.* 2019;**114**. doi:10.1007/s00395-018-0712-z
- 69 Christia P, Frangogiannis NG. Targeting inflammatory pathways in myocardial infarction. *Eur. J. Clin. Invest.* 2013;**43**. doi:10.1111/eci.12118
- 70 Kim W, Jho EH. The history and regulatory mechanism of the Hippo pathway. *BMB Rep.* 2018;**51**. doi:10.5483/BMBRep.2018.51.3.022
- 71 Calses PC, Crawford JJ, Lill JR, *et al.* Hippo Pathway in Cancer: Aberrant Regulation and Therapeutic Opportunities. *Trends in Cancer.* 2019;**5**. doi:10.1016/j.trecan.2019.04.001
- 72 Zanconato F, Cordenonsi M, Piccolo S. YAP/TAZ at the Roots of Cancer. *Cancer Cell.* 2016;**29**. doi:10.1016/j.ccell.2016.05.005
- 73 Davis JR, Tapon N. Hippo signalling during development. *Dev* 2019;**146**. doi:10.1242/dev.167106
- 74 Piccolo S, Dupont S, Cordenonsi M. The biology of YAP/TAZ: Hippo signaling and beyond. *Physiol Rev* 2014;**94**. doi:10.1152/physrev.00005.2014
- 75 Zheng Y, Wang W, Liu B, *et al.* Identification of Happyhour/MAP4K as Alternative Hpo/Mst-like Kinases in the Hippo Kinase Cascade. *Dev Cell* 2015;**34**. doi:10.1016/j.devcel.2015.08.014
- 76 Hao Y, Chun A, Cheung K, *et al.* Tumor suppressor LATS1 is a negative regulator of oncogene YAP. *J Biol Chem* 2008;**283**. doi:10.1074/jbc.M709037200

- 77 Moon S, Kim W, Kim S, *et al.* Phosphorylation by NLK inhibits YAP -14-3-3- interactions and induces its nuclear localization . *EMBO Rep* 2017;**18**. doi:10.15252/embr.201642683
- 78 Wang P, Gong Y, Guo T, *et al.* Activation of Aurora A kinase increases YAP stability via blockage of autophagy. *Cell Death Dis* 2019;**10**. doi:10.1038/s41419-019-1664-4
- 79 Kim MK, Jang JW, Bae SC. DNA binding partners of YAP/TAZ. *BMB Rep.* 2018;**51**. doi:10.5483/BMBRep.2018.51.3.015
- 80 Pocaterra A, Romani P, Dupont S. YAP/TAZ functions and their regulation at a glance. *J Cell Sci* 2020;**133**. doi:10.1242/jcs.230425
- 81 Dupont S, Morsut L, Aragona M, *et al.* Role of YAP/TAZ in mechanotransduction. *Nature* 2011;**474**. doi:10.1038/nature10137
- 82 Wang J, Liu S, Heallen T, *et al.* The Hippo pathway in the heart: pivotal roles in development, disease, and regeneration. *Nat. Rev. Cardiol.* 2018;**15**:672–84. doi:10.1038/s41569-018-0063-3
- 83 Seo J, Kim J. Regulation of Hippo signaling by actin remodeling. *BMB Rep.* 2018;**51**. doi:10.5483/BMBRep.2018.51.3.012
- 84 Yu FX, Zhao B, Panupinthu N, *et al.* Regulation of the Hippo-YAP pathway by G-protein-coupled receptor signaling. *Cell* 2012;**150**. doi:10.1016/j.cell.2012.06.037
- 85 Gong R, Hong AW, Plouffe SW, *et al.* Opposing roles of conventional and novel PKC isoforms in Hippo-YAP pathway regulation. *Cell Res.* 2015;**25**. doi:10.1038/cr.2015.88
- 86 Mo JS, Yu FX, Gong R, *et al.* Regulation of the Hippo-YAP pathway by protease-activated receptors (PARs). *Genes Dev* 2012;**26**. doi:10.1101/gad.197582.112
- 87 Santinon G, Pocaterra A, Dupont S. Control of YAP/TAZ Activity by Metabolic and Nutrient-Sensing Pathways. *Trends Cell Biol.* 2016;**26**. doi:10.1016/j.tcb.2015.11.004
- 88 Shao D, Zhai P, Del Re DP, *et al.* A functional interaction between Hippo-YAP signalling and FoxO1 mediates the oxidative stress response. *Nat Commun* 2014;**5**. doi:10.1038/ncomms4315

- 89 Ma B, Cheng H, Gao R, *et al.* Zyxin-Siah2-Lats2 axis mediates cooperation between Hippo and TGF- $\beta$  signalling pathways. *Nat Commun* 2016;**7**. doi:10.1038/ncomms11123
- 90 Hong AW, Meng Z, Yuan H, *et al.* Osmotic stress-induced phosphorylation by NLK at Ser128 activates YAP . *EMBO Rep* 2017;**18**. doi:10.15252/embr.201642681
- 91 Koo JH, Guan KL. Interplay between YAP/TAZ and Metabolism. *Cell Metab.* 2018;**28**. doi:10.1016/j.cmet.2018.07.010
- 92 Chen J, Cheng J, Zhao C, *et al.* The hippo pathway: A renewed insight in the craniofacial diseases and hard tissue remodeling. *Int J Biol Sci* 2021;**17**. doi:10.7150/ijbs.63305
- 93 Mullen PJ, Yu R, Longo J, *et al.* The interplay between cell signalling and the mevalonate pathway in cancer. *Nat. Rev. Cancer.* 2016;**16**. doi:10.1038/nrc.2016.76
- 94 Yuan L, Mao Y, Luo W, *et al.* Palmitic acid dysregulates the Hippo-YAP pathway and inhibits angiogenesis by inducing mitochondrial damage and activating the cytosolic DNA sensor cGAS-STING-IRF3 signaling mechanism. *J Biol Chem* 2017;**292**. doi:10.1074/jbc.M117.804005
- 95 Noto A, De Vitis C, Pisanu ME, *et al.* Stearoyl-CoA-desaturase 1 regulates lung cancer stemness via stabilization and nuclear localization of YAP/TAZ. *Oncogene* 2017;**36**. doi:10.1038/onc.2017.75
- 96 Peng C, Zhu Y, Zhang W, *et al.* Regulation of the Hippo-YAP Pathway by Glucose Sensor O-GlcNAcylation. *Mol Cell* 2017;**68**. doi:10.1016/j.molcel.2017.10.010
- 97 Zhang X, Qiao Y, Wu Q, *et al.* The essential role of YAP O-GlcNAcylation in high-glucose-stimulated liver tumorigenesis. *Nat Commun* 2017;**8**. doi:10.1038/ncomms15280
- 98 Heallen T, Zhang M, Wang J, *et al.* Hippo pathway inhibits wnt signaling to restrain cardiomyocyte proliferation and heart size. *Science (80- )* 2011;**332**. doi:10.1126/science.1199010
- 99 Xiao Y, Leach J, Wang J, *et al.* Hippo/Yap Signaling in Cardiac Development and Regeneration. *Curr. Treat. Options Cardiovasc. Med.* 2016;**18**. doi:10.1007/s11936-016-0461-y

- 100 Vincent SD, Buckingham ME. How to make a heart. The origin and regulation of cardiac progenitor cells. In: *Current Topics in Developmental Biology*. 2010. doi:10.1016/S0070-2153(10)90001-X
- 101 Xin M, Kim Y, Sutherland LB, *et al.* Development: Regulation of insulin-like growth factor signaling by Yap governs cardiomyocyte proliferation and embryonic heart size. *Sci Signal* 2011;4. doi:10.1126/scisignal.2002278
- 102 Xin M, Kim Y, Sutherland LB, *et al.* Hippo pathway effector Yap promotes cardiac regeneration. *Proc Natl Acad Sci U S A* 2013;110:13839–44. doi:10.1073/pnas.1313192110
- 103 Li J, Gao E, Vite A, *et al.* Alpha-catenins control cardiomyocyte proliferation by regulating yap activity. *Circ Res* 2015;116. doi:10.1161/CIRCRESAHA.116.304472
- 104 Odashima, M., Usui, S., Takagi, H., Hong, C., Liu, J., Yokota, M., & Sadoshima J. Inhibition of endogenous Mst1 prevents apoptosis and cardiac dysfunction without affecting cardiac hypertrophy after myocardial infarction. *Circ Res* 2007;100:1344–1352.
- 105 Tsao CW, Aday AW, Almarzooq ZI, *et al.* Heart Disease and Stroke Statistics - 2023 Update: A Report from the American Heart Association. *Circulation*. 2023;147. doi:10.1161/CIR.0000000000001123
- 106 Brazma A, Hingamp P, Quackenbush J, *et al.* Minimum information about a microarray experiment (MIAME) - Toward standards for microarray data. *Nat. Genet.* 2001;29. doi:10.1038/ng1201-365
- 107 Tulacz D, Mackiewicz U, Maczewski M, *et al.* Transcriptional profiling of left ventricle and peripheral blood mononuclear cells in a rat model of postinfarction heart failure. *BMC Med Genomics* 2013;6. doi:10.1186/1755-8794-6-49
- 108 Berg Jeremy, Tymoczko John LS. *Biochemistry*. 7th ed. New York: W.H. Freeman and Company 2010.
- 109 Tol MJ, van der Lienden MJC, Gabriel TL, *et al.* HEPES activates a MiT/TFE-dependent lysosomal-autophagic gene network in cultured cells: A call for caution. *Autophagy* 2018;14. doi:10.1080/15548627.2017.1419118

- 110 van der Lienden MJC, Aten J, Boot RG, *et al.* HEPES-buffering of bicarbonate-containing culture medium perturbs lysosomal glucocerebrosidase activity. *J Cell Biochem* 2022;**123**. doi:10.1002/jcb.30234
- 111 Lin Z, Von Gise A, Zhou P, *et al.* Cardiac-specific YAP activation improves cardiac function and survival in an experimental murine MI model. *Circ Res* 2014;**115**. doi:10.1161/CIRCRESAHA.115.303632
- 112 Heallen T, Morikawa Y, Leach J, *et al.* Hippo signaling impedes adult heart regeneration. *Dev* 2013;**140**. doi:10.1242/dev.102798
- 113 Correction (JACC: Basic to Translational Science (2020) 5(9) (931–945), (S2452302X20303417), (10.1016/j.jacbts.2020.07.009)). *JACC Basic to Transl. Sci.* 2021;**6**. doi:10.1016/j.jacbts.2021.06.007
- 114 Zhao B, Li L, Tumaneng K, *et al.* A coordinated phosphorylation by Lats and CK1 regulates YAP stability through SCF(beta-TRCP). *Genes Dev* 2010;**24**:72–85. doi:10.1101/gad.1843810
- 115 Hao Y, Chun A, Cheung K, *et al.* Tumor suppressor LATS1 is a negative regulator of oncogene YAP. *J Biol Chem* 2008;**283**:5496–509. doi:10.1074/jbc.M709037200
- 116 Wang P, Gong Y, Guo T, *et al.* Activation of Aurora A kinase increases YAP stability via blockage of autophagy. *Cell Death Dis* 2019;**10**:432. doi:10.1038/s41419-019-1664-4
- 117 Isogai S, Nishimura A, Kotaka A, *et al.* High-Level Production of Isoleucine and Fusel Alcohol by Expression of the Feedback Inhibition-Insensitive Threonine Deaminase in *Saccharomyces cerevisiae*. *Appl Environ Microbiol* 2022;**88**. doi:10.1128/aem.02130-21
- 118 Dimou A, Tsimihodimos V, Bairaktari E. The Critical Role of the Branched Chain Amino Acids (BCAAs) Catabolism-Regulating Enzymes, Branched-Chain Aminotransferase (BCAT) and Branched-Chain  $\alpha$ -Keto Acid Dehydrogenase (BCKD), in Human Pathophysiology. *Int. J. Mol. Sci.* 2022;**23**. doi:10.3390/ijms23074022
- 119 Wada KI, Itoga K, Okano T, *et al.* Hippo pathway regulation by cell morphology and stress fibers. *Development* 2011;**138**. doi:10.1242/dev.070987

- 120 Wang J, Sinnett-Smith J, Stevens J V., *et al.* Biphasic regulation of Yes-associated Protein (YAP) cellular localization, phosphorylation, and activity by G protein-coupled receptor agonists in intestinal epithelial cells: A novel role for Protein Kinase D (PKD). *J Biol Chem* 2016;**291**. doi:10.1074/jbc.M115.711275
- 121 Shreberk-Shaked M, Oren M. New insights into YAP/TAZ nucleo-cytoplasmic shuttling: new cancer therapeutic opportunities? *Mol. Oncol.* 2019;**13**. doi:10.1002/1878-0261.12498
- 122 Das A, Fischer RS, Pan D WC. YAP Nuclear Localization in the Absence of Cell-Cell Contact Is Mediated by a Filamentous Actin-dependent, Myosin II- and Phospho-YAP-independent Pathway during Extracellular Matrix Mechanosensing. *J Biol Chem* 2016;**291**.
- 123 Effendi WI, Nagano T. Connective Tissue Growth Factor in Idiopathic Pulmonary Fibrosis: Breaking the Bridge. *Int. J. Mol. Sci.* 2022;**23**. doi:10.3390/ijms23116064
- 124 Zhang SM, Wei CY, Wang Q, *et al.* M2-polarized macrophages mediate wound healing by regulating connective tissue growth factor via AKT, ERK1/2, and STAT3 signaling pathways. *Mol Biol Rep* 2021;**48**. doi:10.1007/s11033-021-06646-w
- 125 Liu SC, Chuang SM, Hsu CJ, *et al.* CTGF increases vascular endothelial growth factor-dependent angiogenesis in human synovial fibroblasts by increasing miR-210 expression. *Cell Death Dis* 2014;**5**. doi:10.1038/cddis.2014.453
- 126 Moon S, Lee S, Caesar JA, *et al.* A CTGF-YAP Regulatory Pathway Is Essential for Angiogenesis and Barrierogenesis in the Retina. *iScience* 2020;**23**. doi:10.1016/j.isci.2020.101184
- 127 Sharifi-sanjani M, Berman M, Goncharov D, *et al.* Yes-associated protein (Yap) is up-regulated in heart failure and promotes cardiac fibroblast proliferation. *Int J Mol Sci* 2021;**22**. doi:10.3390/ijms22116164
- 128 Garoffolo G, Casaburo M, Amadeo F, *et al.* Reduction of Cardiac Fibrosis by Interference with YAP-Dependent Transactivation. *Circ Res* 2022;**131**. doi:10.1161/CIRCRESAHA.121.319373
- 129 Vainio LE, Szabó Z, Lin R, *et al.* Connective Tissue Growth Factor Inhibition Enhances Cardiac Repair and Limits Fibrosis After Myocardial Infarction. *JACC Basic to Transl Sci* 2019;**4**. doi:10.1016/j.jacbts.2018.10.007

- 130 Matsui Y, Sadoshima J. Rapid upregulation of CTGF in cardiac myocytes by hypertrophic stimuli: Implication for cardiac fibrosis and hypertrophy. *J. Mol. Cell. Cardiol.* 2004;**37**. doi:10.1016/j.yjmcc.2004.05.012
- 131 Du X, You H, Li Y, Wang Y, Hui P, Qiao B, Lu J, Zhang W, Zhou S, Zheng Y DJ. Relationships between circulating branched chain amino acid concentrations and risk of adverse cardiovascular events in patients with STEMI treated with PC. *Sci Rep* 2018;**8**.
- 132 Wang W, Zhang F, Xia Y, *et al.* Defective branched chain amino acid catabolism contributes to cardiac dysfunction and remodeling following myocardial infarction. *Am J Physiol - Hear Circ Physiol* 2016;**311**. doi:10.1152/ajpheart.00114.2016
- 133 Wendel U. Metabolism of branched-chain amino acids in maple syrup urine disease. *Eur J Pediatr Suppl* 1997;**156**. doi:10.1007/pl00014274
- 134 Gannon NP, Schnuck JK, Vaughan RA. BCAA Metabolism and Insulin Sensitivity – Dysregulated by Metabolic Status? *Mol. Nutr. Food Res.* 2018;**62**. doi:10.1002/mnfr.201700756
- 135 Najumudeen AK, Ceteci F, Fey SK, *et al.* The amino acid transporter SLC7A5 is required for efficient growth of KRAS-mutant colorectal cancer. *Nat Genet* 2021;**53**. doi:10.1038/s41588-020-00753-3
- 136 Ong YT, Andrade J, Armbruster M, *et al.* A YAP/TAZ-TEAD signalling module links endothelial nutrient acquisition to angiogenic growth. *Nat Metab* 2022;**4**. doi:10.1038/s42255-022-00584-y